NPS-OC-99-01

NAVAL POSTGRADUATE SCHOOL
Monterey, California

THESIS

CHANGES IN THE HYDROGRAPHY OF CENTRAL CALIFORNIA WATERS ASSOCIATED WITH THE 1997-1998 EL NIÑO

by
Hiromi Asanuma
June 1999

Thesis Advisor: Curtis A. Collins
Second Reader: Carmen G. Castro

Prepared for:
Naval Postgraduate School
Monterey, California 93943

NAVAL POSTGRADUATE SCHOOL

MONTEREY, CALIFORNIA 93943-5000

RADM Robert C. Chaplin
Superintendent

This report was prepared for the National Science Foundation.

This report was prepared by: Hiromi Asanuma, Thomas A. Rago, Curtis A. Collins, Francisco Chavez and Carmen G. Castro.

REPORT DOCUMENTATION PAGE

Form Approved
OMB No. 0704-0188

1. AGENCY USE ONLY *(Leave blank)*	2. REPORT DATE	3. REPORT TYPE AND DATES COVERED
	June 1999	Masters Thesis and Technical Report

4. TITLE AND SUBTITLE CHANGES IN THE HYDROGRAPHY OF CENTRAL CALIFORNIA WATERS ASSOCIATED WITH THE 1997-1998 EL NIÑO

5. FUNDING NUMBERS
OC-9811035

6. AUTHOR(S)
Asanuma, Hiromi, T. A. Rago, C. A. Collins, F. Chavez and Carmen G. Castro

7. PERFORMING ORGANIZATION NAME(S) AND ADDRESS(ES)
Naval Postgraduate School
Monterey, CA 93943-5000

8. PERFORMING ORGANIZATION REPORT NUMBER
NPS-OC-99-001

9. SPONSORING / MONITORING AGENCY NAME(S) AND ADDRESS(ES) National Science Foundation, 4201 Wilson Blvd., Arlington, VA 22230

10. SPONSORING / MONITORING AGENCY REPORT NUMBER
OCE9811035

11. SUPPLEMENTARY NOTES The views expressed in this thesis are those of the authors and do not reflect the official policy or position of the Department of Defense or the U.S. Government.

12a. DISTRIBUTION / AVAILABILITY STATEMENT
Approved for public release; distribution unlimited.

12b. DISTRIBUTION CODE

13. ABSTRACT *(maximum 200 words)* During 1998-1997, oceanographic conditions off Central California were monitored by means of a series of thirteen cruises which measured water properties along an oceanographic section perpendicular to the California Coast. Data were analyzed by utilizing time series plots on isobaric and isopycnal surfaces and by principal component analysis. The following conditions were observed: (a) in June-July 1997, the strong poleward flow at the coast was associated with coastal (within 100 km), subsurface (200-500 dbar) warming of 0.5°C and increased salinity (0.07) on isopycnal surfaces and offshore waters appeared cooler, fresher with stronger equatorward flow; (b) in September 1997, a relaxation of El Niño conditions occurred, with coastal, subsurface waters cooling by 0.3°C, and the band of poleward flow at the coast narrowed; (c) in January 1998, maximum interannual temperature and sea level anomalies were observed with nearsurface (80 dbar), nearshore (within 100 km) warming of 2.5°C , subsurface warming comparable to that observed in June-July 1997, and equatorward flow at the coast; and (d) in March-April 1998, coastal waters freshened greatly, both due to the onshore flow of Subarctic water and to river runoff from winter storms. By summer 1998, hydrographic conditions were near normal. The observed warming in late 1997 was not caused by decreased offshore Ekman transport but does appear to be remotely forced by poleward propagation from the Equatorial Pacific along the Eastern Boundary, possibly by Kelvin waves. The subsequent onshore transport and freshening that took place during Spring 1998 could have been related to onshore Ekman transport associated with winter storms. The observed change in heat content associated with the 1997-1998 El Niño was the same as that observed during a normal seasonal cycle.

14. SUBJECT TERMS	15. NUMBER OF PAGES
California Current System, El Niño, Eastern Boundary Currents	133
	16. PRICE CODE

17. SECURITY CLASSIFICATION OF REPORT	18. SECURITY CLASSIFICATION OF THIS PAGE	19. SECURITY CLASSIFI- CATION OF ABSTRACT	20. LIMITATION OF ABSTRACT
Unclassified	Unclassified	Unclassified	UL

NSN 7540-01-280-5500

Standard Form 298 (Rev. 2-89)
Prescribed by ANSI Std. 239-18

CHANGES IN THE HYDROGRAPHY OF CENTRAL CALIFORNIA WATERS ASSOCIATED WITH THE 1997-1998 EL NIÑO

Hiromi Asanuma
Lieutenant Commander, JMSDF

Submitted in partial fulfillment of the
requirements for the degree of

MASTER OF SCIENCE IN PHYSICAL OCEANOGRAPHY

from the

NAVAL POSTGRADUATE SCHOOL
June 1999

ABSTRACT

During 1998-1997, oceanographic conditions off Central California were monitored by means of a series of thirteen cruises which measured water properties along an oceanographic section perpendicular to the California Coast. Data were analyzed by utilizing time series plots on isobaric and isopycnal surfaces and by principal component analysis. The following conditions were observed: (a) in June-July 1997, the strong poleward flow at the coast was associated with coastal (within 100 km), subsurface (200-500 dbar) warming of 0.5°C and increased salinity (0.07) on isopycnal surfaces and offshore waters appeared cooler, fresher with stronger equatorward flow; (b) in September 1997, a relaxation of El Niño conditions occurred, with coastal, subsurface waters cooling by 0.3°C, and the band of poleward flow at the coast narrowed; (c) in January 1998, maximum interannual temperature and sea level anomalies were observed with nearsurface (80 dbar), nearshore (within 100 km) warming of 2.5°C , subsurface warming comparable to that observed in June-July 1997, and equatorward flow at the coast; and (d) in March-April 1998, coastal waters freshened greatly, both due to the onshore flow of Subarctic water and to river runoff from winter storms. By summer 1998, hydrographic conditions were near normal.

The observed warming in late 1997 was not caused by decreased offshore Ekman transport but does appear to be remotely forced by poleward propagation from the Equatorial Pacific along the Eastern Boundary, possibly by Kelvin waves. The subsequent onshore transport and freshening that took place during Spring 1998 could have been related to onshore Ekman transport associated with winter storms. The observed change in heat content associated with the 1997-1998 El Niño was the same as that observed during a normal seasonal cycle.

TABLE OF CONTENTS

ACKNOWLEGEMENT

I wish to express my sincere appreciation to my advisor, Prof. Curtis. A. Collins. Without his assistance, encouragement, and professional advice, this study would have never been completed. I also wish to express appreciation to my second reader, Dr. Carmen. G. Castro. Her advice was extremely helpful for this study. Thanks also to Dr. Steven. R. Ramp for his guidance, Mr. Tarry Rago for his CTD data collection and processing, Mr. Mike Cook for Matlab help. Other members of the Oceanography faculty I would like to thank for their encouragement were Dr. Mary. L. Batteen, Dr. Peter. C. Chu, Dr. Ching-Sang. Chiu, Dr. Jeffery Paduan. Mr. Mark Orzech, Ms. Arlene Guest, and Ms. Marla Stone.

Cruises were sponsored by the Oceanographer of the Navy, the Naval Oceanographic Office, the David and Lucile Packard Foundation, and the Monterey Bay National Marine Sanctuary. Additional funding support for data collection was provided by the National Science Foundation (OCE9811035). We thank Mr. Ron Lynn for providing data for Line 67 from the October 1997 cruise of **NOAA Ship David Starr Jordon** and LCDR Chris Moore, NOAA, for providing shore station and wind stress data. Dr. Tim Pennington of Monterey Bay Aquarium Research Institute (MBARI) organized many of these cruises and provided logistical support for others. Mr. Drew Gashler of MBARI and Mr. Rich Muller of Moss Landing Marine Laboratories were responsible for providing high quality CTD support for most of the cruises, and Ms. Reiko Michisaki. of MBARI aided in data processing. Support of the officers and crews of the **R/V Point Sur**, **R/V New Horizon** and the **NOAA Ship McArthur** is gratefully acknowledged.

This thesis was presented at the Fall Meeting of the American Geophysical Union in December 1998 and at the Monterey bay National Marine Sanctuary Science Symposium on March 20, 1999.

I. INTRODUCTION

While the oceanic effects of El Niño are greatest in the tropical Pacific (Rasmusson and Wallace, 1983), it also produces significant modifications to oceanic conditions off Central California (Simpson, 1984; Lenartz et al.,1995; Chavez, 1996; Ramp et al., 1997; McGowan et al., 1998). The primary physical effects are associated with warming of local waters which can be caused by either poleward advection of equatorial waters, onshore advection of offshore waters, or a decrease in the coastal upwelling of cool, nutrient rich subsurface waters. Secondary physical effects are increased coastal sea levels (which lead to shoreline erosion during winter storms) and changes in the salinity of coastal waters. These warm events in the California Current result in episodic lowerings of the nutricline, decreasing primary production (Chavez, 1996) and affecting population and community dynamics; zooplankton and kelp forest declining (McGowan et al., 1998), displacement or reduction in fish and marine populations and increasing mortality amongst marine mammals.

Although long-range forecast models failed to predict the 1997-1998 El Niño, the large areal extent and warming of waters in the Eastern Tropical Pacific were easily detected by satellite and in-situ measurements in 1997. Since these equatorial effects are known to subsequently propagate to higher latitudes along eastern boundaries, it was possible to organize a program of in-situ ocean observations off Central California. This thesis examines the results of thirteen cruises which took place from February 1997

through January 1999. These cruises were designed to augment long-term monitoring systems and to determine the effect of the 1997-1998 El Niño on the California Current system off Central California.

A. CALIFORNIA CURRENT SYSTEM (CCS)

The California Current System is a complex system of equatorward and poleward flows located off the West Coast of North America from Washington to Baja California. For simplicity, it is usually described as consisting of three currents, the equatorward flowing California Current (CC), and the poleward flowing California Inshore Current (CIC) (sometimes referred to as the Davidson Current) and California Undercurrent (CUC). The CC is a surface current (0-300 m) that constitutes the eastern limb of the North Pacific Subtropical gyre, connecting the westward North Pacific Drift with the North Equatorial Current. As such, it transports Subarctic waters equatorward throughout the year so that near-surface waters are lower in temperature and salinity and higher in dissolved oxygen than oceanic waters to the east (Lynn and Simpson 1987). The average speed of the CC off the coast of California is typically less than 25 cm/s (Reid and Schwartzlose, 1962) although daily average surface speeds may be as high as 50 cm/s (Davis, 1985). Maximum CC velocities are found at or near the surface (Lynn and Simpson, 1987).

Near the California coast there is a reversal of the equatorward flow. This poleward flow is called the Inshore Countercurrent (IC) or the Davidson Current. The poleward flowing IC transports waters derived from Equatorial Pacific sources which are

warmer and saltier than Subarctic waters. The IC is most noticeable in fall and winter when it is associated with an offshore dynamic trough (Lynn and Simpson, 1987). Current speeds are similar to those found in the CC (Collins et al., 1999).

The CU appears as a subsurface maximum of flow between 100 and 250 m over the continental slope and also transports warm, saline equatorial waters poleward (Lynn and Simpson, 1987). Off Point Sur (36°20'N), California, in water 800 m deep, the average speed (direction) was 7.6 cm/s (326°T) at 350 m (Collins et al., 1996). Alongshore geostrophic velocity shows that the position of the undercurrent core varies from 12 to 42 km from shore while its strength varied from less than 5 cm/s to 35 cm/s, with the maximum flow occurring in winter off Point Sur (Tisch et al., 1992). Collins et al. (1999) examined a series of bimonthly sections off Point Sur during 1988-1991 and showed that the region of mean poleward flow extended to a distance of about 100 km from the coast.

Coastal upwelling results in significant modification of surface waters in the California Current System. Persistent strong northwesterly winds over the CCS in spring and summer results in an acceleration of the CC and geostrophic adjustment result in a shoaling of the pycnocline near the coast. At the coast, the northwesterly winds combine with the earth's rotation to effect an offshore transport of the surface waters (Reid et al., 1952) resulting in upwelling. Although coastal upwelling can occur at any time of the year, it is most effective biologically during the spring and summer when the pycnocline is shallow and nutrient rich pycnocline waters are more easily brought to the surface. These upwelled waters are also colder and saltier than surface waters; they are transported

offshore into the California Current, mostly at headlands, and are easily visible on AVHRR images of the sea surface.

B. THE EFFECT OF EL NIÑO ON THE CCS

Figure 1 shows a time series for 1950-1999 El Niño events based upon a tropical index. El Niños occurred every five- to seven years with varying intensity, but seem to be increasing in both frequency and intensity. Time series studies of sea level (McLain and Thomas, 1983) and temperature (Cole and McLain, 1989) along the Pacific coast show that elevated sea levels and warming occur along California during tropical El Niño events.

The major El Niños that have been studied in California waters were in 1957-8 (Reid, 1960) and 1982-3 (Simpson, 1984); Ramp et al (1996) describe a smaller El Niño event in 1991-2. The 1957-8 event occurred 7 years after systematic surveys of the California and Alaska Current had begun and during the first cooperative international study of the ocean, the International Geophysical Year (IGY). In early 1957, elevated surface temperature and salinity conditions anomalies appeared. The temperature and salinity anomalies accounted for a steric rise of sea level of about five centimeters averaged roughly over the California Current System. The sea level rise at the coast was about twice the steric rise. It was noted that these features were consistent with three possible causes: reduced coastal upwelling, reduced lateral flow due to wind stress, and geostrophic readjustment by moving new surface water from the west and south into the region.

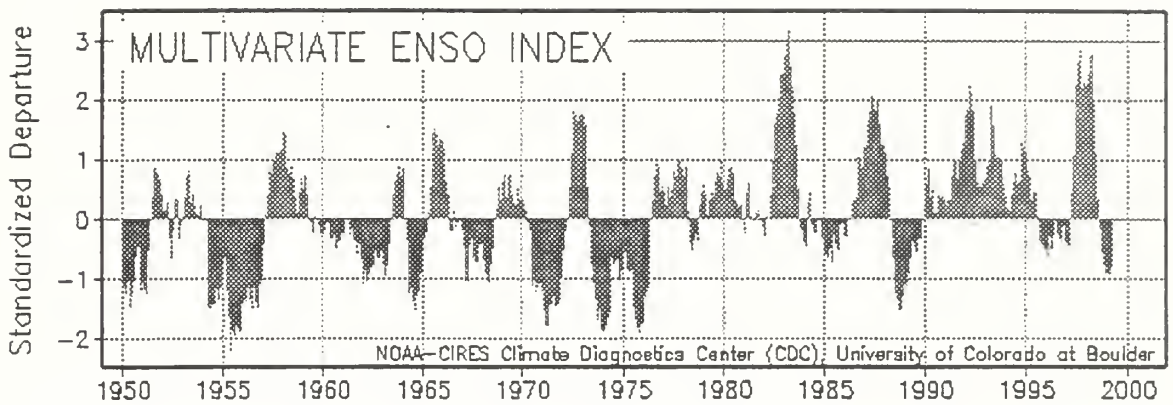

Figure 1. Multivariate ENSO Index. The multivariable ENSO Index is derived from observed conditions over the tropical Pacific. It includes the following six variables: sea-level pressure, the east-west and north-south components of the surface wind, SST, surface air temperature, and total amount of cloudiness (Wolter et al., 1998).

Simpson (1984) studied the effect of the 1982-3 El Niño on the CCS and concluded that the expansion and intensification of the Aleutian low and the decrease in strength of the Pacific high produced the 1982-3 Californian El Niño. This resulted in anomalous onshore transport which produced downwelling at the coast and also caused higher sea level. The onshore transport and following downwelling caused warmer temperatures and fresher salinities. The transport of the IC increased during late summer and fall. Simpson (1984) noted that theoretical studies suggested that this anomalous poleward geostrophic flow was induced by a poleward propagating Kelvin waves. Simpson (1984) also noted that transports of the CC increased during late spring and early summer.

The 1991-2 El Niño off Central California was associated with an anomalously strong Aleutian low which formed in the Gulf of Alaska in late 1991, broadening and strengthening with time. By February 1992 this low-pressure system engulfed the entire U.S. West Coast, causing poleward, downwelling favorable wind stress, onshore transport, and a depressed main thermocline. As with the 1983-4 event, poleward propagating coastal-trapped Kelvin waves also raised the coastal sea level and enforced the CU although the mass transport associated with these waves was not clear. The local upwelling favorable winds, if present at all, could no longer reach the cold, nutrient rich lower layer. During August 1991 and particularly February 1992 the thermocline was strongly depressed, causing warm, fresh T-S anomalies accompanied by a larger fraction of CU water in the region.

To summarize, these previous studies show two possible causes of Californian El Niño events. One is associated with poleward, downwelling favorable wind stress, especially during winter. The second is poleward propagating coastal trapped Kelvin waves which would raise the coastal sea level, increase poleward transport of inshore waters, and deepen the pycnocline (resulting in upwelling of warmer waters).

C. ORGANIZATION OF THESIS

The goal of this thesis is to document effects of the 1997-8 El Niño off Central California. Background information on the California Current System and El Niño are discussed above. Chapter II discusses cruise design, sampling procedures, and data processing. Results are shown for coastal time series and as section means and standard deviations, time series of properties on isobaric and isopycnal surfaces, and principal component analysis in Chapter III Chapter IV summarizes results and presents conclusions. Appendices include hydrographic sections for each cruise, vector plots of current measurements, and complete results of principal component analysis.

II. DATA AND METHODS

Hydrographic data collected during thirteen research cruises in 1997-8 are the principal basis for this thesis. Data from local shore stations (Granite Canyon and Southeast Farallon Island), the sea level gauge at Monterey, and wind stress computed by Pacific Fisheries Environmental Laboratory will also be used.

A. CRUISE DESIGN

Hydrographic data collection protocols for the California Current System were established in 1950 by the California Cooperative Fisheries Investigations (CalCOFI). Stations are typically located at 74 km intervals along lines which were directed from 060° toward 240°T, i.e. perpendicular to the trend of the California coastline. Near shore the station spacing was half or less (Lynn and Simpson,1987). These lines were in turn 74 km apart and extended from the Southern Baja California (Line 140) to Point Reyes (line 60). Where water depth permitted, data was collected to a depth of 500 m.

The CalCOFI line which extended through Monterey Bay was line 67. The position of stations that was occupied along this line is listed in Table 1 and shown in Figure 2. The first station was located at the head of Monterey Submarine Canyon where the water depth was 240 m.

CalCOFI Line 67 Stations

Latitude(N),	Longitude(W),	Distance from shore (km),	Water Depth(m),	Station name
36.7967,	121.847,	5.4,	240,	C1
36.7350,	122.020,	22.2,	1144,	H3
36.6783,	122.200,	39.4,	1170,	NPS1
36.6200,	122.415,	59.6,	2745,	67-55
36.5367,	122.595,	78.0,	3175,	NPS2
36.4533,	122.773,	96.3,	2862,	67-60
36.3700,	122.952,	114.7,	2700,	NPS3
36.2867,	123.130,	129.1,	3267,	67-65
36.2033,	123.308,	151.5,	3472,	NPS4
36.1200,	123.485,	169.8,	3583,	67-70
36.0367,	123.663,	188.2,	3756,	NPS5
35.9533	123.842,	206.8,	3892,	67-75
35.8700,	124.018,	225.1,	3916,	NPS6
35.7867,	124.195,	243.5,	3990,	67-80
35.7033,	124.372,	262.0,	4081,	NPS7
35.6200,	124.550,	280.5,	4215,	67-85
35.5367,	124.727,	298.9,	4350,	NPS8
35.4533,	124.903,	317.3,	4409,	67-90

Table 1. Hydrographic Stations.

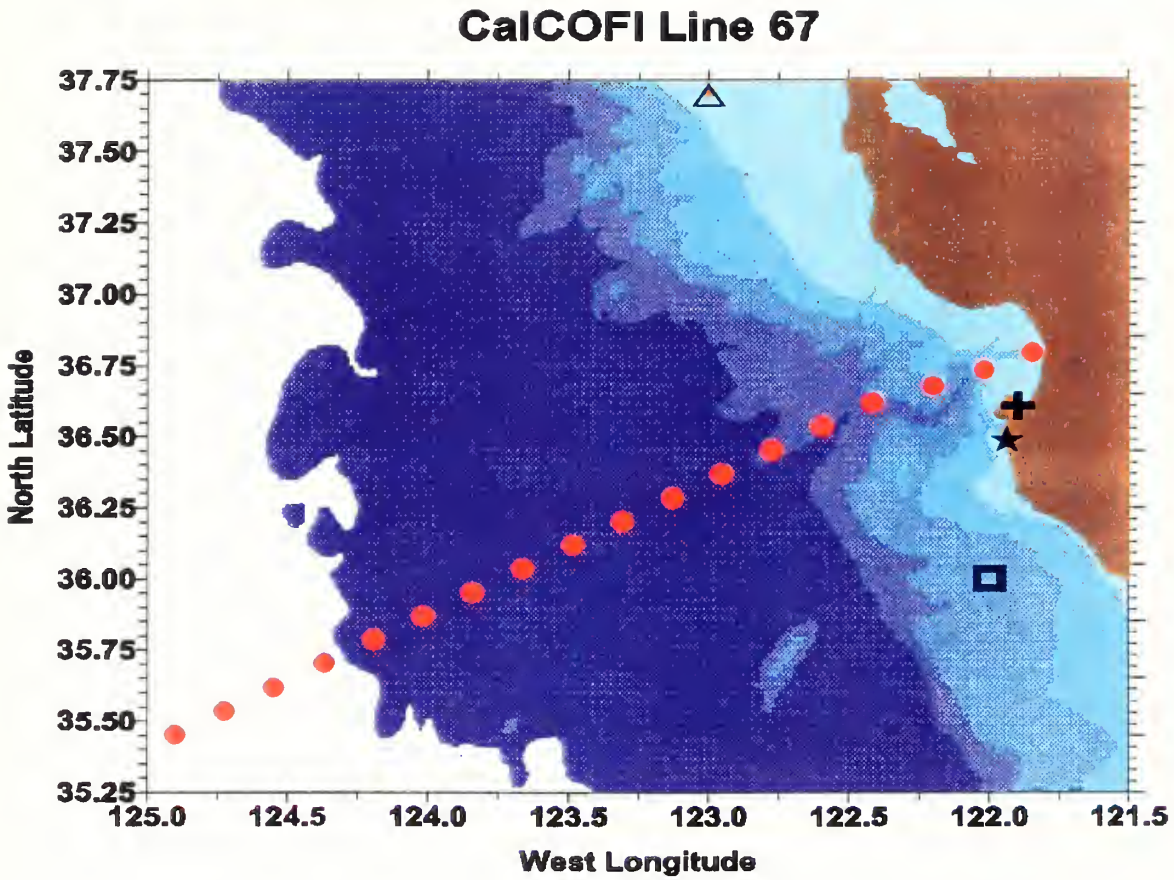

Figure 2. Measurement Locations. Circles are locations of hydrographic stations along CalCOFI Line 67. The star and triangle represent shore stations at Granite Canyon and Southeast Farallon Island, respectively. The location of the Monterey tide gauge is shown by '+' and the position for which Ekman transports were estimated by a square (36°N, 122°W). Land is colored brown and the shades of blue represent the 200 m, 1000 m, 2000 m, 3000 m, and 4000 m isobaths.

The second station, H-3, corresponded to a CalCOFI station in Monterey Bay that was sampled by Hopkins Marine Station; here the water depth is 1140 m. Since the Rossby internal radius of deformation for these waters is 15-20 km, intermediate stations were located between CalCOFI stations. This provided 18 km (10 n. mile) spacing so that mesoscale flow features could be resolved. The station farthest from shore (CalCOFI station 67-90) was 315 km from the first station and was about 20 km to the west of the mean position of the axis of the California Current. Where water depth permitted, samples were collected to 1000 dbars except that the full water column (4.4 km) was sampled at station 67-90. The elapsed time between the first and last stations was 2.5 days.

Dates of cruises and vessels used are given in Table 2. Cruises were sponsored by the Oceanographer of the Navy, the Naval Oceanographic Office, Monterey Bay Aquarium Research Institute, and the Monterey Bay National Marine Sanctuary. Additional support for data collection was provided by the National Science Foundation.

B. HYDROGRAPHIC DATA

Conductivity, temperature and pressure were measured using SeaBird 911 Plus™ CTDs. Salinity was computed using the 1978 Practical Salinity Scale. Measurement accuracy (resolution) was 0.001°C (0.0002°C), 0.0003 S/m (0.00004 S/m), and 0.9 dbars (0.06 dbars). Salinity accuracy was maintained by comparison of CTD derived values with laboratory measurements of water samples collected during CTD casts by Niskin bottles. CTD data were processed using software provided by SeaBird™ and data were averaged

Cruise	Cruise Dates	Research Vessel	Data
	1997		
1	February 23-4	R/V Point Sur	CTD,ADCP[1]
2	March 6-7	R/V Western Flyer	CTD
3	June 2-5	R/V Point Sur	CTD,ADCP[1]
4	July 26-28	R/V Point Sur	CTD,ADCP[1]
5	September 12-14	R/V New Horizon	CTD,ADCP[1]
	1998		
6	January 21-24	R/V Point Sur	CTD,ADCP[1]
7	March 21-23	R/V New Horizon	CTD,ADCP[1]
8	April 14-17	NOAA Ship McArthur	CTD,ADCP
9	May 9-12	R/V New Horizon	CTD,ADCP
10	July 2-4	R/V Point Sur	CTD,ADCP[1]
11	August 22-25	R/V New Horizon	CTD,ADCP
12	November 6-9	R/V New Horizon	CTD,ADCP
	1999		
13	January 14-16	R/V Point Sur	CTD,ADCP[1]

Table 2. Cruise Schedule

[1] Gyro offset monitored using an Ashtech GPS-based instrument.

into 2-dbar bins. Derived quantities (density anomaly, specific volume anomaly, geopotential anomaly) were computed using the 1980 Equation of State (Fofonoff, 1985).

Figure 3 shows both the temporal and spatial location of stations that were actually occupied along line 67 during the 1997-8. Not all stations were occupied on each cruise due to weather and time constraints. In order to have a uniform grid of data, sections were objectively analyzed to produce samples every 18 km horizontally and 10 dbar vertically. For the objective analysis, Distance from shore, x, was used as the horizontal dimension with a Gaussian correlation function e^{-d^2/d_c^2}, where $d^2 = \left[(\Delta x)^2 / L^2 + z^2\right]$, and z was pressure in dbar. After a number of trials using different parameters values for d_c and L to represent the large scale field, a value of 1 was chosen for the decay scale, d_c, and a value of $10^{½}$ km for L.

Except for the ***R/V Western Flyer*** cruise, ocean current observations were collected continuously on each cruise using vessel mounted RD Instruments Acoustic Doppler Current Profilers (ADCP). 150 kHz narrowband instruments were used on the ***R/V Point Sur*** and ***R/V New Horizon*** and a 150 kHz broadband instrument was used on the *NOAA Ship McArthur*. Data were processed using CODAS3 software provided by the University of Hawaii and averaged by 0.1° longitude bins. For cruises where attitude measurements were available (Table 2), ADCP data were accurate to 1 cm/s; on other cruises, the accuracy was 2 cm/s.

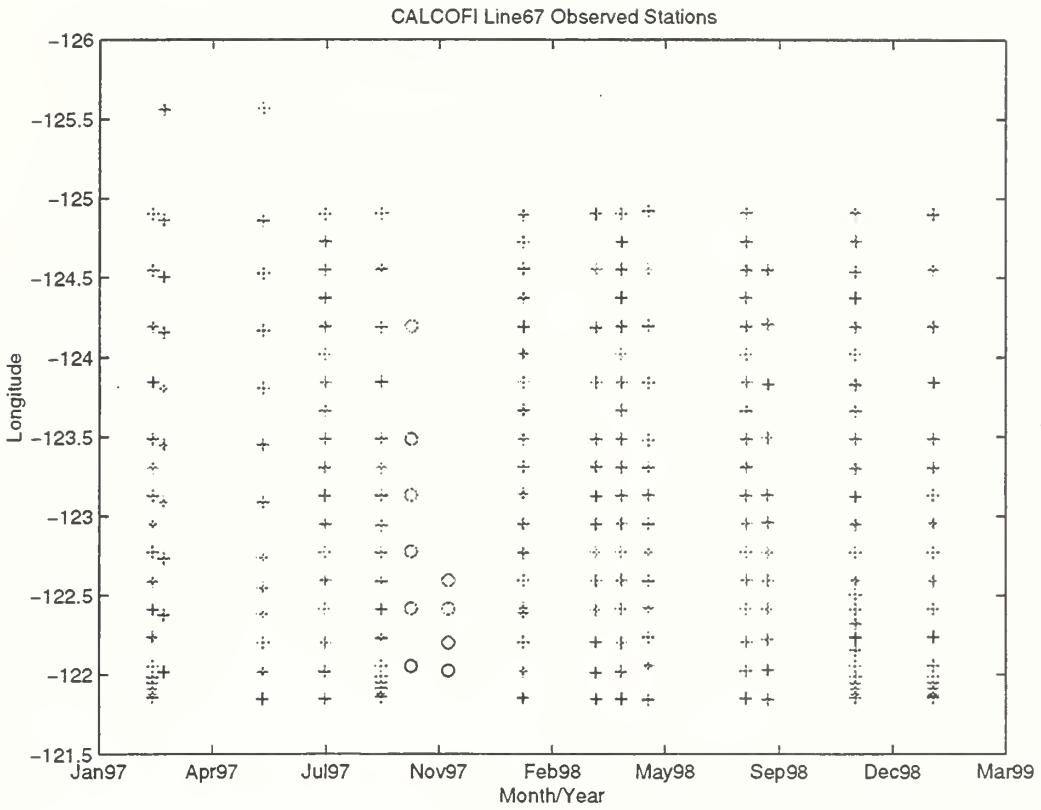

Figure 3. Temporal and Spatial Location of Stations. ('o' are not used in Chapter 3.)

In addition to the collection of hydrographic data, a program of biological and chemical sampling was carried out by the Monterey Bay Aquarium Research Institute. These data are not considered here.

c. LONG TIME SERIES DATA

For coastal waters, Eulerian and Lagrangian time scales are 18 and 5 days, respectively (Collins et al., 1996, Garfield et al., 1999). This means that each of the thirteen sections can be considered both synoptic and independent. It also means that the ~2 month sampling interval does not provide good temporal resolution for the evolution of the synoptic scale fields. Also, the hydrographic section along line 67 was not frequently sampled by the CalCOFI program, so we do not have an estimate of either long term means or seasonal variability. To overcome both of these problems---temporal resolution and long term sampling---it was necessary to use other data.

Three long-term data sets were used: shore station data, sea level observations, and geostrophic wind estimates. The shore station data consisted of daily observations of sea surface temperature and salinity at SW Farallon Island and Granite Canyon. Data collection and processing procedures are described in UCSD (1994). For SW Farallon Island, the data span the period 1925 to present but there were no observations collected during the period from March 1943 to December 1956. At Granite Canyon, observations began in 1971.

Sea level observations were made by the National Ocean Service by means of a tide gauge at Monterey. Monthly means were available from 1974. The datum used for the sea level observations was mean lower low water.

Six-hourly estimates of geostrophically-derived Ekman transports for the period 1967 to present were calculated by the Pacific Environmental Fisheries Laboratory for 36°N, 122°W. This data is used to derive an upwelling index that is widely used (Schwing, et.al., 1996). The geostrophic winds agree well with buoy and ship measurements of wind (Moore, personal communication).

III. RESULTS

Results of long time series measurements are described first. These provide a comparison with long term means as well as showing the temporal evolution of the 1997-8 El Niño event. Next, the 13 line 67 sections are analyzed: means and standard deviations are computed, time series of properties at given levels are derived, and principal component analysis is used to show annual and El Niño variability.

A. LONG TERM TIME SERIES

Long time series show that local anomalies peak during the winter of 1997-8. The sea surface temperatures at Granite Canyon (Figure 4) and SE Farallon Island (Figure 5) increase in two steps in June and September,1997. At Granite Canyon the temperature continues to increase until late November 1997 and temperatures approach one standard deviation greater than the mean in February. At SE Farallon, temperatures decrease after the September maximum but remain well above normal until February. At Granite Canyon, upwelling began about a month sooner than normal in 1997, with maximum salinities occurring in February. From March through January, 1998, salinities are close to average. During winter, the fresh-water tidal prism from San Francisco Bay occasionally sweeps across SE Farallon Island. Two of these events occurred in January 1997, the first resulting in salinities lower than 29. As at Granite Canyon, salinities are close to the annual average from March through January 1998. In winter and spring of 1998, salinities remained low at SE Farallon Island.

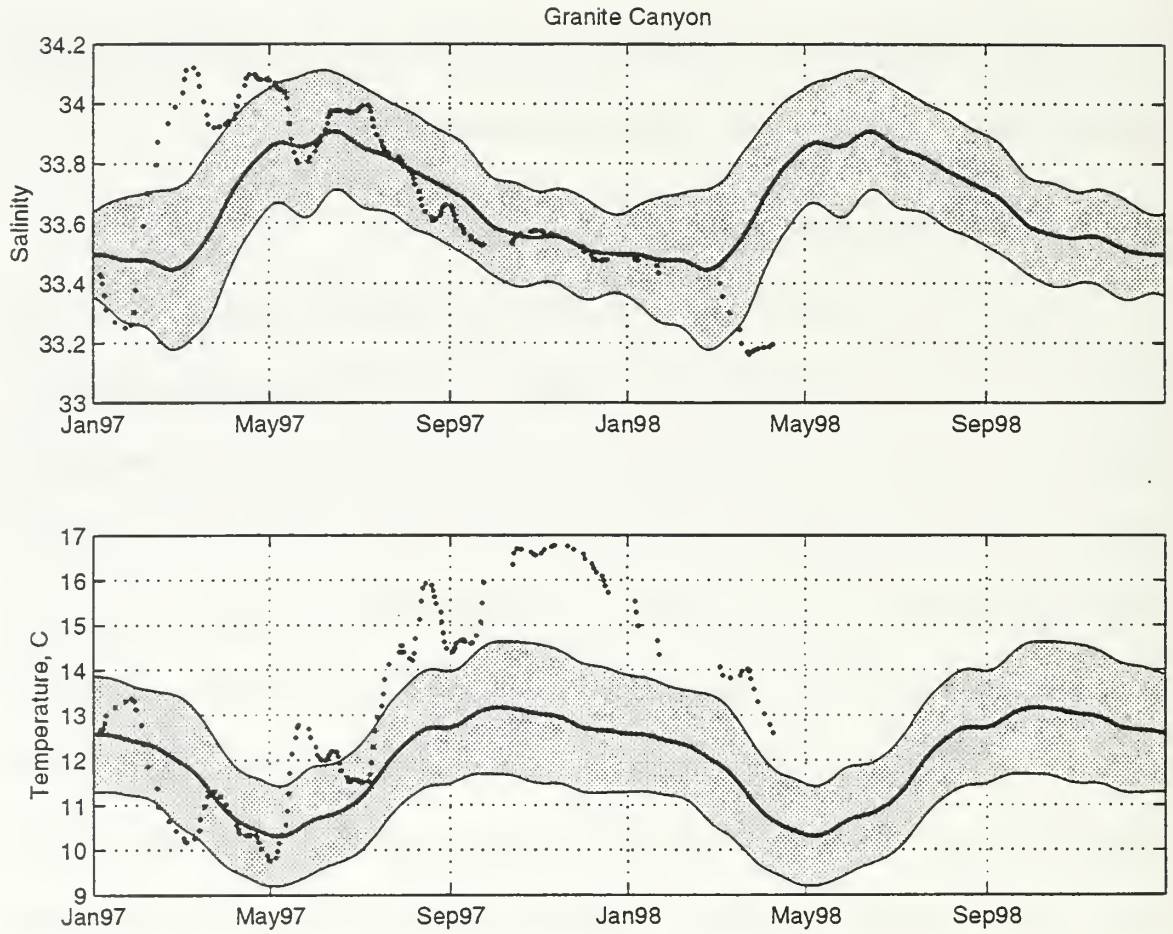

Figure 4. Time series of salinity (Upper) and temperature (Lower) at Granite Canyon. Mean value is shown by solid line, 1997-8 data are shown by doted line, and shadowed zone indicates the area within one standard deviation. Data for summer and fall 1998 are not yet available.

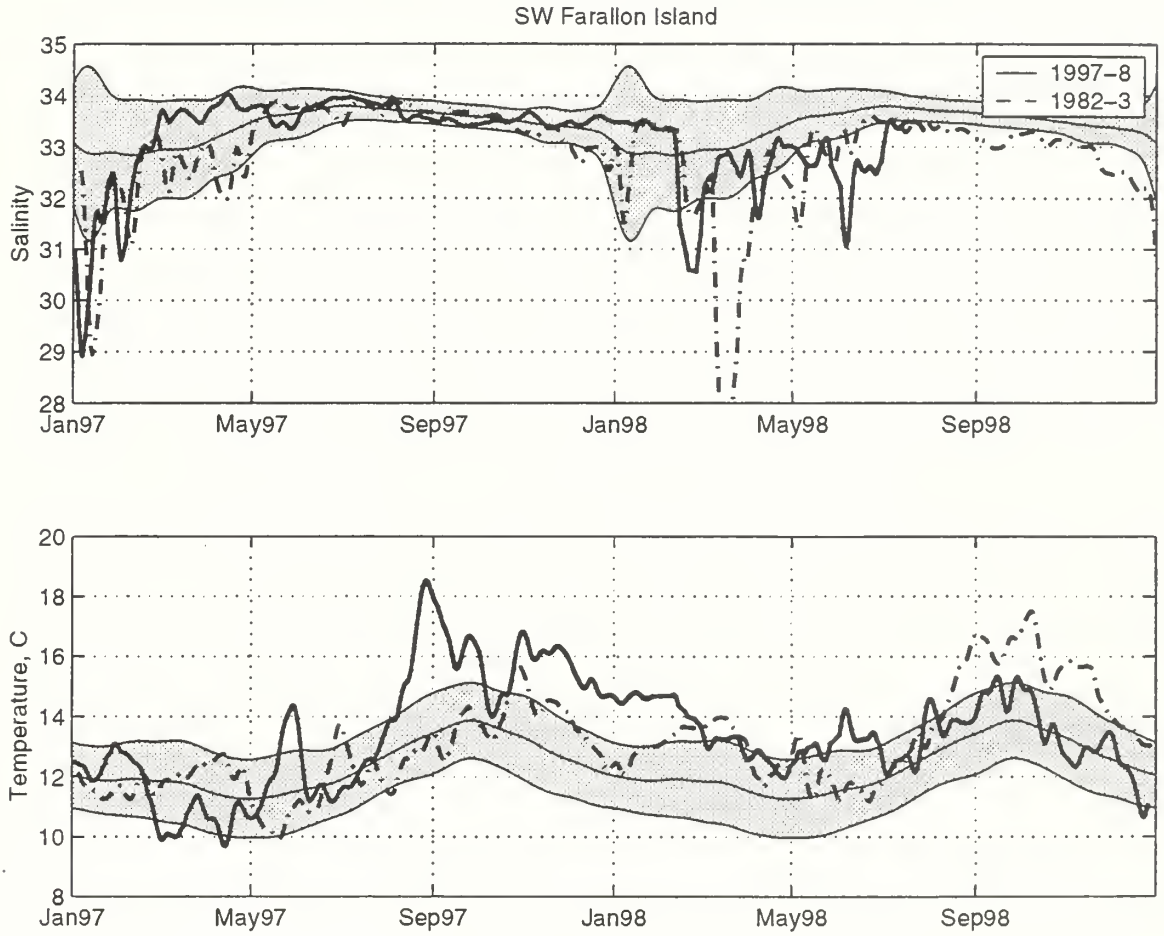

Figure 5. Time series of salinity (Upper) and temperature (Lower) at SW Farallon Island. Mean value is shown by solid line, 1997-8 data are shown by doted line, and shadowed zone indicates the area within one standard deviation. Data for summer and fall 1998 are not yet available.

Sea level and barometric pressure time series are shown in Figure 6. From November 1997 through January 1998, sea levels were higher than normal. The 1982-83 sea level showed peaks in January and October 1982.

Ekman transports (Figure 7) show the early onset of upwelling in February 1997, but appear close to normal through November, 1997. During November 1997 and January 1998 large onshore transports occurred, the latter exceeding 200 tonnes/s. The former event was associated with poleward transports and the latter with equatorward transports. The 1982-3 transports also appeared normal except winter storms which occurred slightly later and were less than those observed in 1997-8.

B. MEAN PLOTS AND STANDARD DEVIATION

Mean sections (Figures 8-10) resemble those derived from CalCOFI data (Lynn et al., 1982, Lynn and Simpson, 1987, Collins et al., 1999). Isopycnals, isotherms and isohalines shoal toward shore in the upper 150 dbar so that offshore, near surface waters were lighter, warmer, and fresher than they were near the coast. This feature is associated with both the southward flow of the California Current, and nearshore, coastal upwelling. At pressures of 150 dbar to 800 dbar, the slope of the isopycnals changed at a distance of about 110 km, deepening both to the onshore and offshore of this location. The inshore region, where the isopycnals deepen toward shore, was associated with warmer and saltier waters on a given isobar, so that isotherms slope down toward shore in this region and isohalines shoal toward the coast. In the mean, there is no sharp front between the fresh

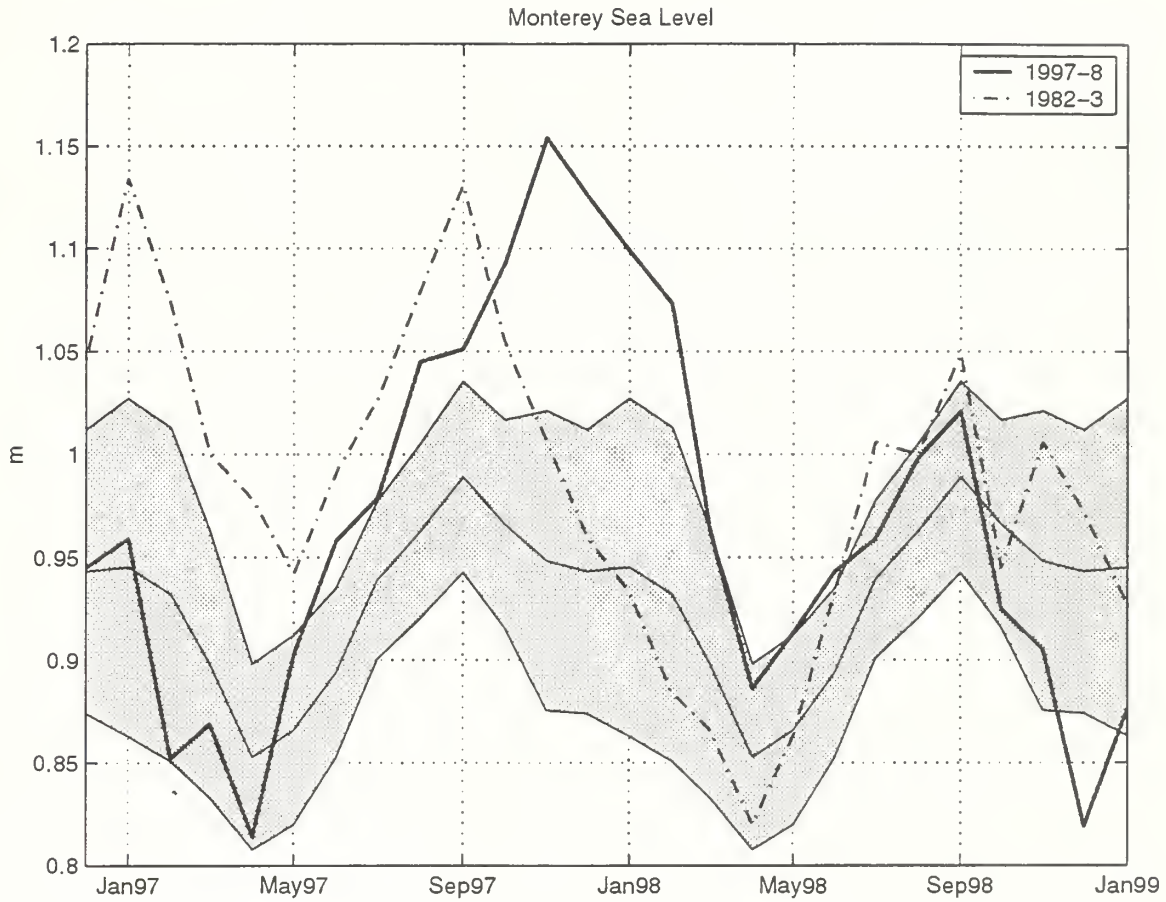

Figure 6. Monterey Sea Level. Mean value is shown by solid line, observation periods are shown by bold line (1997-98) and solid-dot line (1982-83), shadow zone indicates the area within one standard deviation.

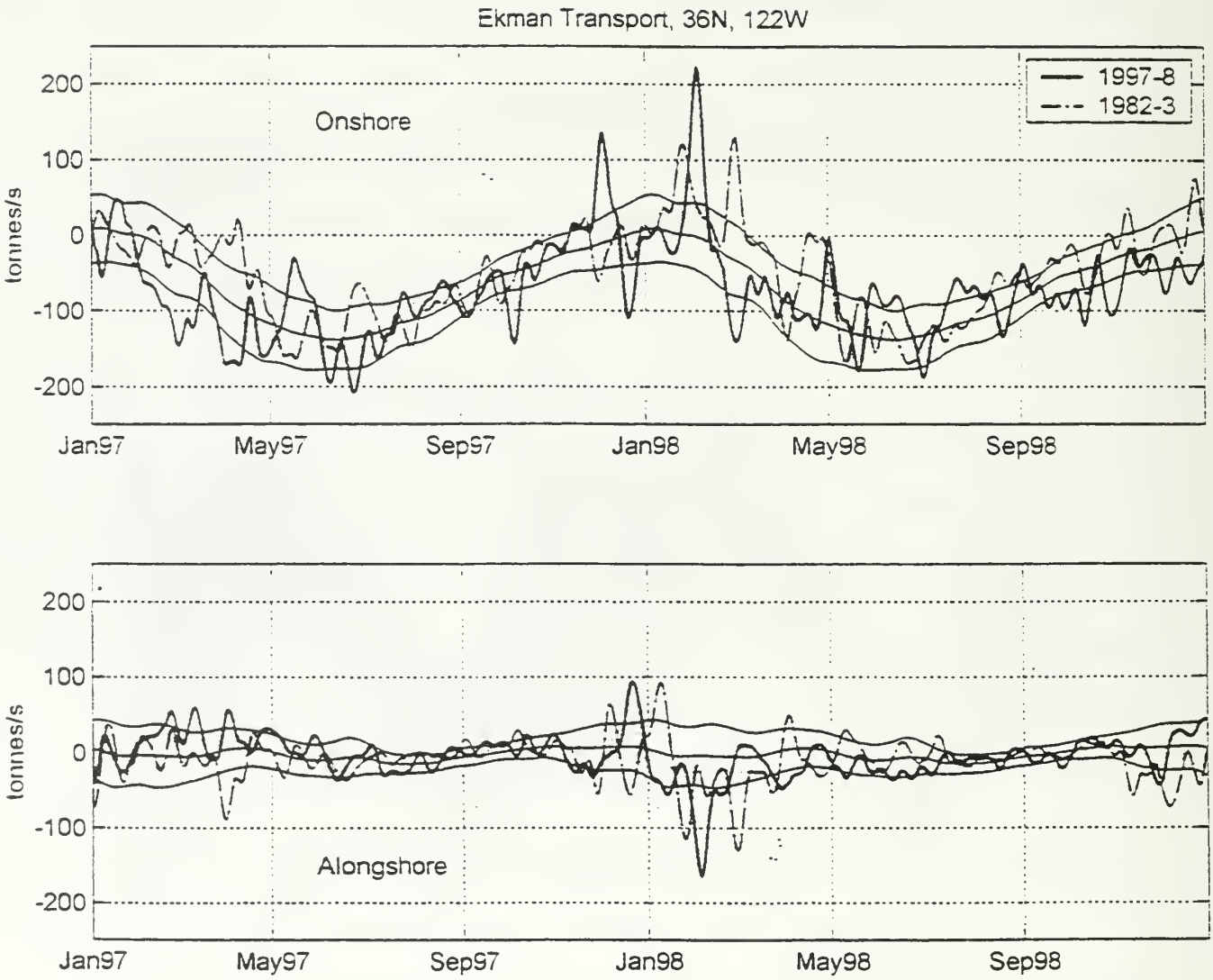

Figure 7. Ekman Transport

core of the California Current and inshore waters in the upper layer. In the region between 200 and 400 dbars, the character of the lower part of the halocline changed markedly at about the halfway point due to the existence of the fresher Pacific Intermediate water at densities of 26.6-26.7 kg/m^3 in offshore waters.

In general, standard deviations are largest at the surface and closer to shore. This is due to the effect of air sea interactions upon surface waters and to the coastal boundary which supports coastally trapped waves as well as requiring vertical displacements to balance changes in offshore Ekman transport. There are exceptions to this pattern of variability. For example, at 10 km the surface waters vary more than those waters farther from shore due to the existence of cooler surface waters at the entrance to Monterey Bay. The subsurface maximum of standard deviation along the strongest part of the thermocline (about 11°C) occurred below the bottom of the winter mixed layer. For salinity, it was expected that largest variability would be associated with meandering of the low salinity core of California Current waters which occurred near the offshore edge of the section; instead, largest variability occurred in the upper 20 dbar at a distance of 60 km, and above 100 dbar.

Mean velocity fields are shown in figures 11-13. The geostrophic velocities (Figure 11) were calculated using 1000 dbar as the reference level. Only the upper 200 dbar are shown to facilitate comparison with ADCP observations. The geostrophic velocities show two distinct cores of poleward flow which increase with depth at 90 km and 300 km from

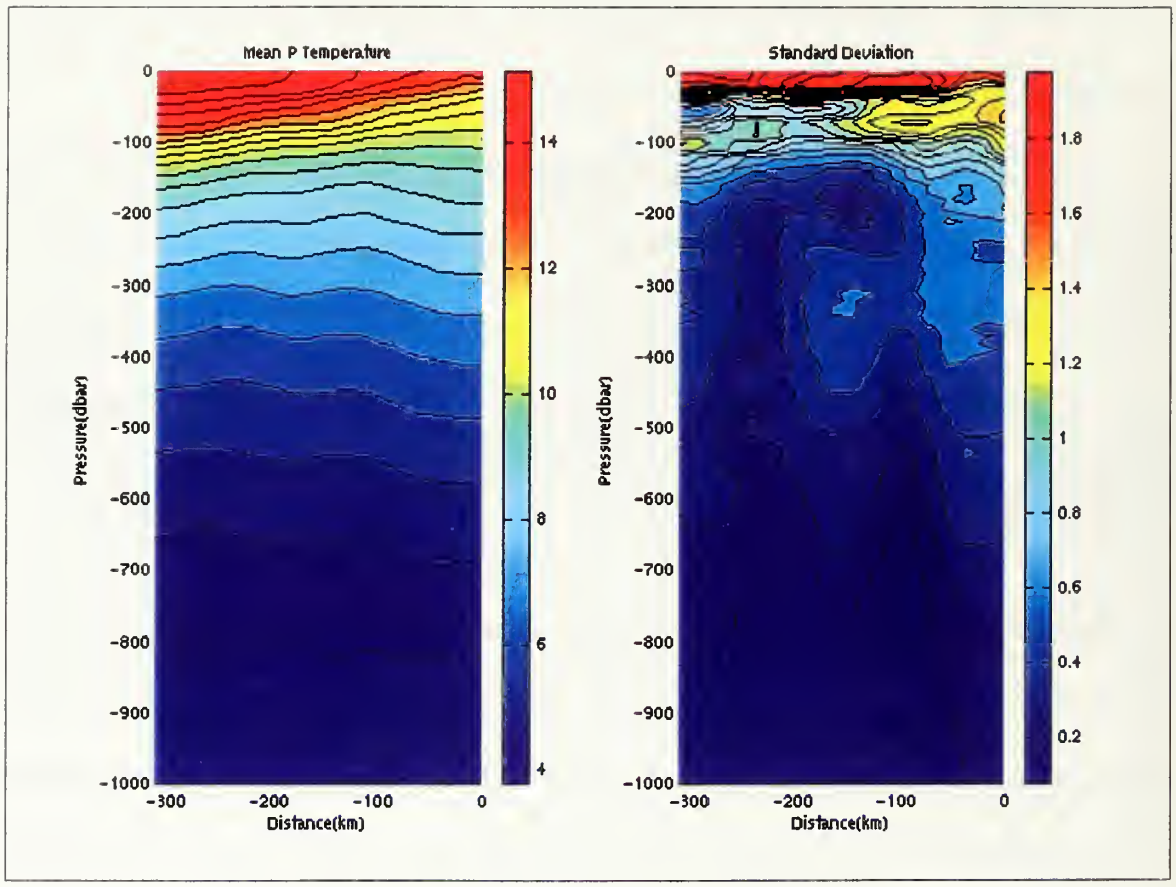

Figure 8. Mean (left) and Standard Deviation (right) of Potential Temperature, °C.

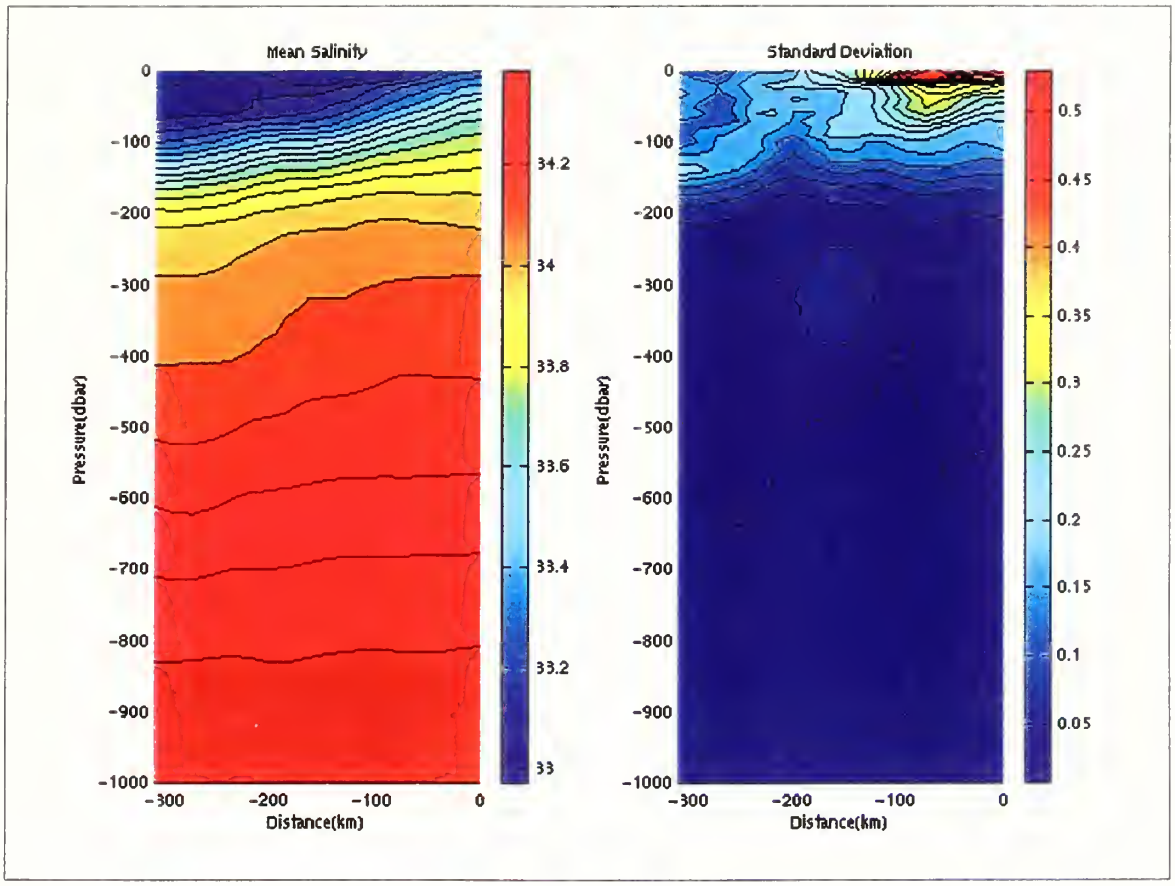

Figure 9. Mean (left) and Standard Deviation (right) of Salinity.

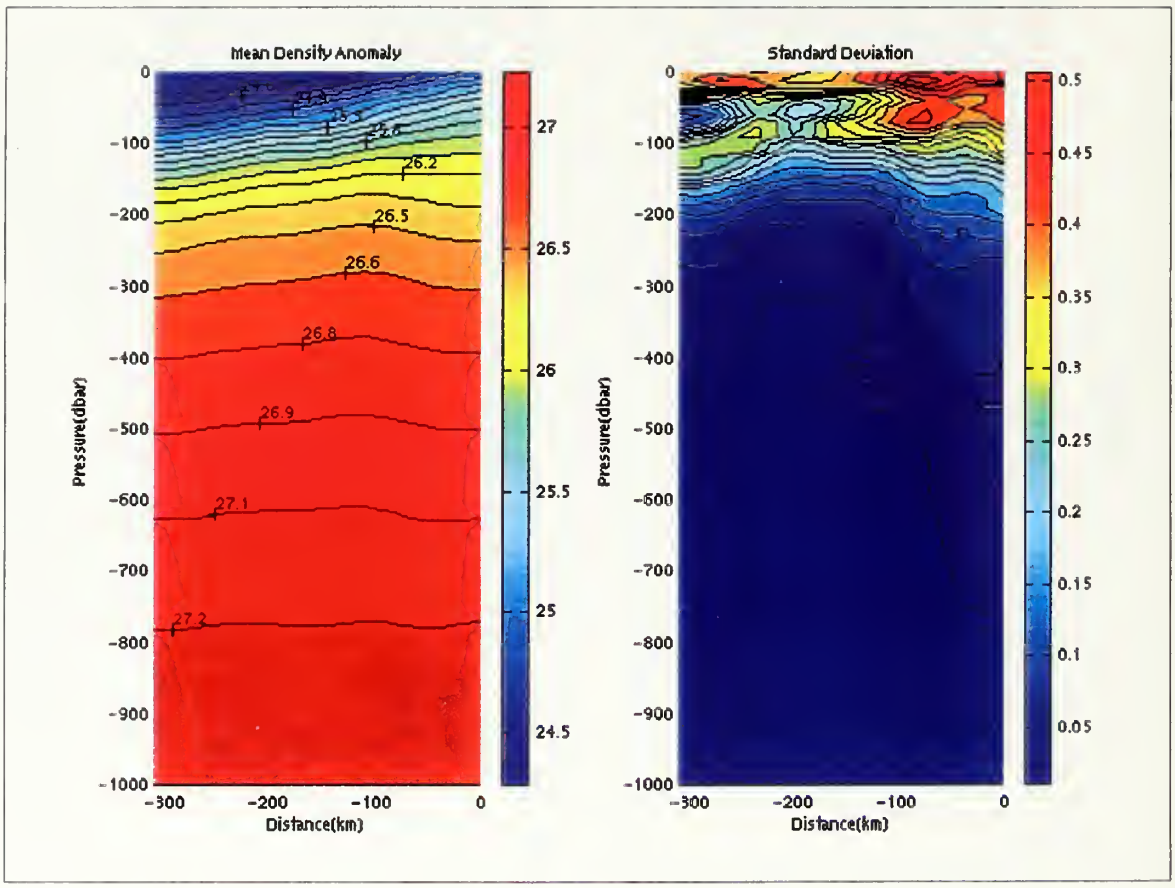

Figure 10. Mean (left) and Standard Deviation (right) of Density Anomaly, kg/m^3.

the coast; maximum poleward speeds were 2 and 1 cm/s respectively. Surface geostrophic flow was equatorward everywhere, with strongest velocities at the surface, exceeding -8 cm/s. Three cores of equatorward flow appeared, the weakest, -5 cm/s, at the entrance to Monterey Bay and the other two cores appeared at 150 km and 260 km from the coast with peak speeds of -9 cm/s. The ADCP alongshore velocities, Figure 12, had a similar pattern to the geostrophic velocities with alternating cores of poleward and equatorial flow in about the same locations and the same relative strengths. Peak velocities were higher for the ADCP, -11 cm/s for the equatorward flow and 7 cm/s for the region of strongest poleward flow which was centered at about 70 km from the coast. Differences between the ADCP and geostrophic velocities were greatest inshore: the ADCP showed a broader region of poleward flow at the coast than geostrophy and the region of equatorward flow immediately to the west was narrower.

Standard deviations for the alongshore velocity fields showed that the largest variability coincided with the location of the poleward flows. Variability decreased with depth (expected for geostrophic fields) and was also reduced within Monterey Bay. The minimum observed ADCP standard deviations were 4 cm/s.

The mean and standard deviation of the onshore flow derived from ADCP observations are shown in Figure 13. The pattern and scale of the onshore flow was similar to that of the alongshore flow. There were two broad areas of onshore flow, from the coast to 115 km and from 175 km to 290 km, which encompassed the cores of poleward flow. Regions of offshore flow corresponded to cores of equatorward flow. The

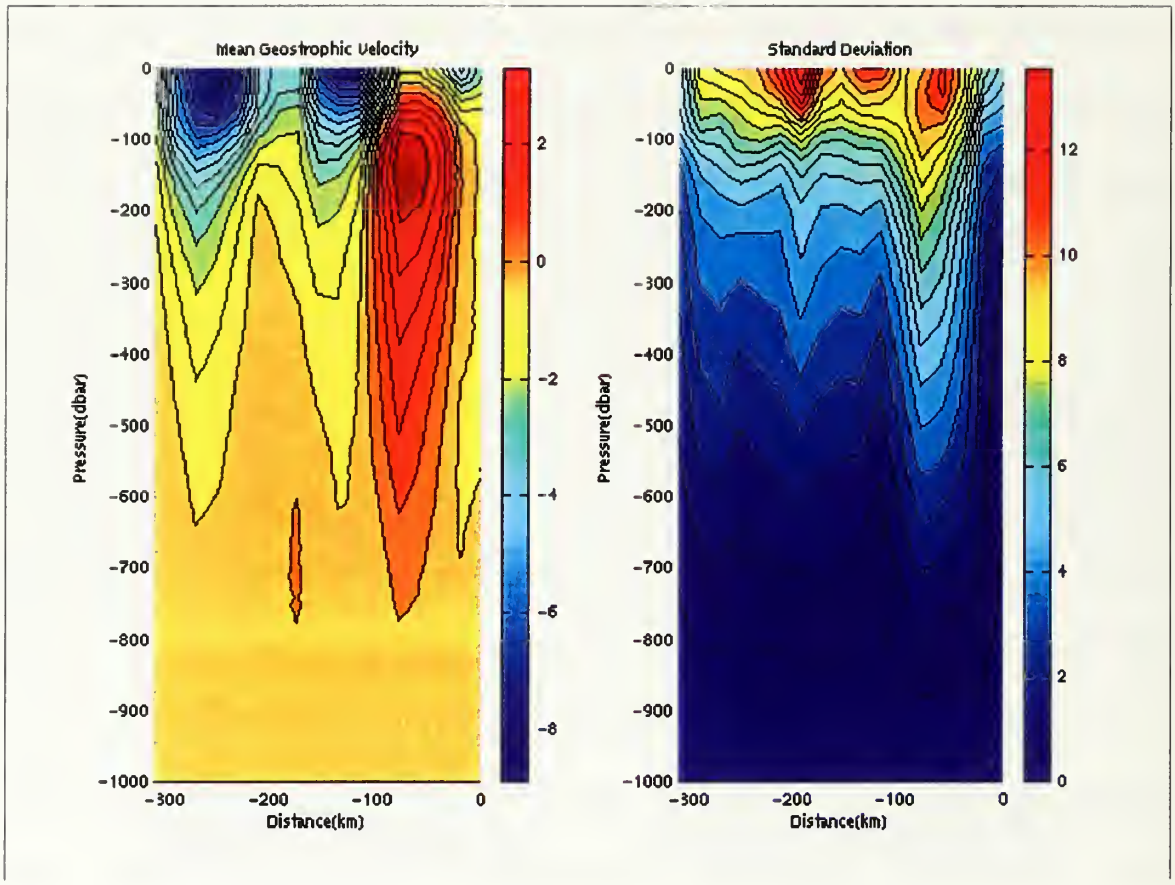

Figure 11. Mean (left) and Standard Deviation (right) of Geostrophic Velocity, cm/s.

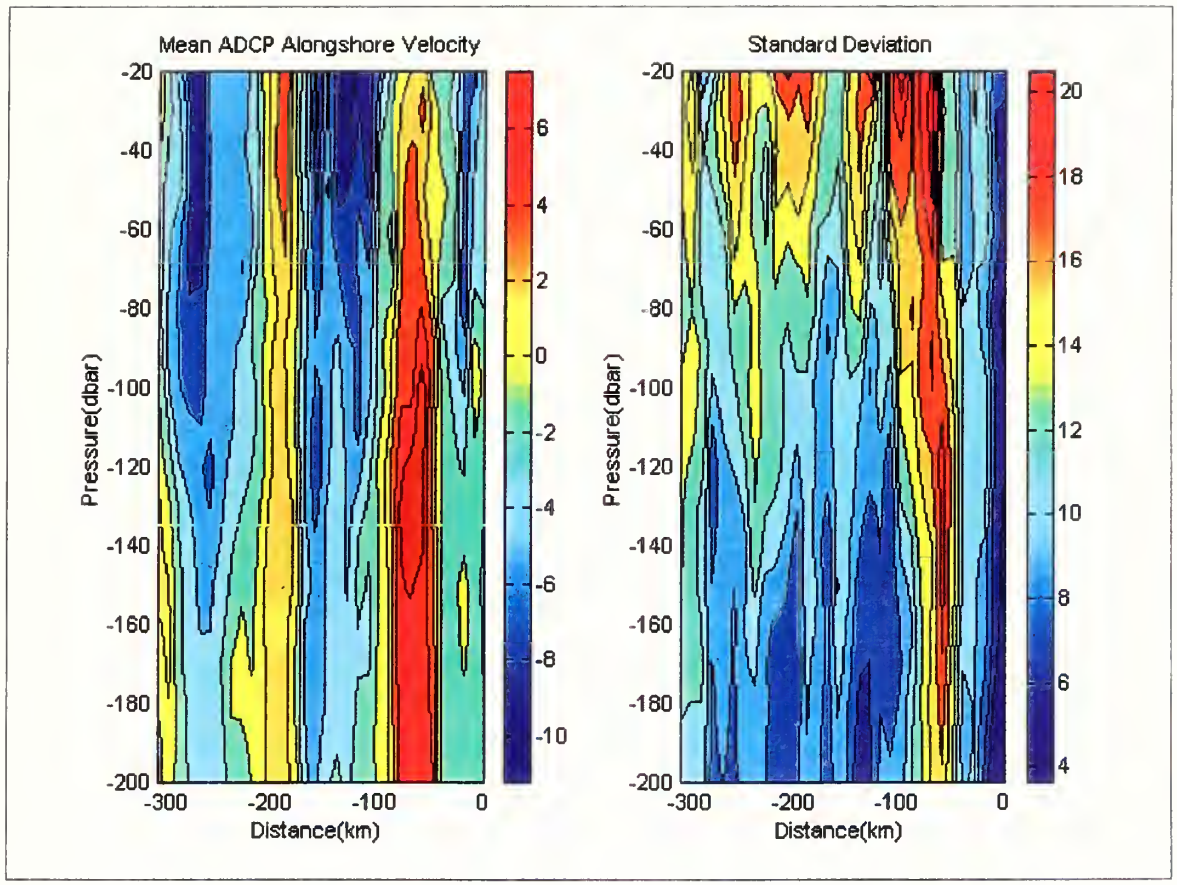

Figure 12. Mean (left) and Standard Deviation (right) of ADCP Alongshore Velocity, cm/s. Positive flow is directed toward 330°T.

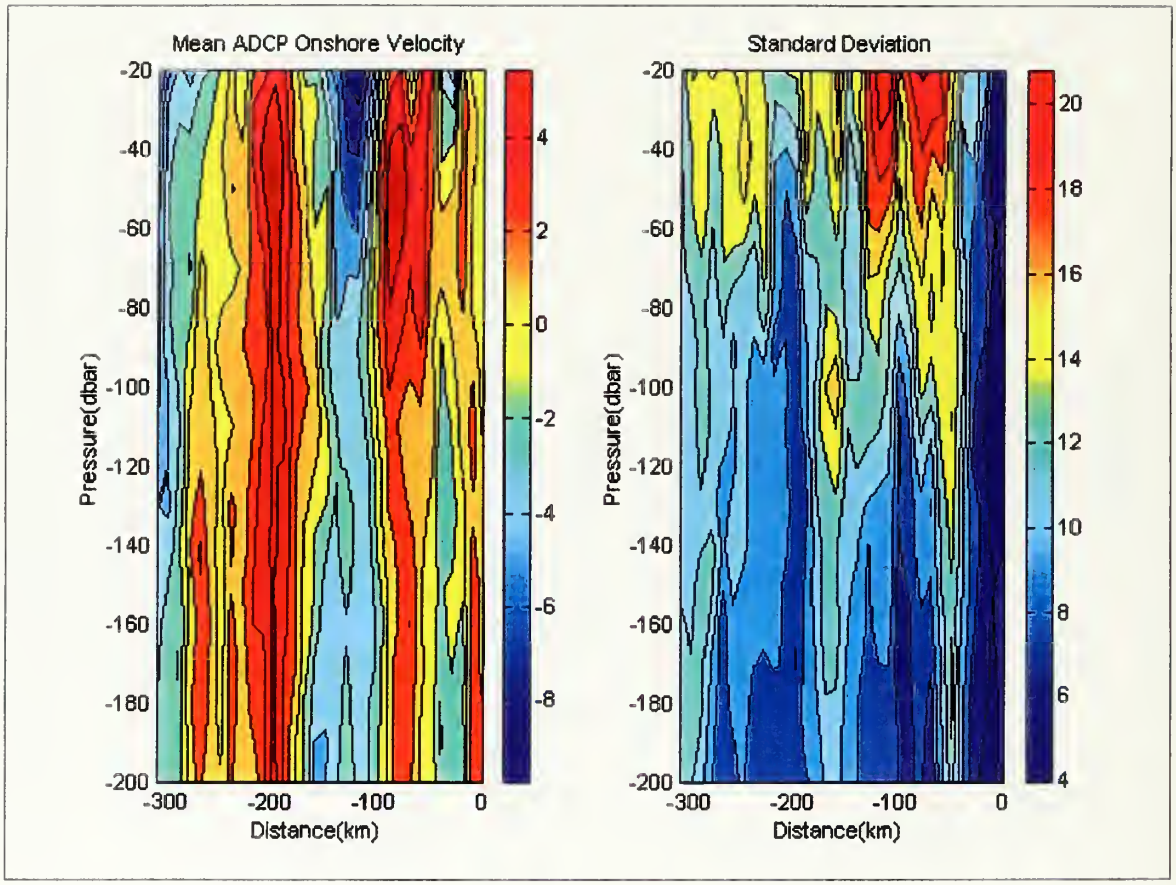

Figure 13. Mean (left) and Standard Deviation (right) of ADCP Onshore Velocity, cm/s. Positive flow is directed toward 060°T.

largest standard deviations, 20 cm/s, were observed above 40 m between 40 km and 135 km from the coast.

Since water mass changes are associated with El Niño conditions, the variability of salinity on density surfaces was examined. To assure 13 observations for each data point, it was necessary to eliminate isopycnals which were less than the maximum density observed at the surface, about 25.7 kg/m^3. As shown in Figure 9, the mean pressure of this isopycnal increases from 70 dbar at the coast to 140 dbar offshore. The mean value of salinity on isopycnals is shown in Figure 14. The rate of increase of salinity with density was remarkably uniform except for the region between 26.4 and 26.8 kg/m^3 where North Pacific Intermediate waters are found. At densities less than 27.2 kg/m^3, minimum salinities occurred about 260 km from shore, suggesting that for the mean fields, the core of the California Current was resolved. Inshore and offshore of this minimum, salinities increased both toward the coast (indicating the presence of waters which had been modified by equatorial water) and offshore (the saline waters to the west are North Pacific Central waters). The variability of salinity on these isopycnals was relatively small, about 0.1; maximum variability occurred along shallower isopycnals between 50 km and 100 km from the coast and at the offshore edge of the section. A region of large variability was associated with the boundary between North Pacific Intermediate Water (NPIW) and Pacific Equatorial Water (PEW) on the 26.7 kg/m^3 at a distance of 160 km.

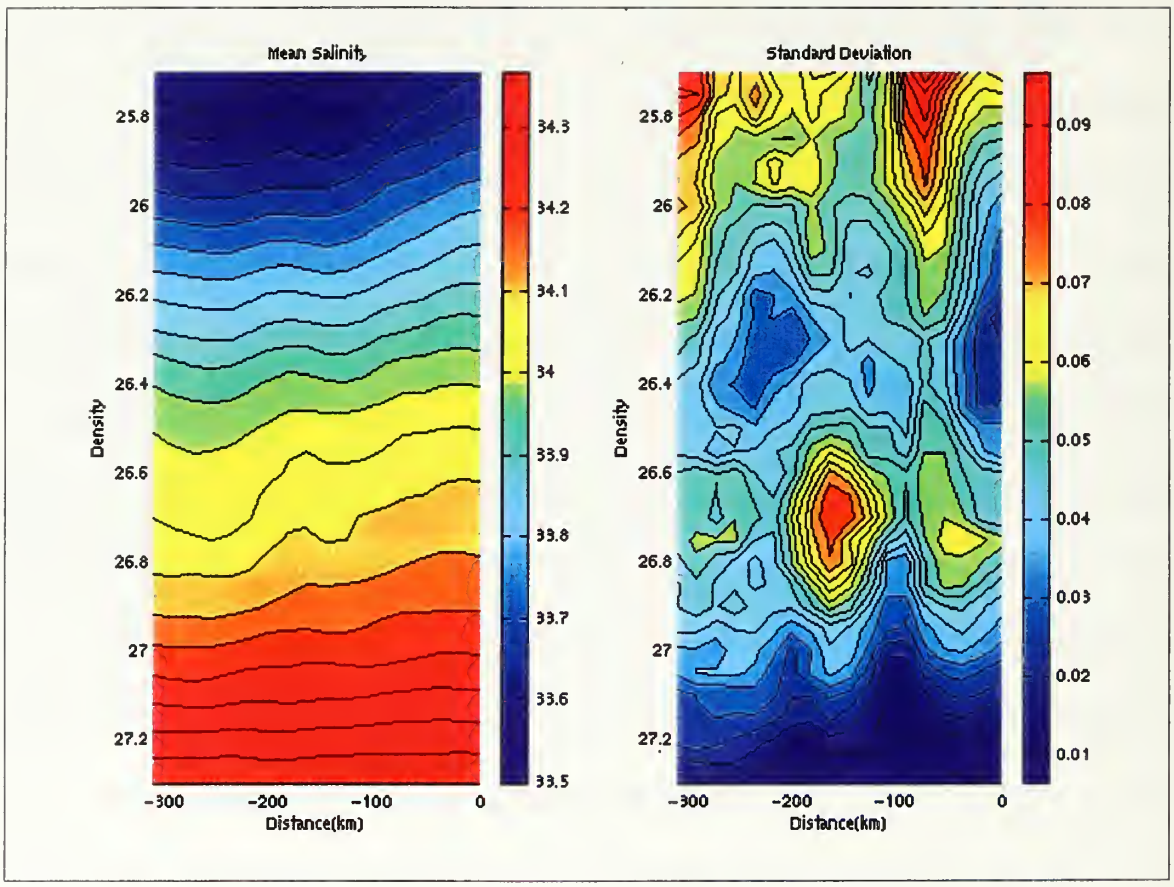

Figure 14. Mean (left) and Standard Deviation (right) of Salinity on Density.

C. TIME SERIES

Time series of water properties on isobaric surfaces for CALCOFI line 67 are shown in Figures 15-17. Potential temperature, salinity, and density anomaly contours are shown for the period from February 1997 through January 1999 at four levels (surface, 80 dbar, 150 dbar, and 300 dbar). The variability of salinity on several isopycnals is also shown (Figure 18). The chosen levels were determined in part by the results of the Principal Component Analysis (PCA) which are described in the next section. The temporal variation of potential temperature and density anomaly were similar at common levels. This suggested that locally, the density anomaly was mainly controlled by temperature (Batteen, et al., 1995).

At the surface, seasonal warming appeared to propagate shoreward while cooling propagated offshore (Figure 15). Compared to 1998, 1997 was warm for an extended period of time. The surface warming in 1997 began in February offshore, was interrupted briefly in July, and surface waters were warmest in August. Inshore, surface waters were about 3°C warmer in the winter of 1998 than either 1997 or 1999. As pressure increases, this pattern changed due to variations in thermocline depth. At 80 dbar, offshore waters were warmer than inshore waters except for January 1998 when the warming appeared along the entire section; note that the offshore warming occurred in winter. At 150 dbar, the wintertime warming offshore is matched, in January 1998, by a region of coastal warming. At 300 dbar, offshore and coastal warming occurred in January and February 1998. At 300 dbar, periods of coastal warming also occurred in April-July, 1997 and July 1998.

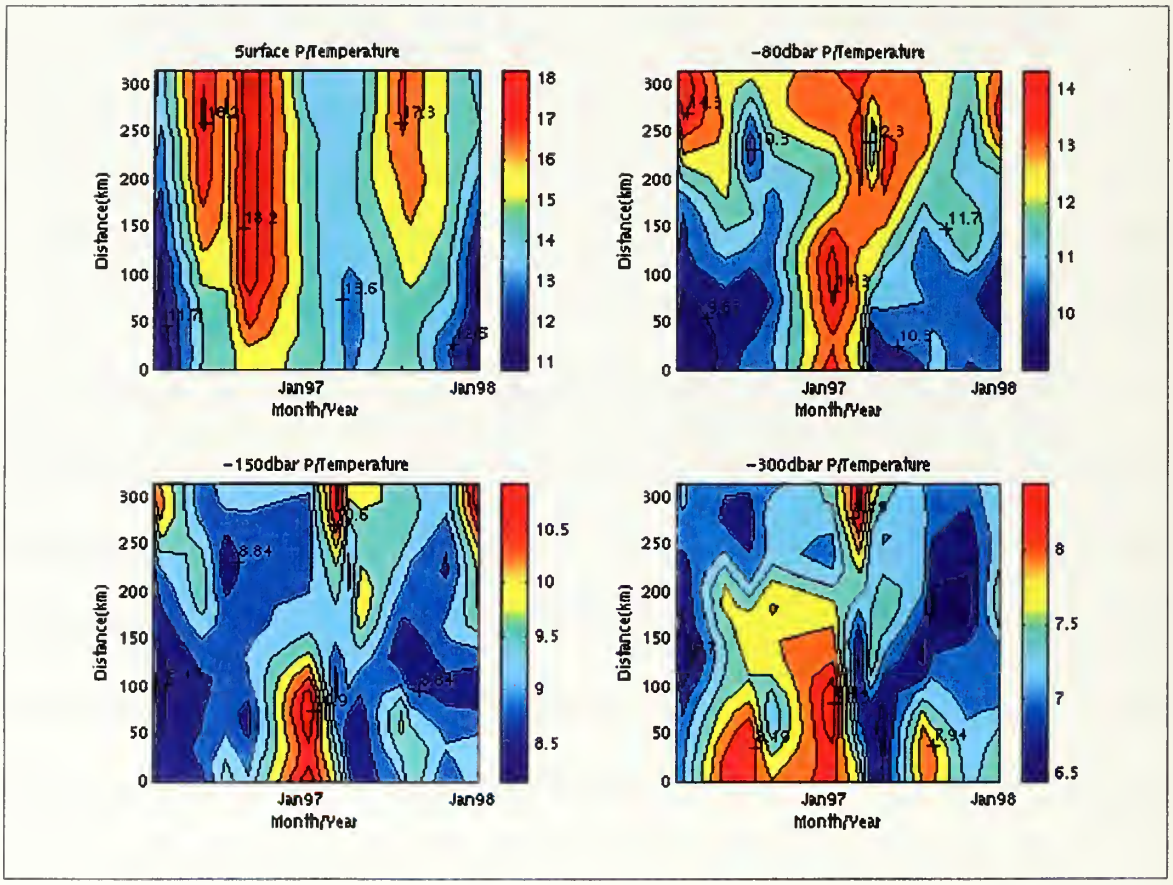

Figure 15. Time series of Potential Temperature, C°.

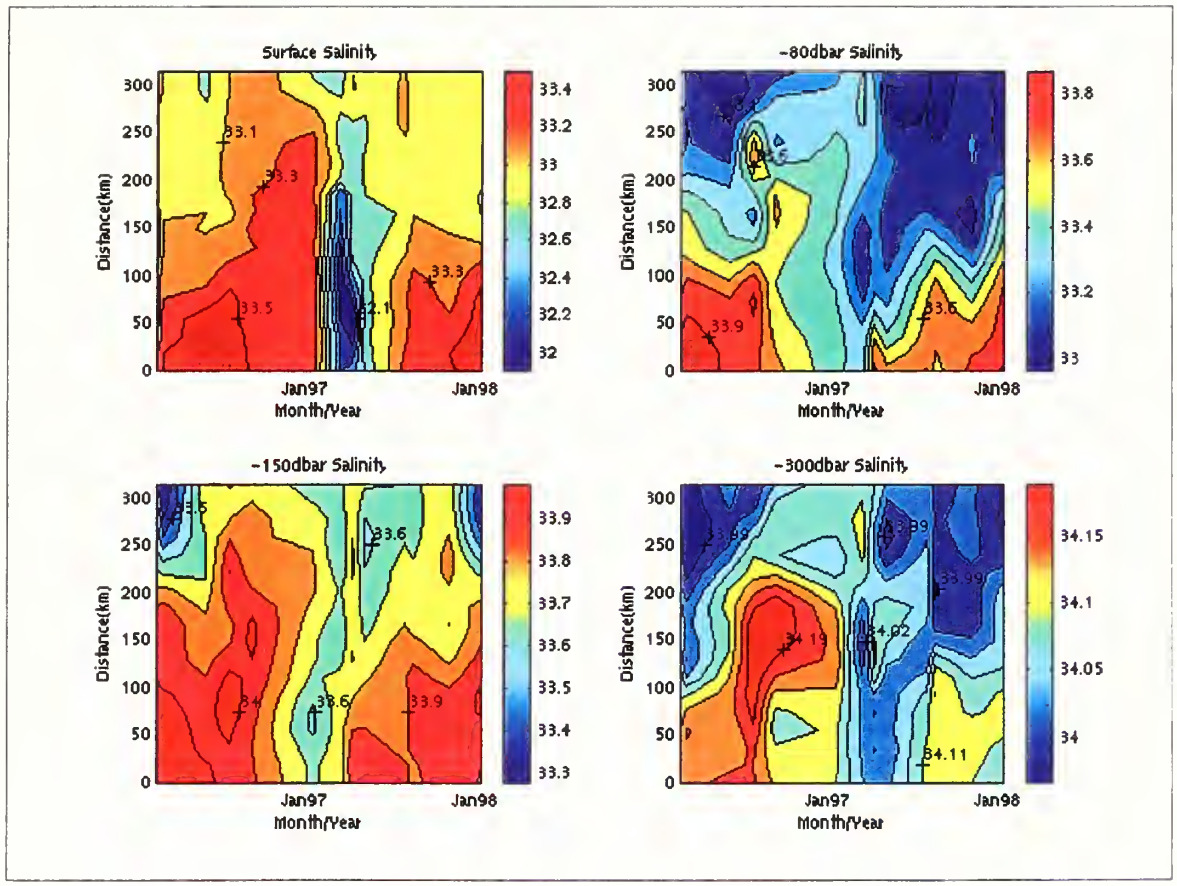

Figure 16. Time Series of Salinity.

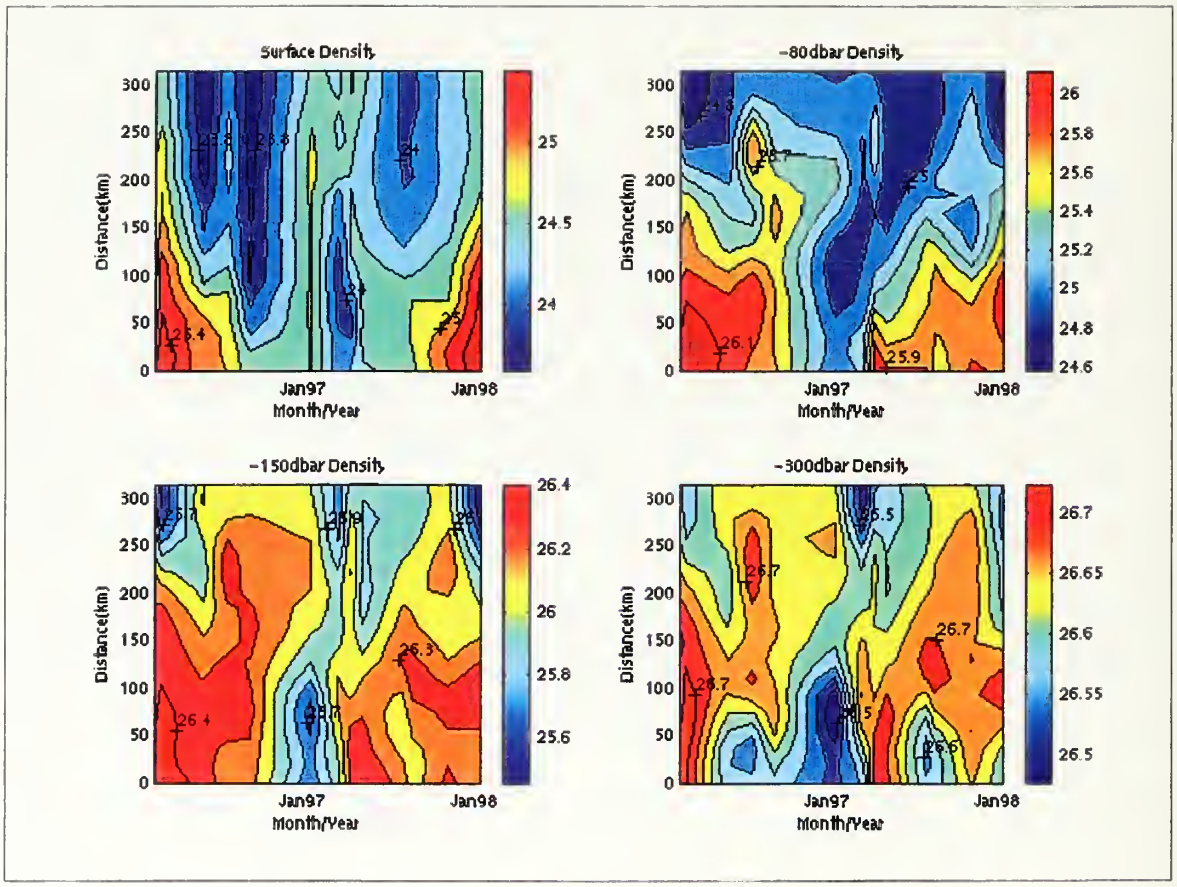

Figure 17. Time series of Density Anomaly, kg/m^3.

At all levels, salinity (Figure 16) tended to decrease with distance from shore. The exception to this pattern occurred in spring 1998 when waters freshened near the coast, to 31.8. This freshening was not observed in February 1997 and January 1999. On pressure surfaces, waters were generally more saline in 1997 than 1998. At 300 dbar, a lens of $S > 34.15$ at about 150 km from shore was replaced by $S < 34$ during the corresponding period in 1998. On density surfaces, the pattern of salinity variability was noisier, in part due to the fact that the range of salinity is reduced and intrusive mixing can more easily create 'bullseyes' (Lynn and Simpson, 1990). But the pattern of offshore freshening, increased salinity of coastal waters in summer, and a greater extent of saline in water in 1997 than 1998 existed on density surfaces between 25.8 and 26.8 kg/m^3 (Figure 18). The 27.25 kg/m^3 isopycnal surface was below 900 dbar; at this level the movement of a patch of water with $S > 34.4$ from the coast in early 1997 to the offshore edge in January 1998 of our section in 1997 was observed. This was preceded by a freshening of offshore waters in February 1997 and followed by a freshening of inshore waters in January 1998. Note the total change in salinity on this deep isopycnal was only 0.06.

The final time series figure shows the evolution of the dynamic thickness of several layers during 1997-9 (Figure 19). Per the discussion of climatology, a dynamic trough should exist midway along our section, with higher dynamic height at the coast and offshore. The 200/1000 dbar and 200/500 dbar layers showed this trough most clearly, moving from 100 km in February 1997 to 200 km in January 1998 and back to 100 km in

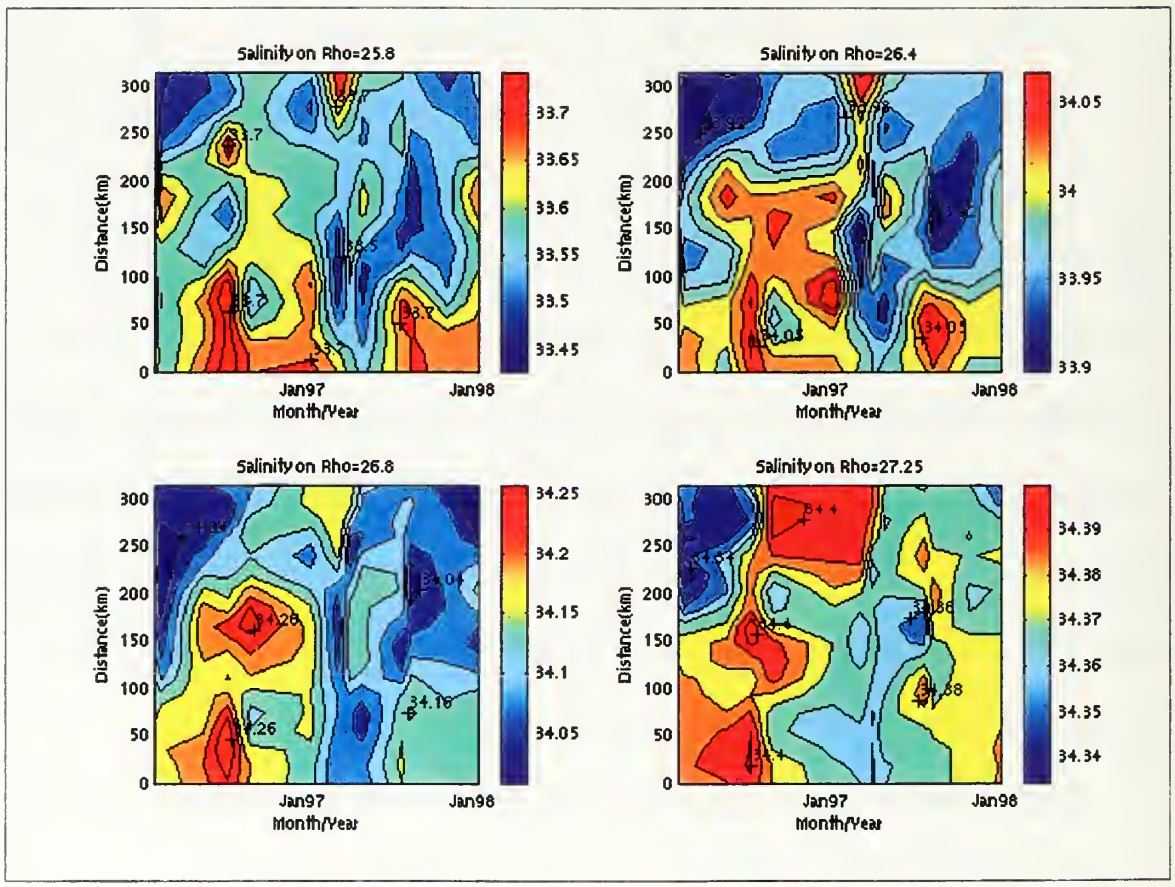

Figure 18. Time series of Salinity on Isopycnal Surfaces.

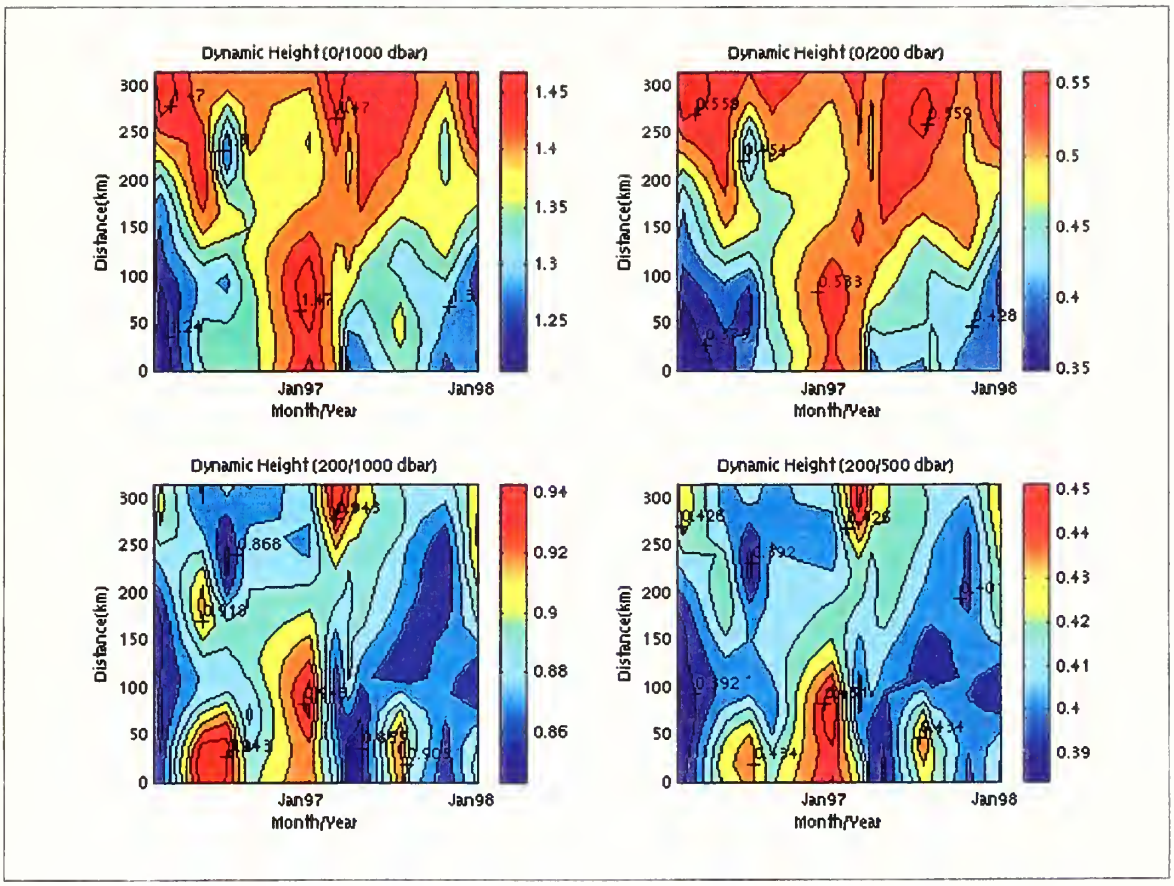

Figure 19. Time series of Dynamic Height, dynamic meters.

January 1999. The intensification of the geostrophic poleward flow at the coast in spring/summer 1997 and 1998 occurred and the 1997 event appeared to be deeper and stronger than in 1998. The winter of 1998 differed from other winters at the coast in that the poleward flow strengthened to the magnitude seen in spring and summer and extended to almost twice the distance from shore. Note that offshore, the dynamic heights increase in winter and this appeared greater in 1998 than 1997 or 1999.

As observed by others, the surface layer (0/200 dbar) is lowest at the coast during most of the year. This pattern too was disrupted in January 1998 by an increase in the dynamic thickness at the coast to a value close to that found offshore.

D. PRINCIPAL COMPONENT ANALYSIS (PCA)

The time series illustrated the deep warming that occurred next to the Central California Coast from spring 1997 through January 1998 and the subsequent surface freshening at the coast in March and April. To better understand the changes that occurred along line 67, principal component analysis was used. Bray and Greengrove (1993) have used PCA to study sections along the California coast; the technique was useful for separating annual and interannual variability and showing the distribution of these changes with depth and distance from shore. PCA decomposes the variance into a set of principal components or modes that are ranked by the percentage of variance that is explained. Each PC consists of a pattern of Z scores that is uncorrelated with other PCs. It also produces a time series of amplitude coefficients that show how a given principal component varied with time. PCA was accomplished by using the MATLAB™ Statistics

Toolbox. The first three principal component patterns typically accounted for 80% to 90% of the variance. The temporal variability of the amplitude patterns was used to "filter" the principal components. Amplitude patterns that had a strong peak during observed El Niño conditions off Central California are discussed below as are principal components that resembled the annual cycle. Note that some caution is needed in examining principal components; results are derived statistically and patterns may not have any physical meaning. Also note that a complete set of the first three modes and their temporal behavior is given in Appendix C.

1. Annual Variability

The principal component that best showed a pattern of annual variability was the first principal component for temperature (Figure 20) which accounted for 39.6% of the variability. The amplitude function showed minima and maxima in each year associated with winter and late summer. Note that the amplitude of the annual variability mode for temperature was only about half (.24) that observed in 1997 (0.41). The pattern of Zscores showed cooling (warming) of waters above 60 m in winter (summer) with maximum amplitude corresponding to decrease (increase) in temperature at the sea surface of 2.4°C (3.0°C) in 1997. The '0' Zscore occurred at a pressure of about 50 dbar at the offshore edge of the section; it increased in depth toward the coast gradually, reaching a pressure of 70 dbar at about 70 km, where it suddenly deepened, moved offshore, and returned to the coast at a pressure of 600 dbar, encompassing the region of the IC. This suggests that winter (summer) cooling (warming) extended to great depths at the coast and was likely associated with an upward (downward) displacement of isotherms

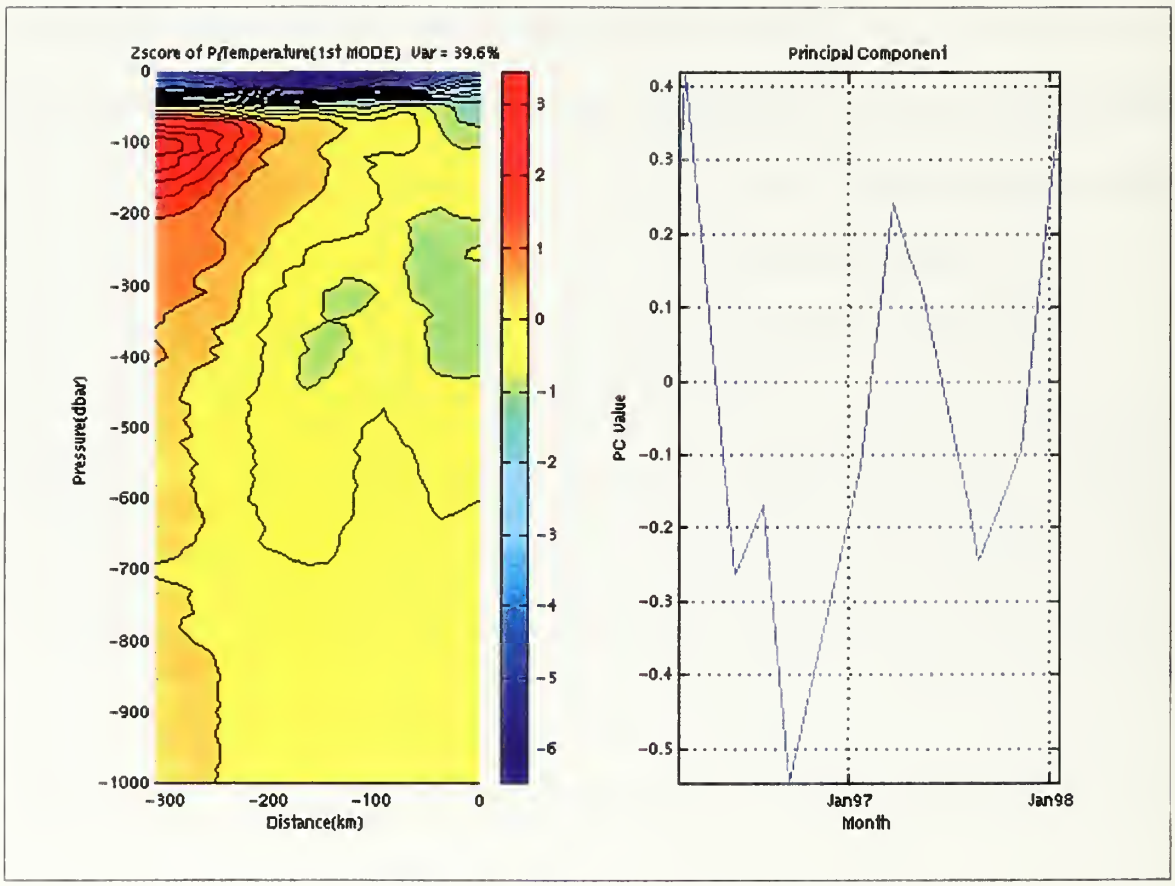

Figure 20. The First Mode for Potential Temperature, °C.

associated with a relaxation (acceleration) of the IC. Offshore, centered at 100 dbar, a region of subsurface winter (summer) warming (cooling) occurred with an amplitude of about 1.5°C due to entrainment of warm waters from the mixed layer during seasonal cooling of surface waters. Winter warming at greater depth at the offshore edge of the section could be caused by a deepening of isotherms, either due to a change in their tilt or an onshore displacement of the CC.

2. Interannual Variability

With seasonal variability removed, the second principal component of temperature (Figure 21) showed clearly the cycle of temperature change associated with El Niño. This component accounted for 25.4% of the variance. The pattern of Zscores appeared as a triangular wedge which extended from the coast at a depth of 80 m to a distance of 280 km, intersecting the surface at a distance of 80 km, and with its lower boundary intersecting the coast at 200 dbar. This component remained negative for the first half of 1997 with an amplitude of –0.3, became positive in August, and peaked in January 1998, after which the amplitude rapidly decreased through the first half of 1998. The amplitude of the 80 m coastal warming (surface offshore cooling) in January 1998 was 2.5°C (-2°C). This pattern of Zscores could be partially explained by a downward tilt of the thermocline toward the coast, associated with an acceleration of geostrophic poleward flow or onshore transport of upper layer waters.

The third mode of potential temperature (Figure 22) accounted for only 12.5% of the variance. The temporal pattern of amplitude variation showed some of the character

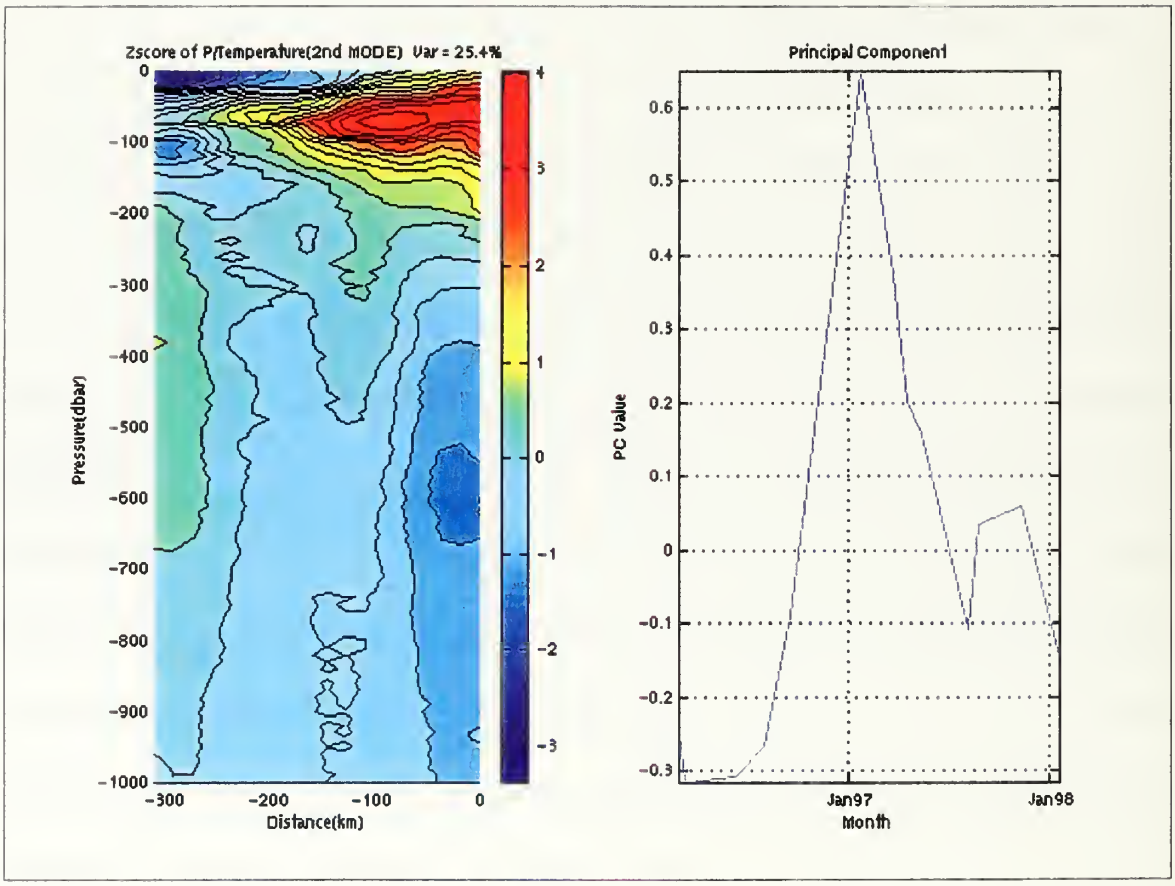

Figure 21. The Second Mode for Potential Temperature, °C.

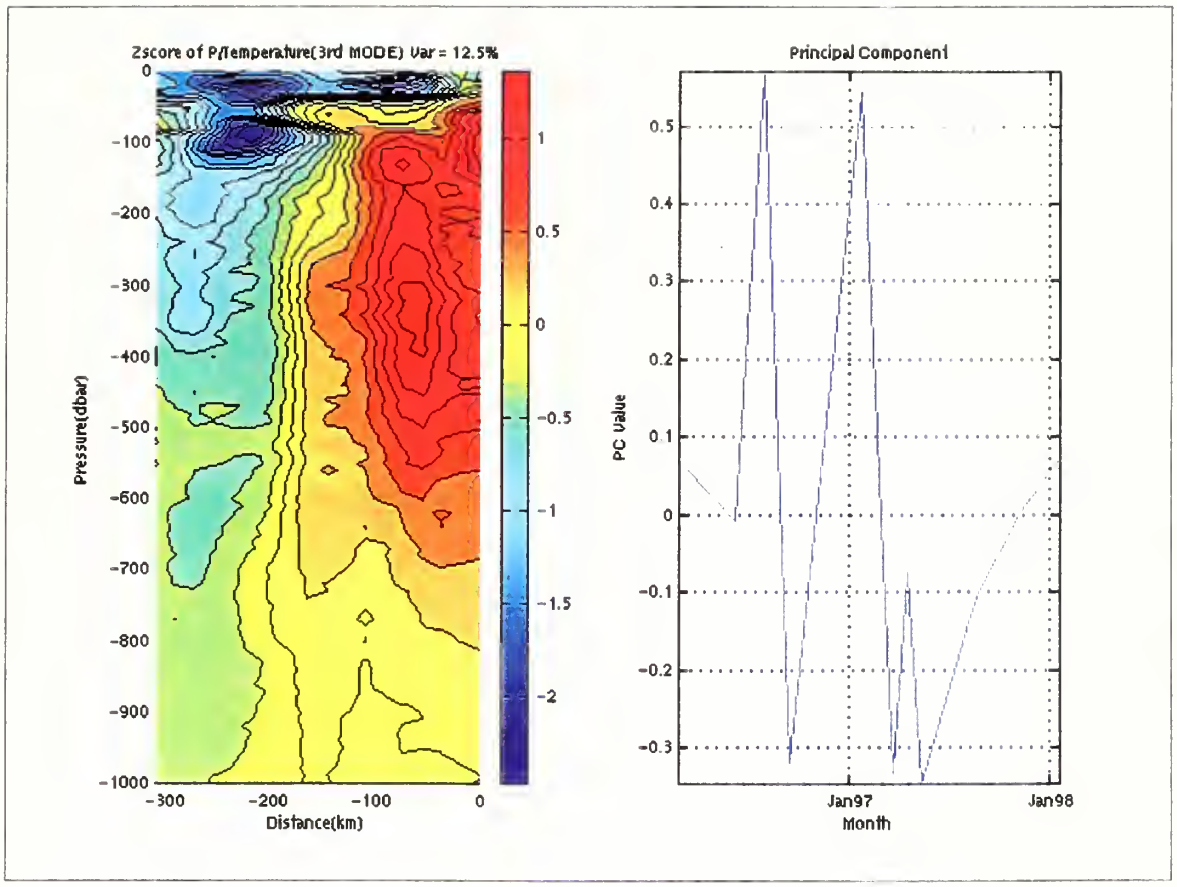

Figure 22. The Third Mode for Potential Temperature, °C.

of the sea level changes in the Tropical Pacific (see next chapter) with peaks which exceeded 0.5 in July 1997 and January 1998. The pattern of Zscores reflected warming of deep nearshore waters and cooling of surface and offshore waters during these events. The greatest warming (cooling) was 0.5°C (-1.3°C). This pattern appeared to be associated with increased upwelling and surface cooling and a tilting of the thermocline about a pivot point at about 200 km, resulting in warmer (cooler) waters inshore (offshore) of the pivot point. ADCP and in situ data showed the CU was intensified in June and July 1997 (Appendix B).

The first principal component of salinity (Figure 23) accounted for 53.8 % of the observed variance, larger than any other principal component. The Zscores greater than zero were confined to an area extending from the coast to 150 km and from the surface to a pressure of about 200 dbar. The amplitudes for this pattern were usually slightly negative except for the spring of 1998 when a minimum amplitude of -1.3 occurred, corresponding to a freshening of S=1 at the surface. Principal components of salinity did not show a pattern of annual variability (see Appendix C).

The second mode for salinity (Figure 24) showed a pattern of increased surface salinity for all but the most seaward 40 km during July 1997 – January 1998. The pattern of temporal variability is similar to that for the second mode of temperature. Also similar was a coastal (0 to 150 km) nearsurface (centered at 110 dbar) feature which indicated a maximum freshening of 0.25 in January 1998.

The first principal component of density anomaly (Figure 25) accounted for 43.1 % of the variance. The temporal variability of the amplitude was clearly interannual, with

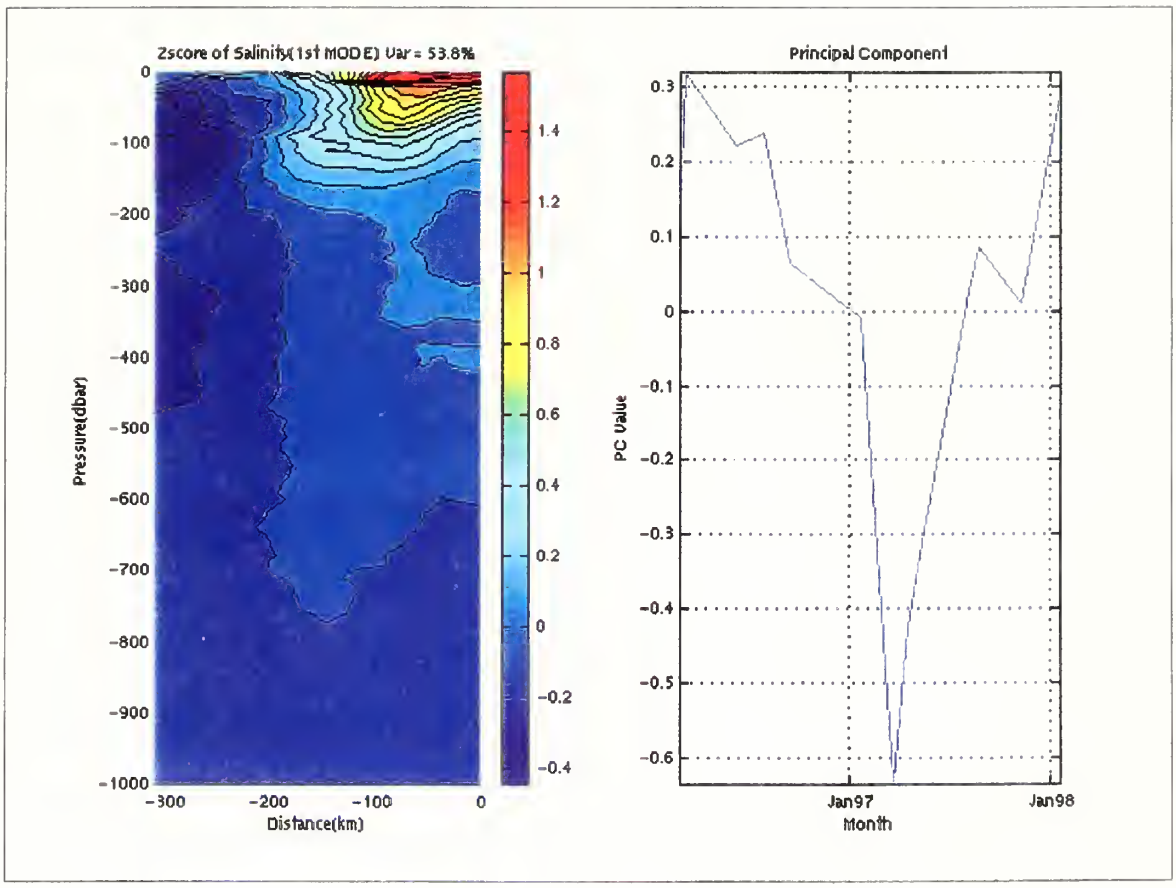

Figure 23. The First Mode for Salinity.

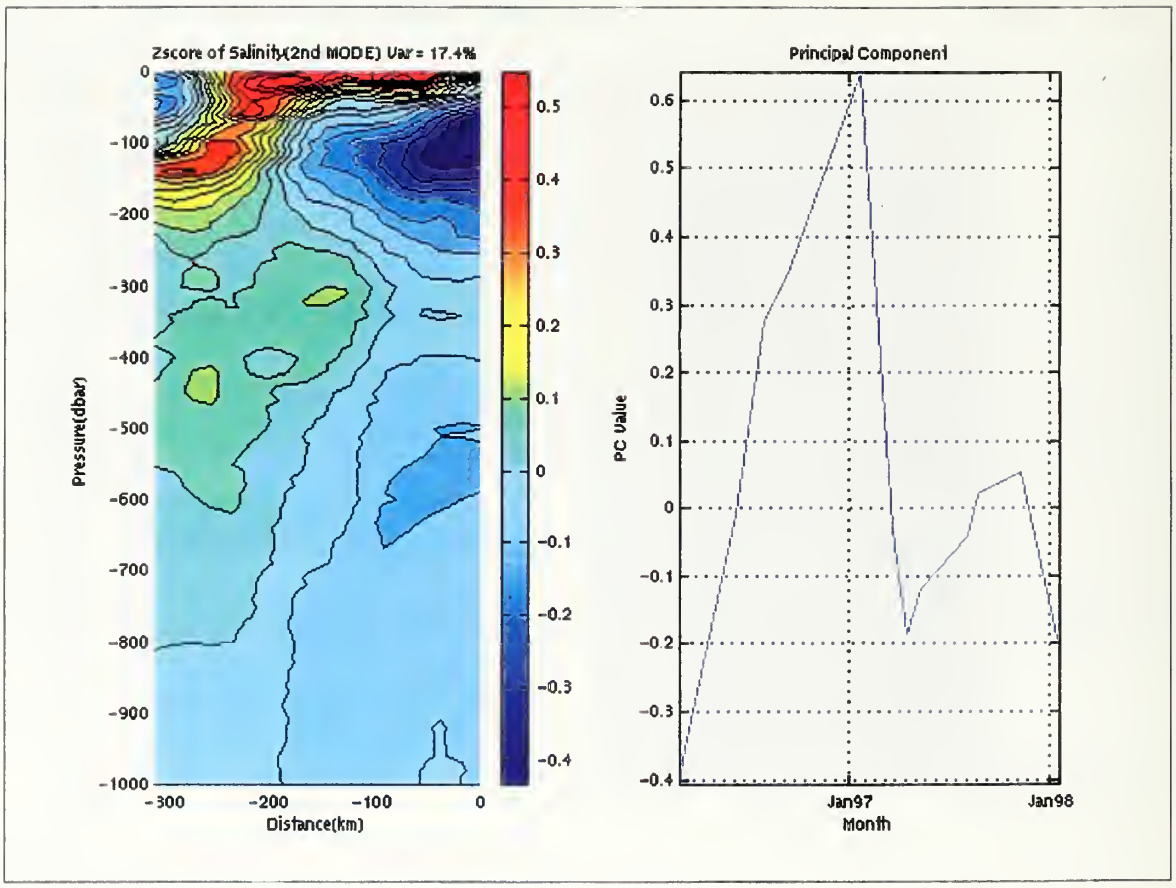

Figure 24. The Second Mode for Salinity.

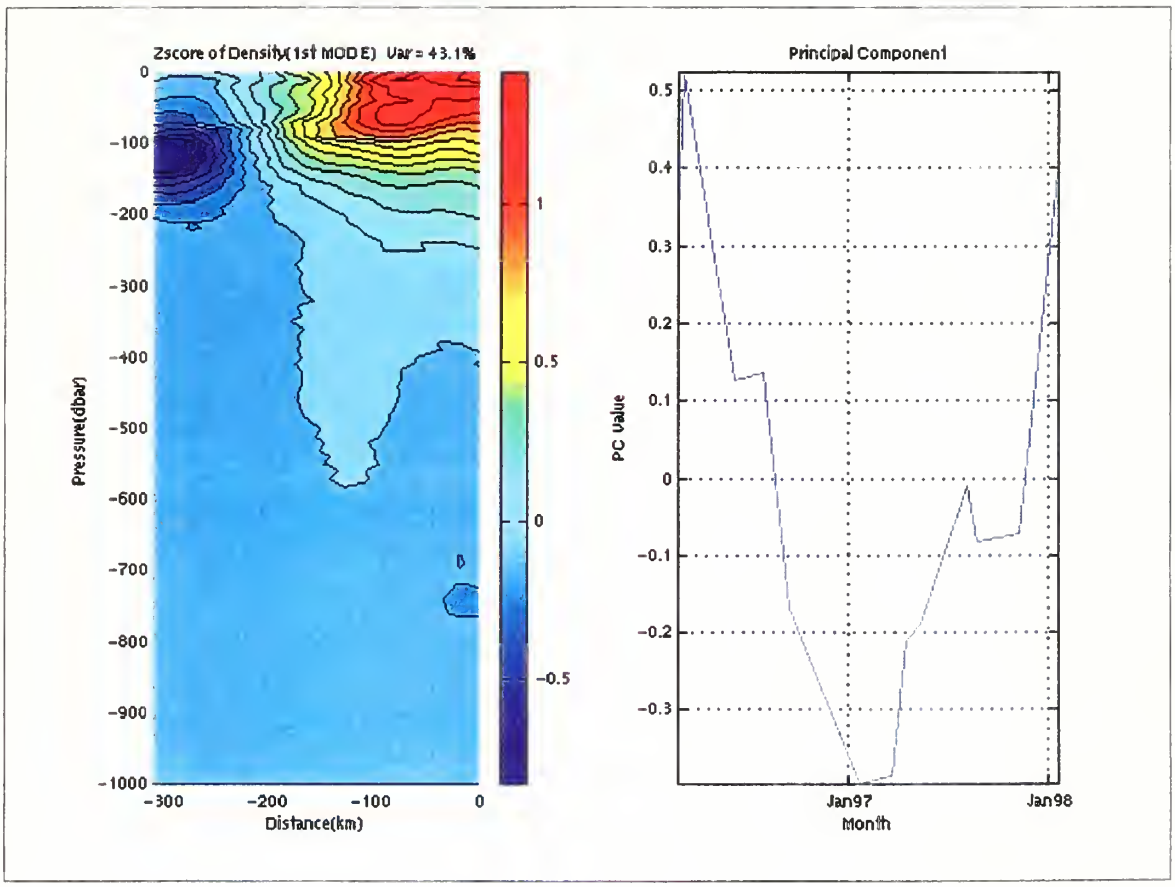

Figure 25. The First Mode for Density Anomaly, kg/m^3.

large positive values of 0.5 and 0.4 in March 1997 and January 1999, respectively, and a minimum value, -0.4 in January, March and April 1998. The pattern of Zscores resembled a combination of the 2nd temperature principal component and the 1st salinity principal component, with a decrease in density anomaly in the upper 200 m within 180 km of shore and an increase in the lower part of the seasonal pycnocline at the offshore boundary of the section. The total change in this pattern from March 1997 to January 1998 was about -1.3 kg/m3 (-0,7 kg/m3) at the surface near the coast (offshore at 120 dbars). Beneath the surface layer, the pattern of variability of the pressure of isopycnals is shown by the first mode of pressure on density (Figure 26) which accounted for 42.2% of the variance. The pattern of the Zscores divided an onshore region within about 130 km of the coast from an offshore region, Positive Zscores were about 50% greater than negative Zscores and maxima were for waters of density 26.6-27.1 kg/m^3 at a distance of 50 km and represented a deepening of isopycnals in this density range of about 50 decibars during July 1997 and January 1998. As noted above, this represented an increase of the downward slope of the pycnocline, corresponding to increased poleward geostrophic flow.

The first mode of the salinity on isopycnal surfaces (Figure 27) showed a pattern of offshore changes. The amplitude was largest in July 1997 and minimum in March 1998. This indicated that salinity of nearshore (offshore) waters decreased (increased) during this time period. Variability was greatest at 25.8 and 26.8 kg/m^3 corresponding to a salinity change of 0.15. The first principal component for the ADCP alongshore velocity (Figure 28) indicated a pattern similar to the mean alongshore flow (Figure 12) and accounted for 30.9% of the variance. The alternating cores of vertically coherent poleward and

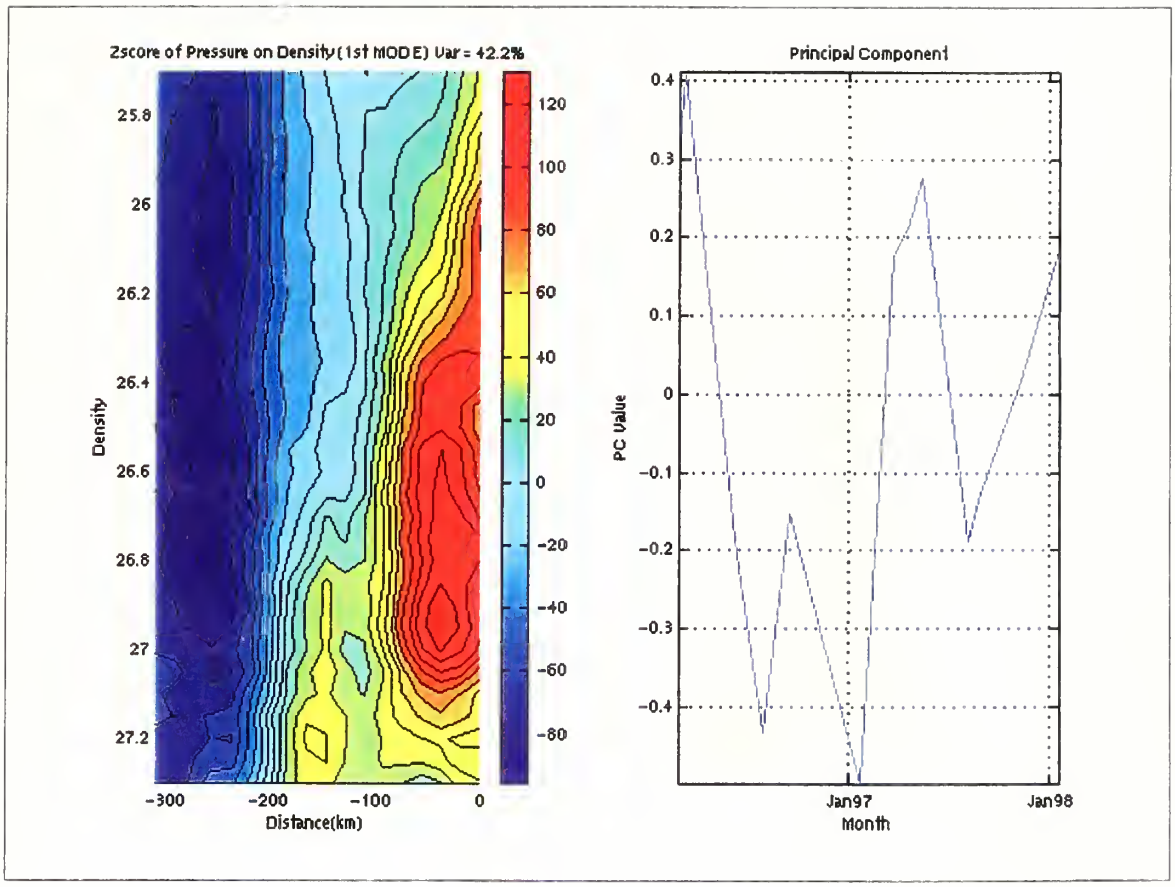

Figure 26. The First Mode for Pressure on Density.

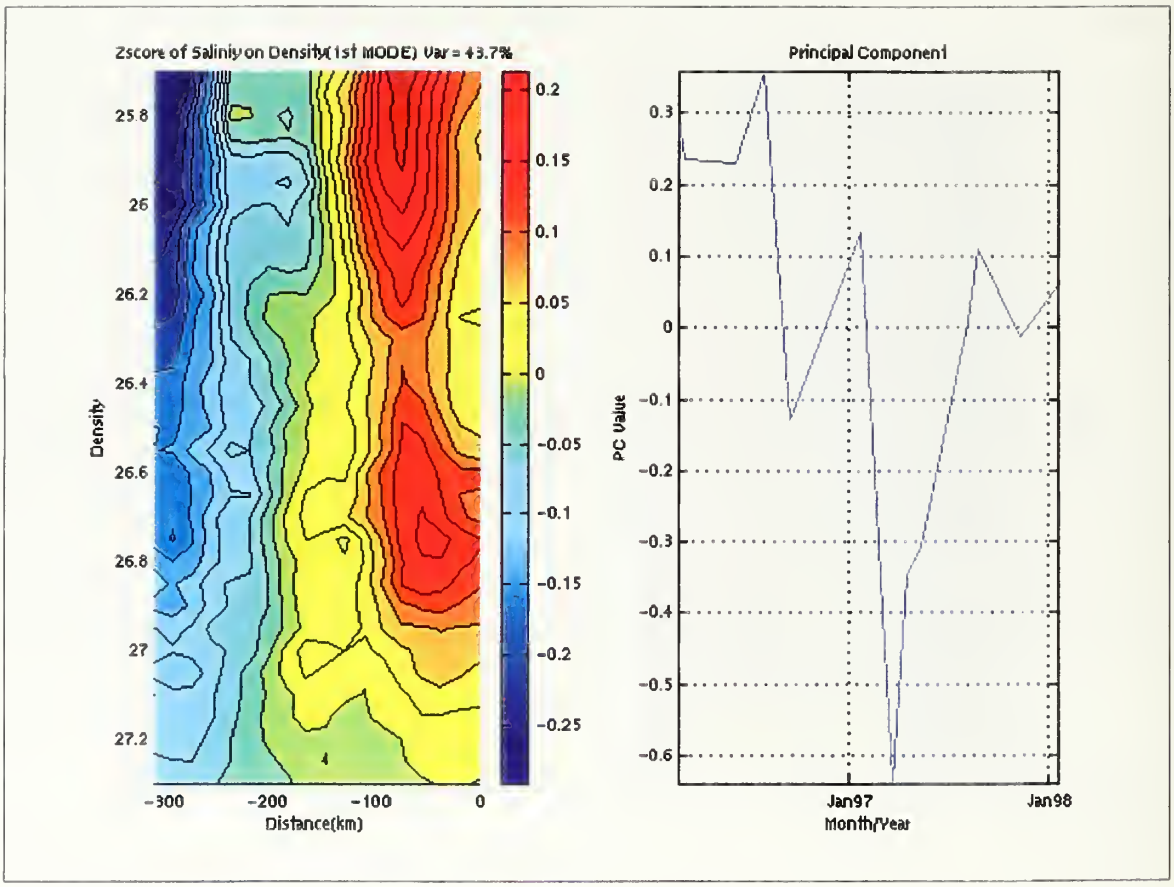

Figure 27. The First Mode for Salinity on Density.

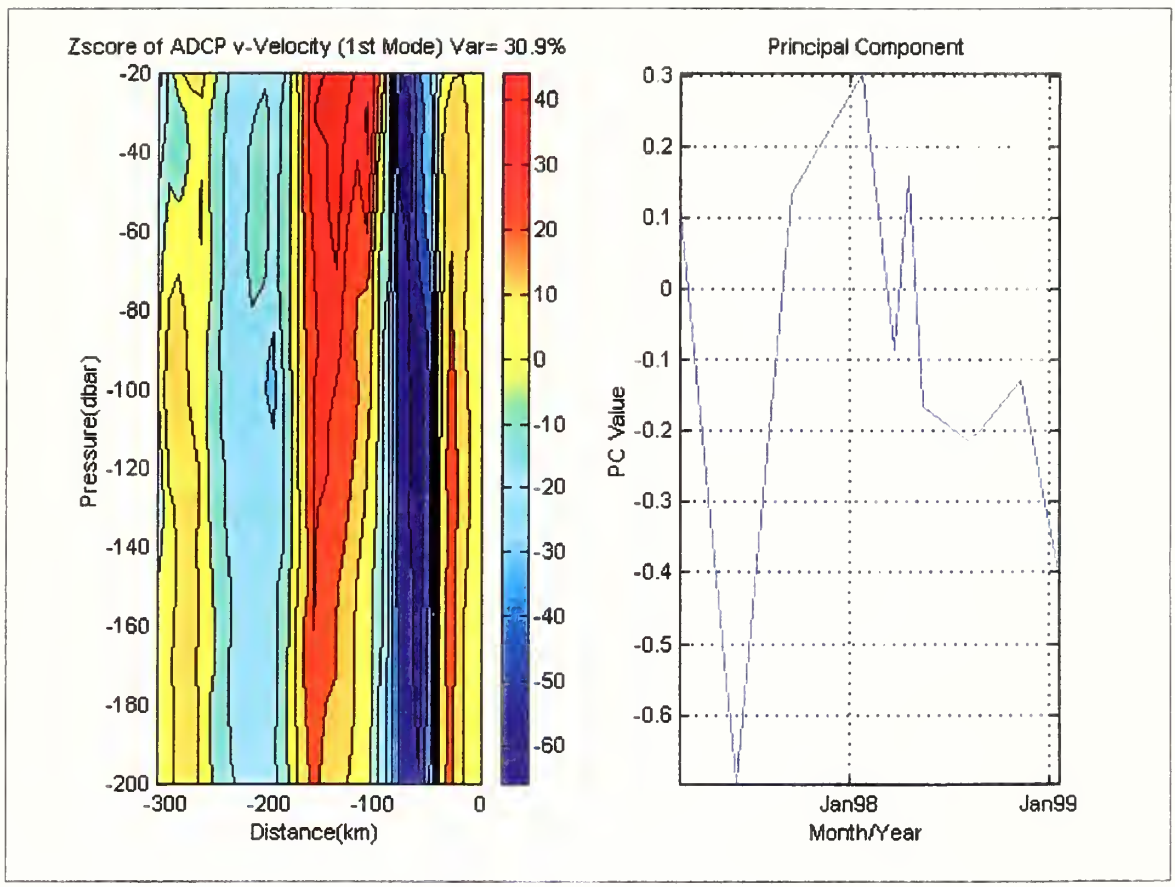

Figure 28. The First Mode for ADCP Alongshore Velocity, cm/s.

equatorward flow were anchored to the same location as the bands of flow in the mean fields (Figure 12). Highest Zscores were associated with band of flow between 115 km and 195 km from the coast and lowest Zscores (with magnitudes 50% greater than the positive Zscores) occurred between 30 km and 115 km from the coast. The amplitude of the first component in July 1997 was -0.6 (40 cm/s for the strong nearshore flow) and for January 1998 was 0.3 (-20 cm/s for the strong nearshore flow). The magnitude of these flows overwhelms the pattern of mean velocities; note that southward flow was associated with the deepened isopycnals and isotherms in January 1998.

The first principal component of ADCP onshore velocity (Figure 29) showed positive Zscores (corresponding to onshore flow) to the west of 195 km from the coast and mostly negative (offshore flow) to the east of 195 km from the coast, with negative Zscores almost twice as large as those for positive Zscores. The temporal variation of the amplitudes of the first principal component showed that this pattern was strongest in February 1997, 0.65, and gradually reversed, reaching minimum amplitude, -0.45 in March 1998. These amplitudes corresponded to peak flows of 25 cm/s near the surface at 115 km from the coast. The strong onshore flow occurred at the same time as the anomalously fresh nearsurface waters.

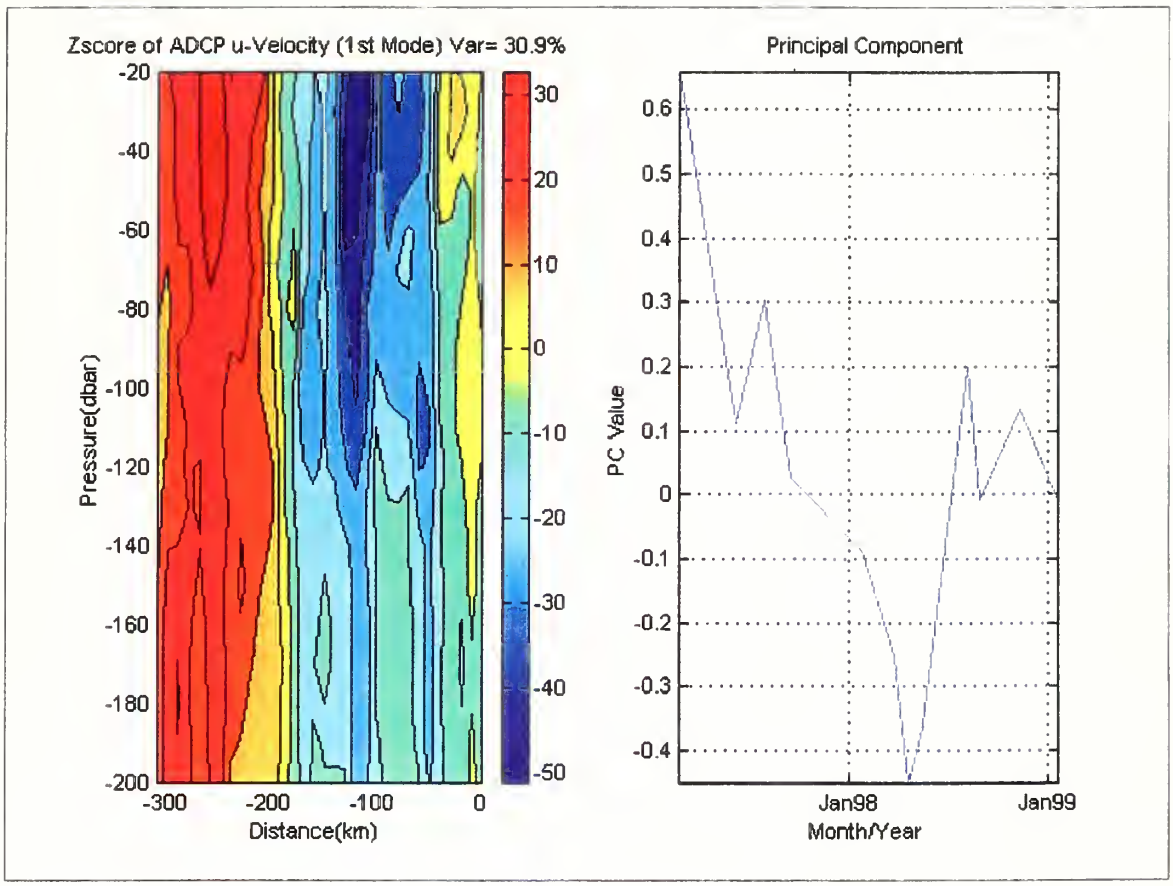

Figure 29. The First Mode for ADCP Onshore Velocity, cm/s.

IV. DISCUSSION AND SUMMARY

In this chapter, the changes in ocean structure that were observed along CalCOFI line 67 during 1997-1998 are summarized and possible mechanisms for the observed changes are discussed. Annual variability is described as well. Finally, suggestions for additional work are made.

A. THE 1997-8 CALIFORNIAN EL NIÑO

The sequence of hydrographic changes that was detected along CalCOFI line 67 using principal component analysis is summarized in Table 3. The chronological sequence of events was:

June-July 1997: Strong poleward flow at the coast was associated with coastal (within 100 km), subsurface (200-500 dbar) warming of 0.5°C and increased salinity on isopycnal surfaces (0.07). Offshore, waters appeared cooler, fresher with stronger equatorward flow.

September 1997: A relaxation of El Niño conditions occurred, with coastal, subsurface waters cooling by 0.3°C, and with a narrow band of poleward flow at the coast.

January 1998: Maximum interannual temperature and sea level anomalies were observed with nearsurface (80 dbar), nearshore (within 100 km) warming of 2.5°C and subsurface warming comparable to that observed in June-July 1997. Despite the large

Date	Mode	Change
June-July, 1997	3rd Temperature	0.5°C warming, 0<x<100km,200<z<500 dbar
	1st Isopycnal Pressure	Isopycnals tilt downward toward coast, maximum displacement 50 dbars at γ =27 kg/m^3
	1st Isopycnal Salinity	Saltier (+0.07) Inshore, Fresher Offshore (-0.07)
	1st Alongshore Flow	Cyclonic Shear at Coast, 40 cm/s
September, 1997	3rd Temperature	0.3°C cooling, 0<x<100 km, 200<z<500 dbar
January, 1998	2nd Temperature, 2nd Salinity	2.5°C warming, 0.3 freshening, 0<x<100 km, 80 dbar
	3rd Temperature	0.5°C warming, 0<x<100 km, 200<z<500 dbar
	1st Isopycnal Pressure	Isopycnals tilt downward toward coast, maximum displacement 60 dbars at γ =27 kg/m^3
	1st Alongshore Flow	Anticyclonic Shear at Coast, 20 cm/s
March-May, 1998	3rd Temperature	0.3°C cooling, 0<x<100 km, 200<z<500 dbar
March-April, 1998	1st Salinity	S=1 freshening at surface next to coast
March, 1998	1st Isopycnal Salinity	Fresher (-0.12) Inshore, Saltier (+0.15) Offshore
March-April, 1998	1st Onshore Flow	Onshore Flow, 50 km<x<175 km

Table 3. Interannual Variability of Principal Components, 1997-1998

downward tilt of isopycnals toward the coast, the flow at the coast was equatorward, with poleward flow occurring toward the center of the section. The salinity of the near surface coastal waters was fresher (0.3) while the subsurface waters were near normal salinity.

March-April 1998: The most remarkable features were the freshening of coastal waters which was accompanied by onshore flow. The freshening was greatest at the surface, with observed salinities less than 32, but the freshening extended to isopycnals as dense as 27 kg/m^3.

Note that the longest time interval between occupation of Line 67 was from September 1997 to January 1998, missing the period in the late fall when warmest waters were observed at Granite Point (Figure 4) and SE Farallon Island (Figure 5) and maximum sea level occurred at Monterey (Figure 6). There were additional data available for this period for line 67: the **NOAA Ship David Starr Jordon** occupied six 500 dbar stations from H-3 to 67-70 along line 67 from October 11-13, 1997 and the **R/V Point Sur** occupied stations H3 to NPS2 from November 8-9, 1997. These data are shown in Figures 30 and 31.

The sections confirmed the results of shore station and sea level measurements. The upper layer continued to warm, from 12°C in September, to 17°C in October and November. The 17°C isotherm formed a core of warm water at the surface at a distance of 150 km from the coast in October (Figure 30) and was fresher than S=33. This core was located in a region where deeper isopycnals slope downward to the west, i.e. southward geostrophic flow, so it resembled the core of the California Current (Simpson

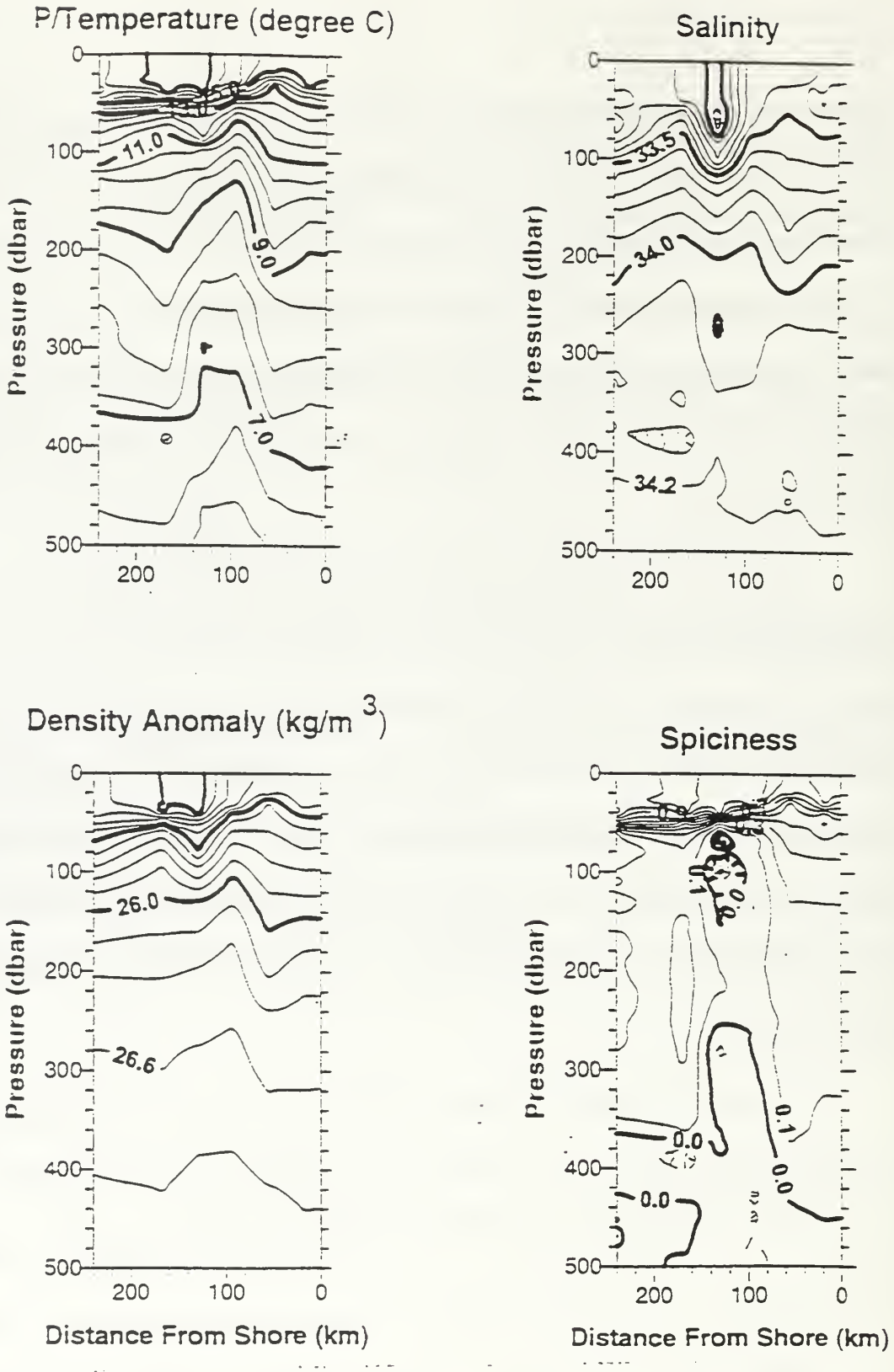

Figure 30. October 11-13, 1997

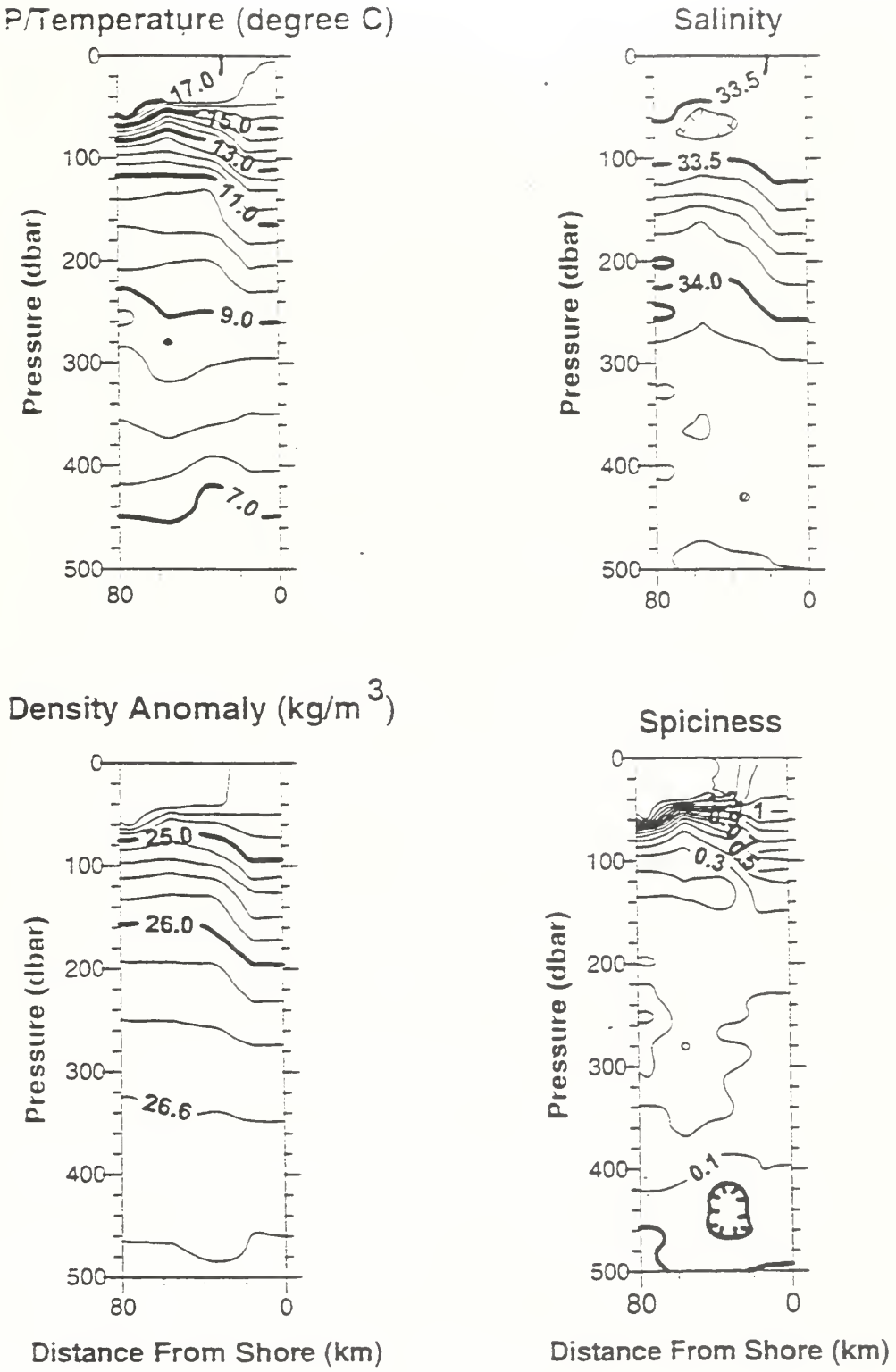

Figure 31. November 8-9, 1997.

and Lynn, 1987) but was displaced about 150 km shoreward from its normal position. Note that to the east of 80 km from shore, the isopycnals slope downward toward the coast, indicating inshore poleward flow.

The November section (Figure 31) only extended 80 km from the coast, but indicated that the 17°C isotherm had moved closer to the coast but with increased salinity, 33.5. In this nearshore region, the 11°C and 9°C isotherm were 50 dbar deeper than in October, and 7°C about 30 dbar deeper. Isopycnals greater than 25.0 kg/m^3 slope downward toward the coast, indicating the continuation of poleward geostrophic flow. Although surface waters had cooled to 14°C in January, this region of deep warming and the associated ridge in dynamic height (not shown) had moved 80 km to the west.

In March and April, the nearshore surface waters were much fresher (S<32) than offshore Subarctic waters (S=32.8), suggesting that the observed freshening was the result of river runoff. Figure 32 shows total river flow in the Sacramento River peaked at 0.4 Sv in late February, 1998. The amount of freshwater, M_2, needed to cause the observed salinity changes on a given isobar, p, is given by $$M_2(p) = M_1(p)\frac{(S_1(p) - S_2(p))}{S_2(p)}$$

where S_1 is the mean salinity in January 1998, S_2 is the mean salinity in March 1998, and M_1 the mass in January. Results were calculated for a section 1 m thick which extended to a distance of 200 km from the coast. The results (Figure 33) show that 3.5×10^5 tonnes of freshwater were needed to account for the observed freshening for each meter of distance along the coastline for the upper 200 m . The Sacramento River outflow could,

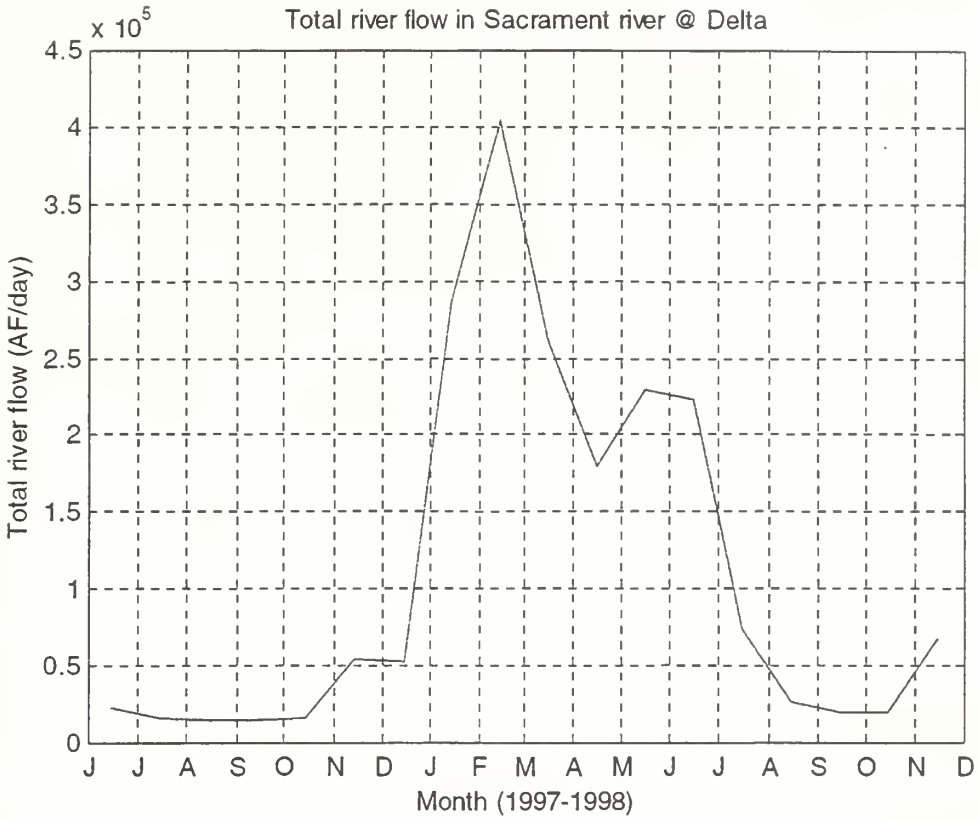

Figure 32. Total River Flow in Sacrament River @ Delta.

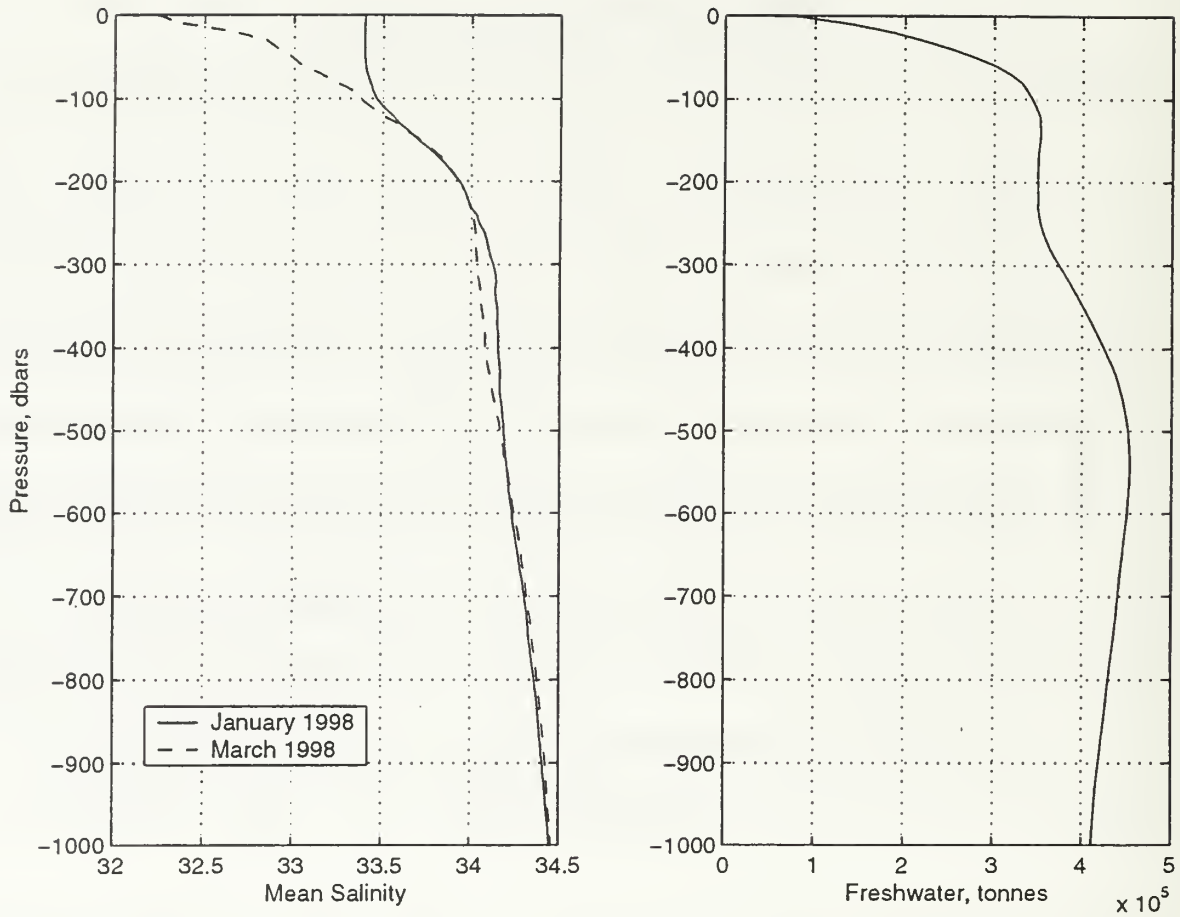

Figure 33. Freshwater budget for Line 67 from the coast to a distance of 200 km from shore for January to March 1998. (left) Mean Salinity. (right) Mass of freshwater required to produce the observed freshning for a 1 m thick section from the surface to a given isobar.

at best, account for 10 % of this volume. Therefore, although waters derived from river outflow could exist in the upper 20-30 m, the upper ocean freshening was mostly due to the presence of Subarctic waters which are normally found offshore.

B. CAUSES OF CALIFORNIAN EL NIÑOS

What causes of the anomalous conditions that were observed off Central California in 1997-1998? Figure 7 shows that the surface winds and associated Ekman transports were near normal except for a series of winter storms that began in December 1997 and ended in March 1998. This means that reduced "upwelling" cannot be responsible for the anomalous warming conditions observed in late 1997. On the other hand, transports associated with winter storms, especially the large pulses (> 100 tonnes/s) in December 1997 and February 1998, could have aided in pushing offshore Subarctic waters toward the coast.

Figure 34 shows sea level height for the Eastern Tropical Pacific for the period 1993 through August 1998. The 1997-1998 El Niño was described by the broad peak of sea level greater than zero in 1997-8. The sea level rise began in January 1997 and steadily increased through July 1997 when sea level reached 24 cm. Sea level then decreased to 11 cm in September, when it resumed rising, reaching a maximum height of 36 cm at the start of 1998. Sea level then decreased rapidly through 1998, crossing zero cm in July 1998. This pattern was similar to that observed at Monterey (Figure 6). At Monterey, the sea level rise began in April 1997, paused in September, and reached a peak in November, about 20 cm greater than the mean. Sea level then decreased, reaching a

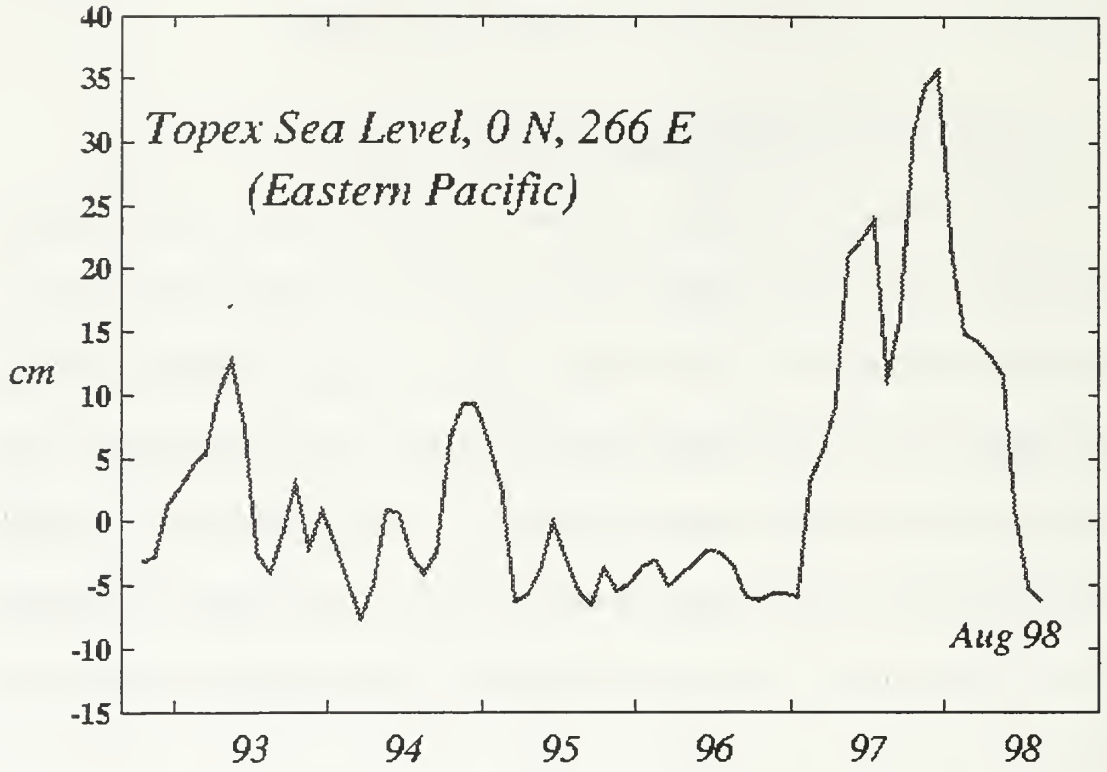

Figure 34. Topex Sea Level Height Anomalies.

minimum in April 1998, after which fluctuations appeared to be near normal. The temporal variations of sea level in the Eastern Tropical Pacific (Figure 1) also resembled the pattern of temporal variation of a number of principal components, e.g. the negative of the first mode of isopycnal pressure. The similarity of temporal variability for Equatorial and Central California waters suggests remote forcing as a factor in causing the 1997-8 Californian El Niño.

Figure 35 shows adjusted sea level at Monterey Harbor for 1997-8. Hourly sea level, referenced to mean lower low water, was filtered to remove tides. The sea level was then adjusted for the inverted barometer effect by adding the observed barometric pressure minus 1000 millibars. Beginning in April 1997, a series of 0.1 m pulses occurred about every two months or so, resembling the poleward propagation of Kelvin waves. These waves should produce equal poleward (rising sea level) and equatorward (decreasing sea level) flows but some of them do not; for example, the July 1997 pulse was associated with a 0.2 m rise in sea level but only a 0.1 m decrease in sea level. To make certain that the sea level pulses are in fact Kelvin waves, the events need to be correlated with current meter measurements and other sea level measurements along the coast. Also note that Kelvin waves cannot account for the onshore and offshore flows that were observed. It seems most likely that a combination of remote forcing and onshore transports associated with winter storms caused the observed 1997-8 Californian El Niño.

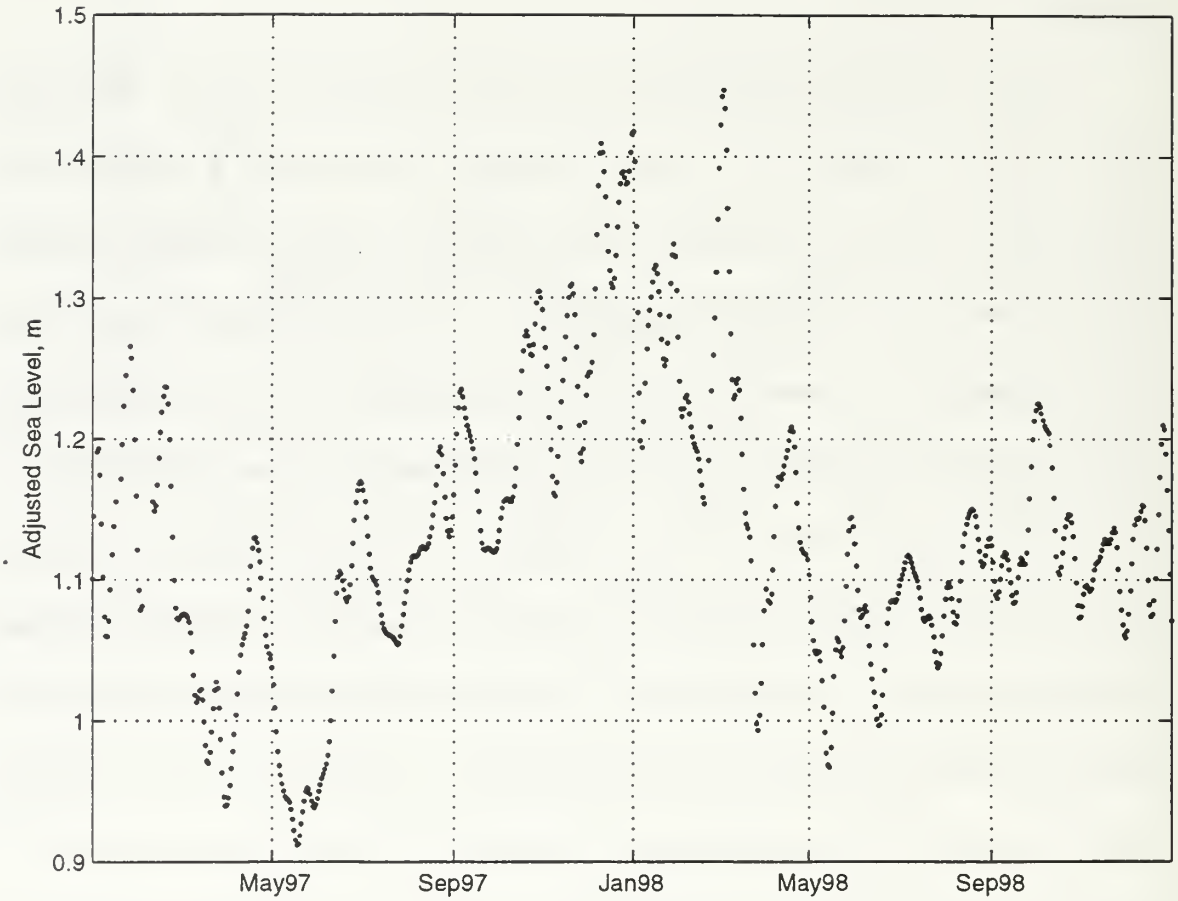

Figure 35. Adjusted sea level for Monterey Harber.

C. ANNUAL VARIABILITY

Annual variability was seen in the temporal variability of the amplitude of three principal components, the first mode of temperature and isopycnal pressure and the second mode for density. This is summarized in Table 4. As expected, the surface cools in winter and its density increases. Offshore, the wintertime heating at 100 dbar resulted from the entrainment of warm water as a result of upper ocean processes associated with the cooling of the surface layer. The change in slope of the isopycnals indicated a weakening of the geostrophic poleward flow in winter.

To estimate the change in heat associated with the annual cycle and El Niño conditions, the heat content of each section was computed as the product of the specific heat of seawater, potential temperature, and density anomaly (Fofonoff and Bacon, 1996). Principal components for heat content were then computed; the Zscores are similar to those shown for temperature. The change in heat content was estimated by subtracting the coldest from the warmest amplitude. The change in heat content, ΔH, was then integrated horizontally and vertically, $\sum_{0}^{p}\sum_{0}^{314.5km}\Delta H(x,p)\Delta x\Delta p$, and results are shown in Figure 36. The change in heat content associated with the annual cycle (first mode), 260 x 10^{12} J was about the same as that associated with El Niño, 250 x 10^{12} J. The corresponding rates of heating are 53 W/m^2 and 25 W/m^2 (the heating associated with El Niño took twice as long as the annual cycle).

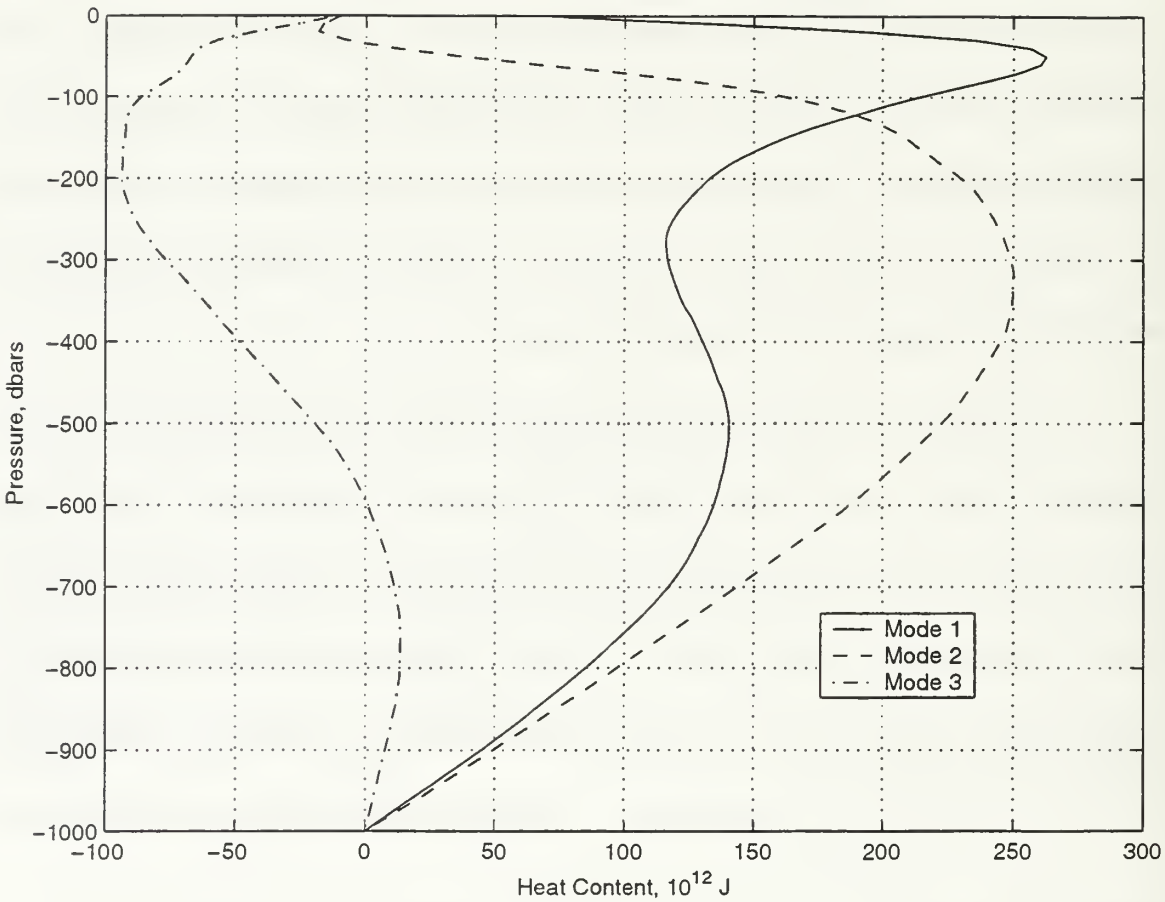

Figure 36. The Change in Heat Content.

Mode	Change	Amplitude
1st Temperature	Cooling above 70 dbar	6°C at surface, x=150 km
	Offshore warming at 100 dbar	1.6°C at 100 dbar, x=300 km
2nd Density	Density increase above 70 dbar	0.25 kg/ surface, x>100 km
	Inshore & Offshore deepening of pycnocline at 100 dbar	0.2 kg/m^3 at 80 km and 300 km
1st Isopycnal Pressure	Upward tilt pycnocline toward the coast	90 dbar/300 km at 26.7 kg/m

Table 4. Winter changes associated with Annual Variability

D. FUTURE WORK

This study illustrates the value of repeated oceanographic sections and their use in understanding ocean variability. The program of measurements that was conducted along Line 67 took 4 days of shiptime and can be carried out on one of the smaller UNOLS vessels, the **R/V Point Sur**. Line 67 is logistically convenient: station C1 is about a half hour from the pier in Moss Landing. The CalCOFI sampling plan is a good pattern for measuring the CC system. The accuracy and ease of use of modern CTDs and the magnitude of density gradients at 500 dbar suggest that 1000 dbar casts should be made. Although this thesis did not comment upon mesoscale variability, the sections that are presented in Appendix A support the view that mesoscale eddies are important in the California Current (Chereskin et al., 1999) so that the distance between stations should be reduced.

Bimonthly sections seemed to resolve the pattern of changes associated with annual and interannual variability. The value of these bimonthly data is greatly increased by the availability of continuous measurements at shore stations or moorings. Nearshore wind measurements would have been especially useful, but both NOAA and MBARI moorings had about six-month gaps during 1997-8.

Finally, it is noted that complete interpretation of the 1997-8 events in Central California waters awaits the analysis of biological and chemical data collected on these cruises. Current and biological measurements were made at moorings close to stations

67-55 and NPS3 in 1998. These data are being processed and will aid in understanding the patterns of variability described in this thesis.

LIST OF REFERENCES

Bacon, S., and Fofonoff, N., Oceanic Heat Flux Calculation, *Journal of Atmospheric and Oceanic Technology*, 13, 1327-1329, 1996.

Batten, M.L., Collins, C.A., and Gunderson, C.R., The effect of Salinity on Density in the California Current System, *Journal of Geophysical Research*, 100(C5), 8733-8749, 1995.

Bray, N.A., and Greengrove, C.L., Circulation over the shelf and Slope off Northern California, *Journal of Geophysical Research*, 98, 18119-18146, 1993.

Chavez, F.P., Forcing and biological impact of onset of the 1992 El Niño in Central California, *Geophysical Research Letters*, 23, 265-268, 1996

Chereskin, T.K., Morris, M.Y., Niiler, P.P., Kosro, P.M., Smith, R.L., Ramp, S.R. Collins, C.A., and Musgrave, D.L., Spatial and Temporal characteristics of the Mesoscale Circulation of the California Current from Eddy-Resolving Moored Measurements, *Journal of Geophysical Research*, in press, 1999.

Chereskin, T.K., and Trunnell, M., Correlation scales, Objective Mapping, and Absolute Geostrophic Flow in the California Current., *Journal of Geophysical Research*, 101(C10), 22 619-22 629, 1996.

Cole, D.A., McLain, D.R., Interannual Variability of Temperature in the Upper Layer of the North Pacific Eastern Boundary region, 1971-1987, NOAA-TM-NMFS-SWFC-125, 12pp, 1989.

Collins, C.A., Garfield, N., Rago, T.A., Rischmiller, F.W., and Carter, E., Mean Structure of the Inshore Countercurrent and California Undercurrent off Point Sur, California, Deep – Sea Research in Press, 1999.

Collins, C.A., Paquette, R.G., and Ramp, S.R., Annual Variability of Ocean Currents at 350-m Depth Over the Continental Slope off Point Sur, California, CalCOFI Rep, 37, 257-263, 1996.

Fofonoff, N.P., A New Salinity Scale and Equation of State for Seawater, *Journal of Geophysical Research*, 90, 3332-3342, 1985.

Flament, P., A Note on Seawater Spiciness and Diffusive Stability, Unpublished, 12pp, 1986.

Garfield, N., Collins, C.A., Paquette, R.G., and Carter, E., Lagrangian Exploration of the California Undercurrent, 1992-95, *Journal of Physical Oceanography*, 29, 560-583, 1999.

Legier, D.M., Empirical Orthogonal Function Analysis of Wind Vectors over the Tropical Pacific Region, *Bulletin American Meteorological Society*, 64(3), 234-241, 1983.

Lenarz, W.H., Van Tresca, D, Graham, W.M., Schiwng, F.B., Chavez, F.P., Explorations of El Niño and associated biological population dynamics off Central California, In El Niño off Central California. CalCOFI Rep, 36, 106-119, 1995.

Lynn, R.J., and Simpson, J.J., The California Current System: The Seasonal Variability of its Physical Characteristics, *Journal of Geophysical Research*, 92(C12), 12947-12966, 1987.

Lynn, R.J., and Simpson, J.J., The Flow of the Undercurrent over the Continental Borderland off Southern California, *Journal of Geophysical Research*, 95, 12995-13008, 1990.

McGowan, J.A., Cayan, D.R., and Dorman, L.M., Climate-ocean variability and ecosystem response in the Northeast Pacific, Science, 281, 210-217, 1998.

McLain, D.R., and Thomas, D.H., Year-to-year Fluctuations of the California Countercurrent and Effects on Marine Organisms, CalCOFI Rep., 24, 165-181, 1983.

Rago, T.A., Locke, J.G.,Collins, C.A., An Atlas of the Hydrographic Stations Off Point Sur, California April 1988-April 1991, Naval Postgraduate School Technical Report NPS-oc-97-006, Monterey, California, 427pp, 1997.

Ramp, S.R., McClean, J.L., Collins, C.A., Semtner, A.J., and Hays, K.A.S., Observations and Modeling of the 1991-1992 El Niño Signal off Central California, *Journal of Geophysical Research*, 102(C3), 5553-5582, 1997.

Rasmusson, E.M., and Wallace, J.M., Meterological aspects of El Niño/Southern Oscillation, Science, 1195-1201, 1983.

Reid, J.L.Jr., Oceanography of the Northeastern Pacific Ocean During the Last Ten Years, CalCOFI Rep., V11, 77-90, 1960.

Reid, J.L.Jr., Roden, G.I., and Wyllie, J.G., Studies of the California Current System, CalCOFI Reports, 6, 28-56, 1959.

Schwing, F., O'Farreu, M., Steger, J., and Balts, K., Coastal Upwelling Indices, West Coast of North America, 1946-1995, U.S. Department of Commerce, NOAA Technical Memorandum NOAA-TM-NMFS-SWFS-231, La Jolla, California, 207pp, 1996.

Simpson, J.J., El Niño-Induced Onshore Transport in the California Current During 1982-1983, *Geophysical Research Letters*, 11(3), 241-242, 1984.

Steger, J.M., Collins, C.A., and Chu, P.C., Circulation in the Archipiélago de Colón (Galapagos Island), November, 1993, Deep-Sea Research 2, 45, 1093-1114, 1998.

Tisch, T.D., Ramp, S.R., and Collins, C.A., Observations of the Geostrophic Current and Water Mass Characteristics off Point Sur,California, From May 1988 Through November 1989, *Journal of Geophysical Research*, 97(C8), 12, 535, 12555, 1992.

University of California, San Diego., Surface Water Temperatures, Salinities and Densities at Shore Stations, United States West Coast, 1994, SIO Reference 95-30, 45pp, 1995.

Wolter, K., and Timlin, M.S., Measuring the Strength of ENSO – how does 1997/98 rank?, *Weather*, 53, 315-324., 1998.

APPENDIX A: HYDROGRAPHIC SECTIONS

For each cruise, sections of potential temperature (θ), salinity, density anomaly (γ_θ), and spiciness (π_θ) have been contoured for the upper 500 dbar and are included in this appendix. Density anomaly was computed using the 1980 Equation of State (Fofonoff, 1987) and spiciness was computed using Flament's algorithm (Flament, 1986). Sections were contoured using a program called SURFER™ using objectively mapped data (objective mapping procedures are described in Chapter 2). Dates for cruises are given in Table 1.

The ocean bottom exists along the lower right ordinate of each section, extending from 240 dbar at a distance of 0 km to 500 kbar at a distance of 10 km. The bottom is not drawn on the sections. Instead, data from offshore stations were objectively mapped onto the ordinate.

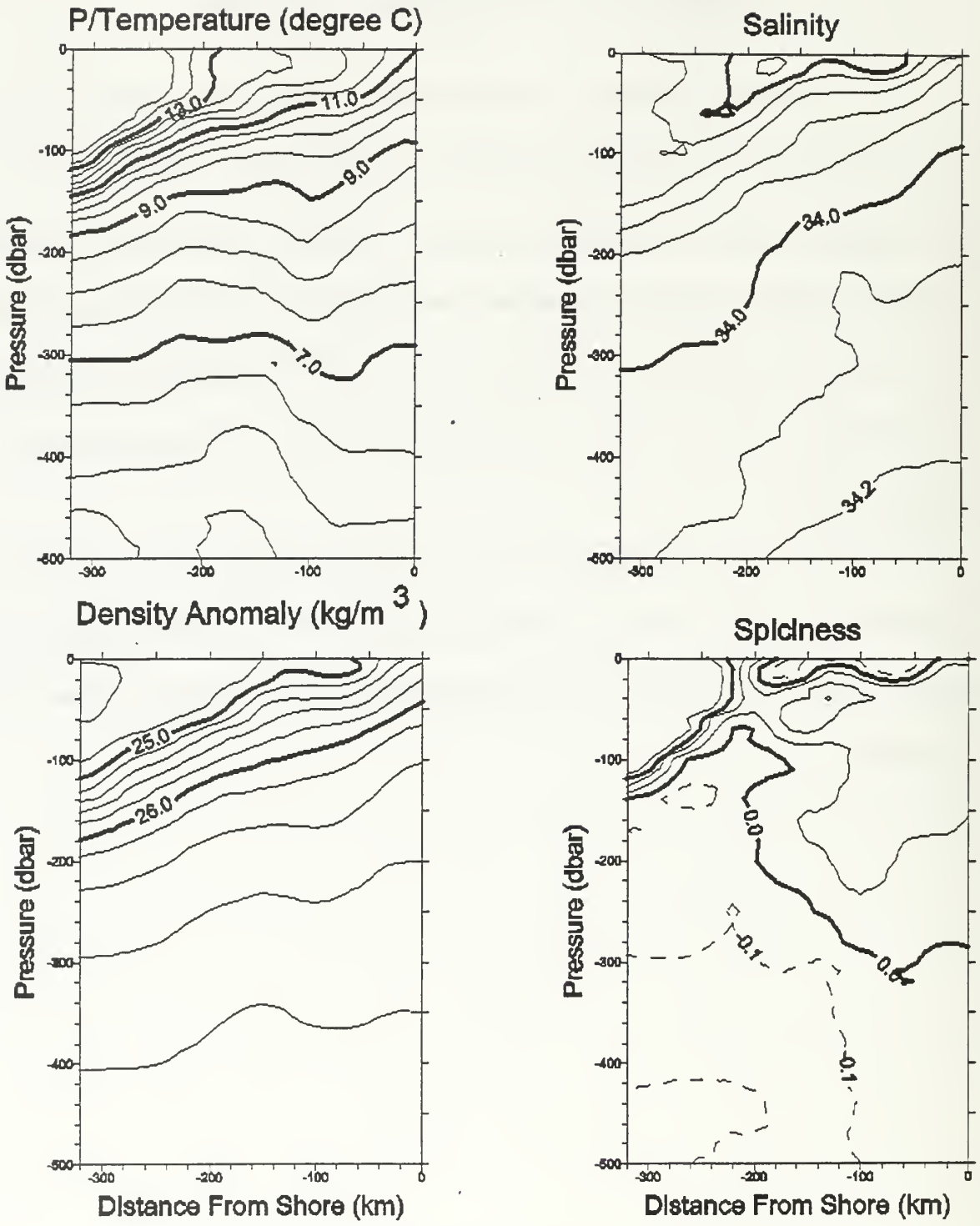

February 23-4 1997

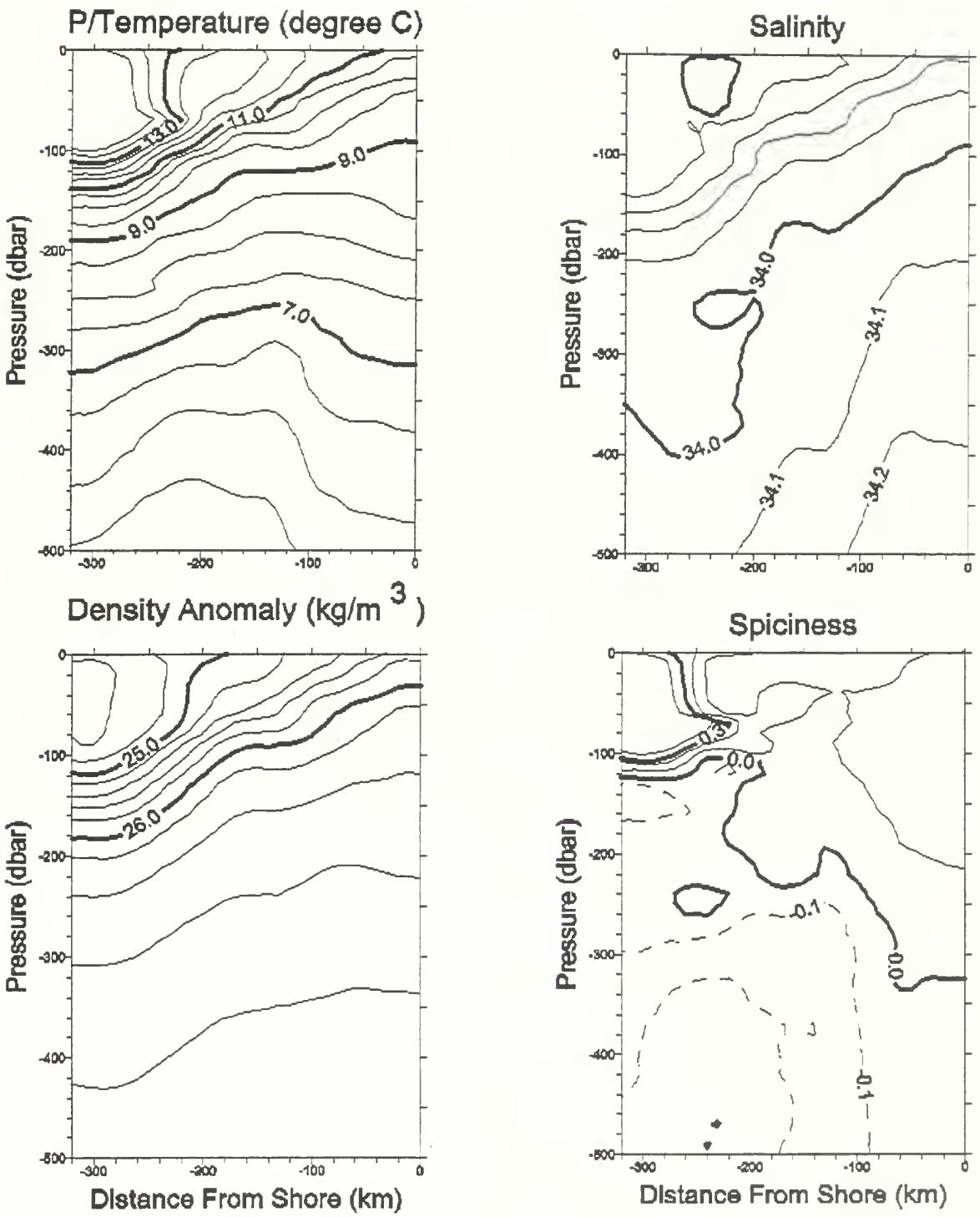
P/Temperature (degree C)
Pressure (dbar)
13.0
11.0
9.0
9.0
7.0
Salinity
Pressure (dbar)
34.0
34.1
34.0
34.1
34.2
Density Anomaly (kg/m 3)
Pressure (dbar)
25.0
26.0
Distance From Shore (km)
Spiciness
Pressure (dbar)
0.3
0.0
0.1
0.0
-0.1
Distance From Shore (km)

March 6-7 199

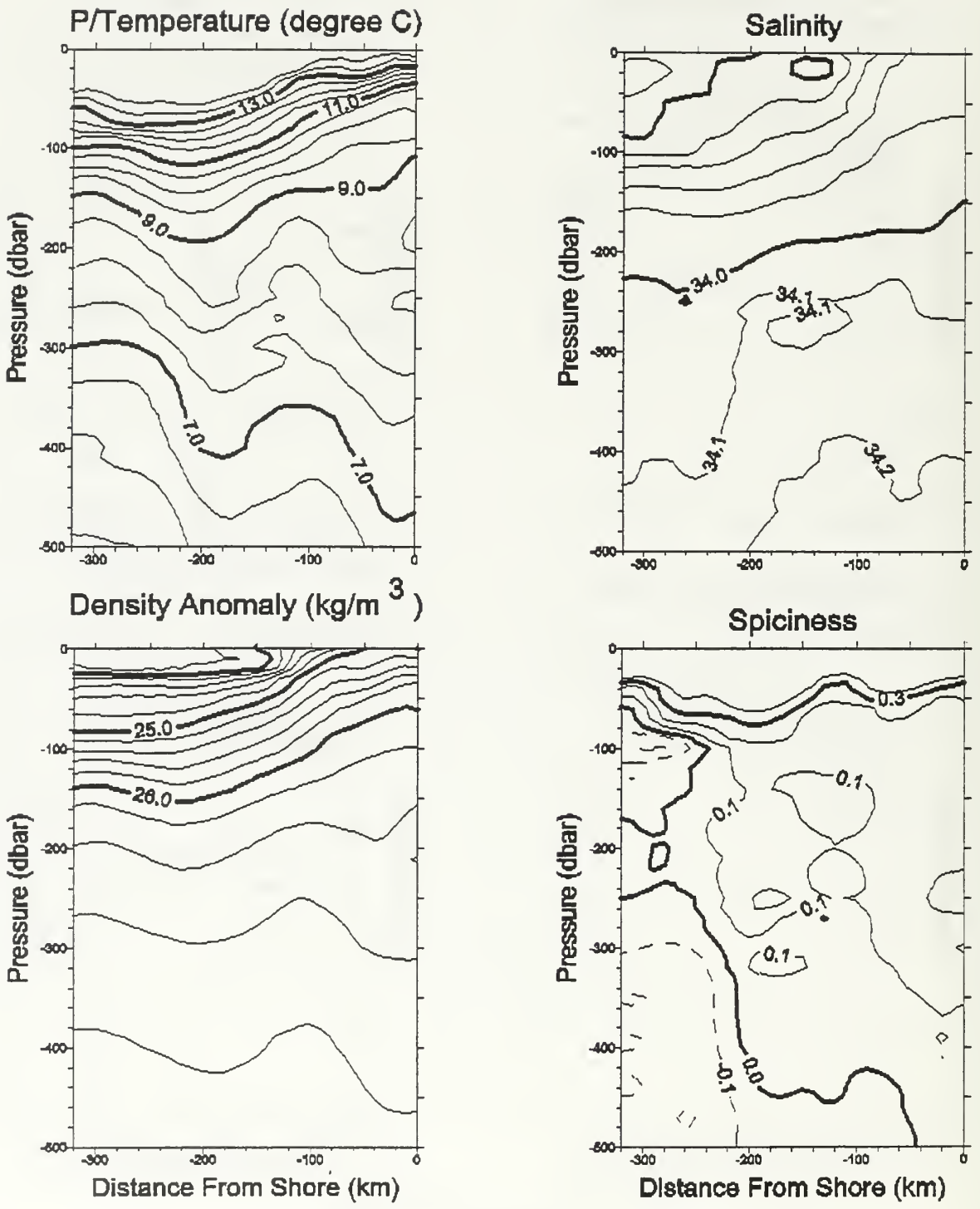
P/Temperature (degree C)
Pressure (dbar)
13.0
11.0
9.0
8.0
7.0
7.0
Salinity
Pressure (dbar)
34.0
34.1
34.1
34.1
34.2
Density Anomaly (kg/m 3)
Pressure (dbar)
25.0
26.0
Distance From Shore (km)
Spiciness
Pressure (dbar)
0.3
0.1
0.1
0.1
0.1
0.0
-0.1
Distance From Shore (km)

June 2-5 1997

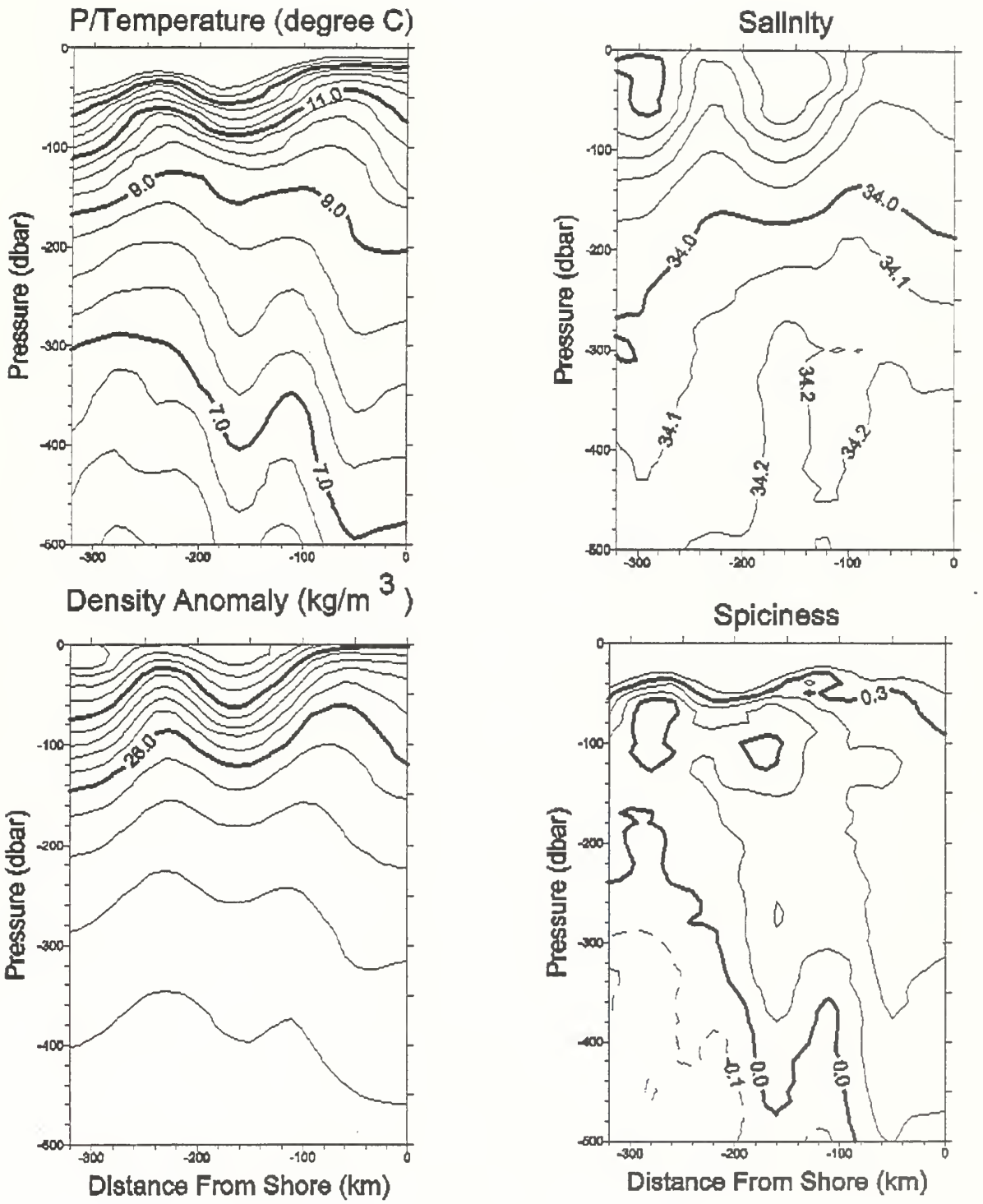

July 26-28 1997

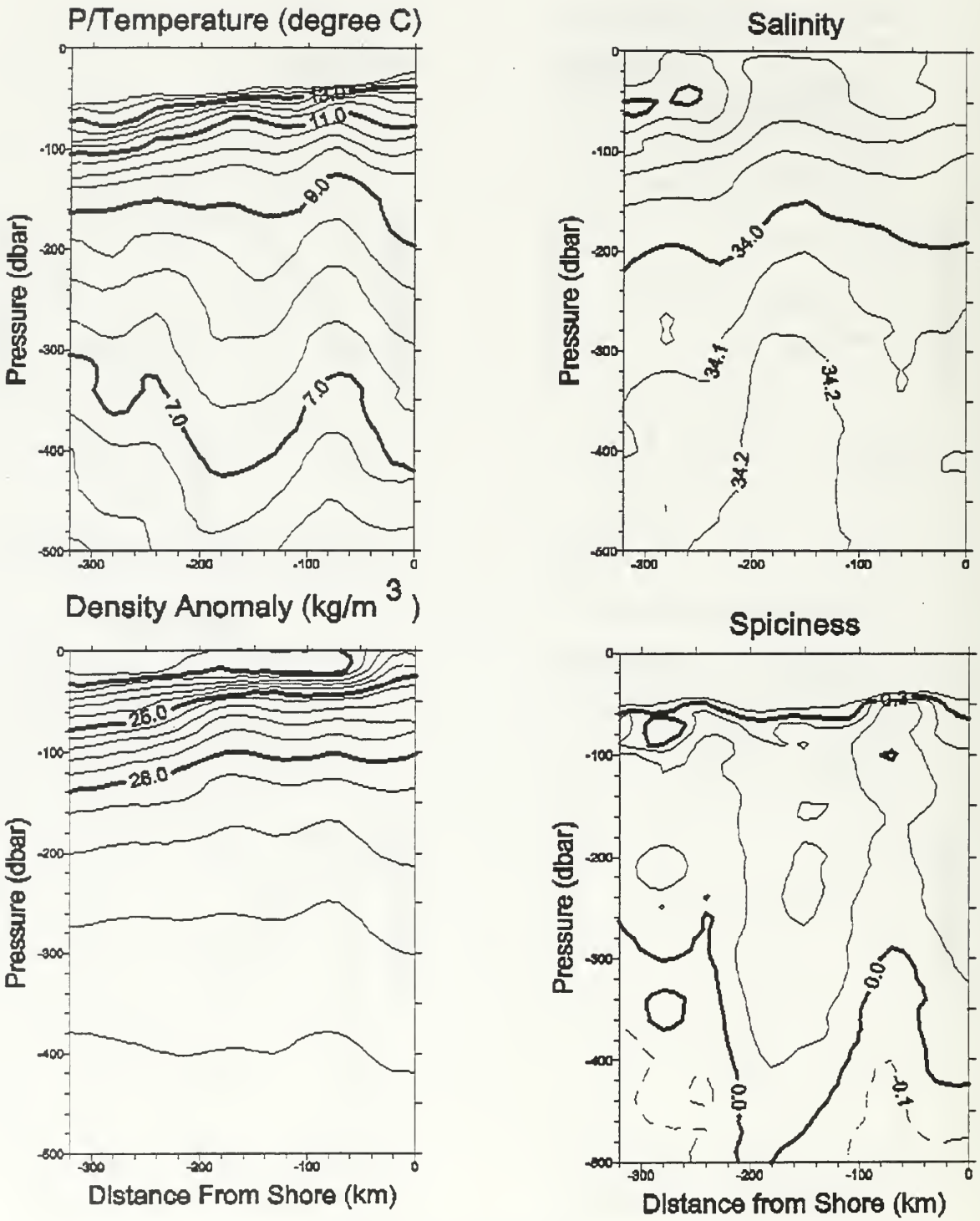

September 12-14 1997

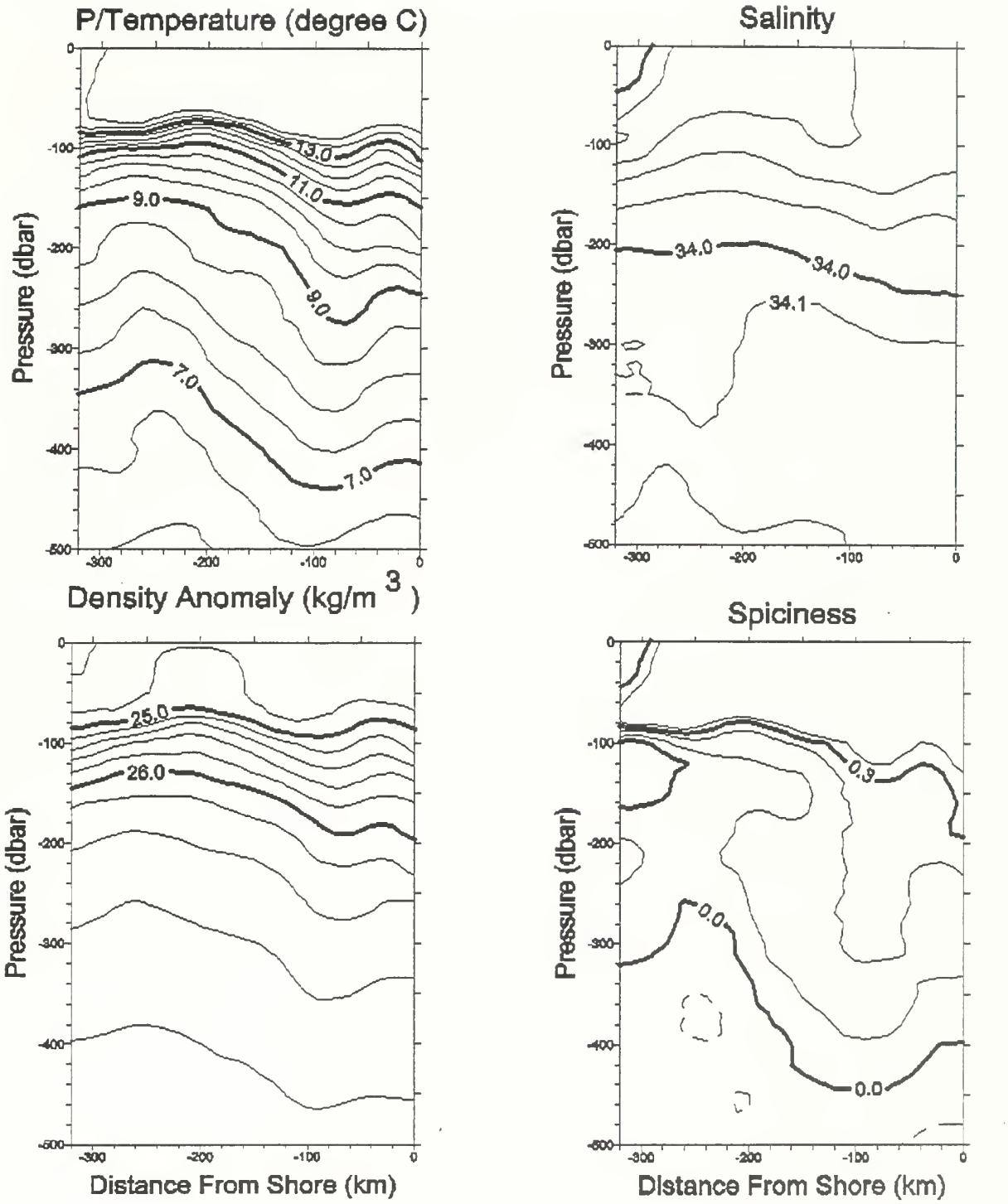

January 21-24 1998

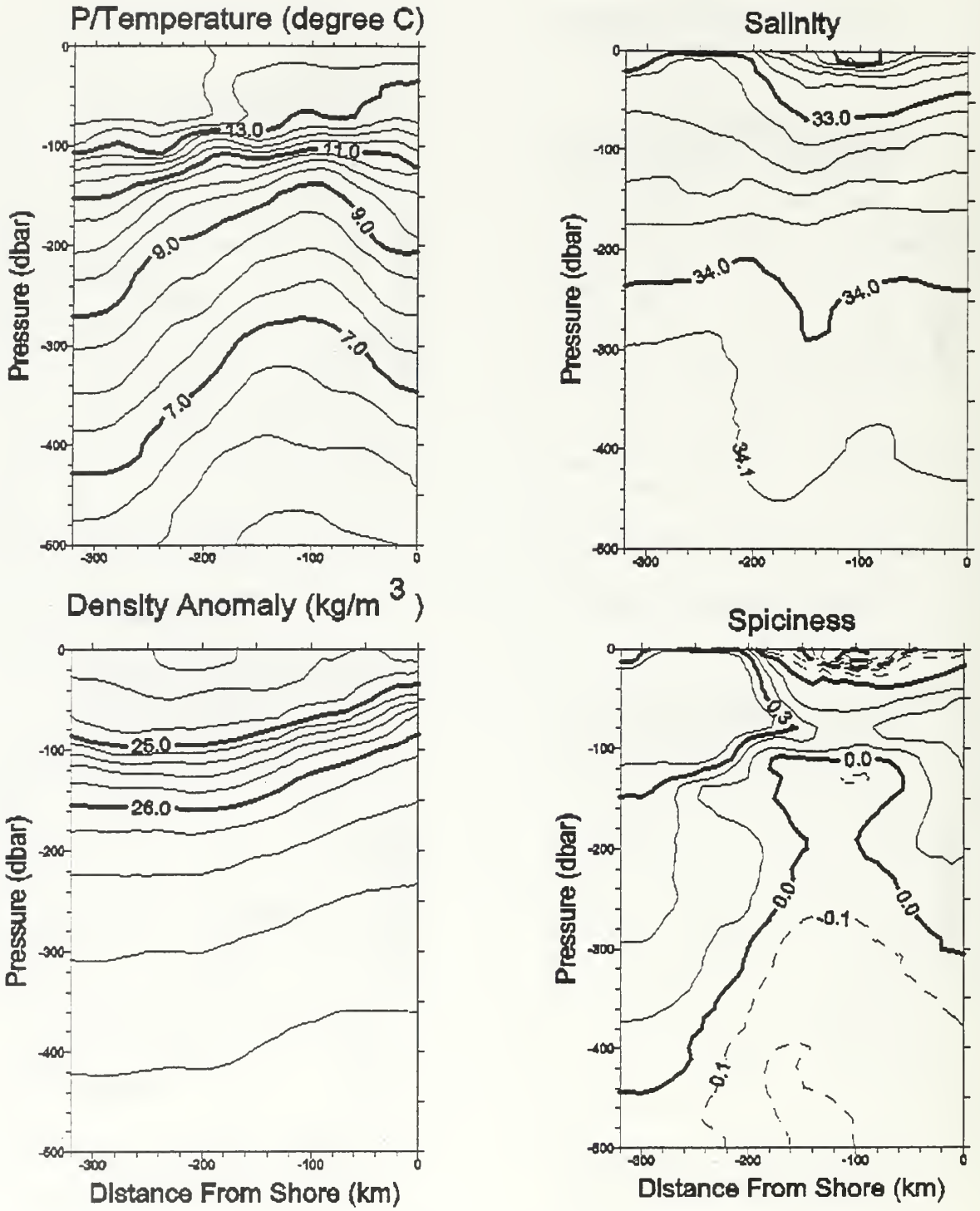

March 21-23 1998

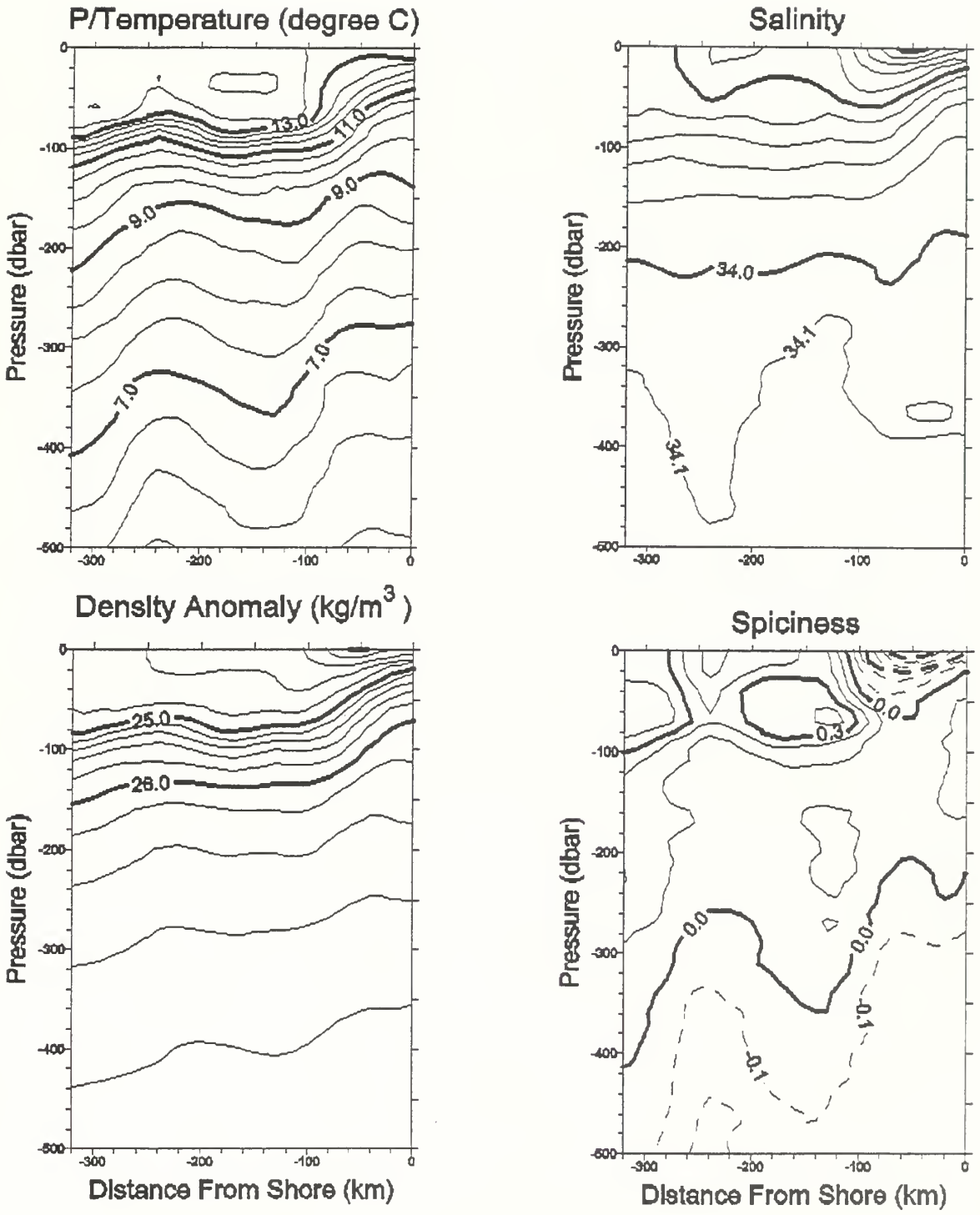

April 14-17 1998

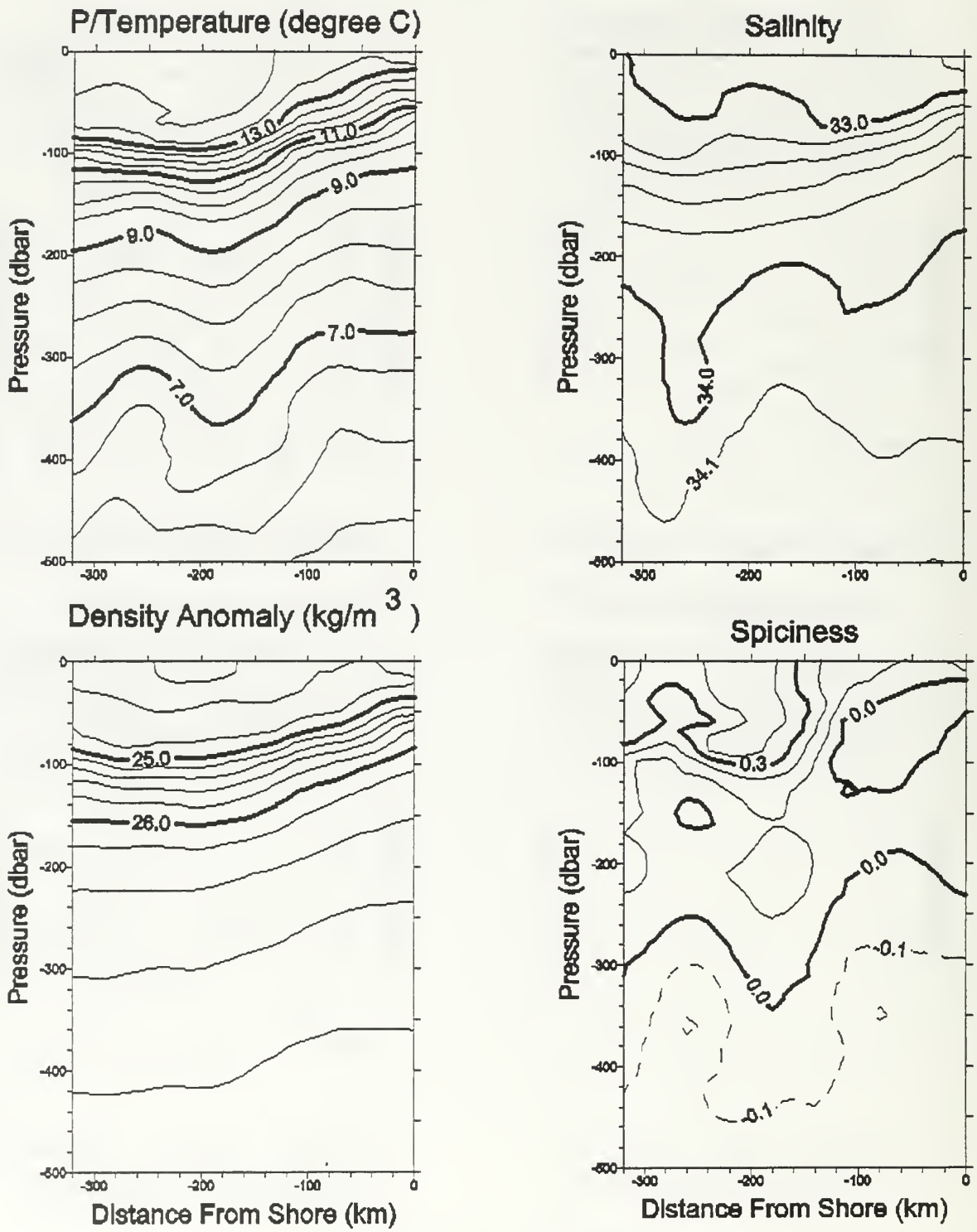
P/Temperature (degree C)
Salinity
Density Anomaly (kg/m 3)
Spiciness
Pressure (dbar)
Distance From Shore (km)
13.0
11.0
9.0
9.0
7.0
7.0
33.0
34.0
34.1
25.0
26.0
0.0
0.3
0.0
0.0
-0.1
-0.1
0
-100
-200
-300
-400
-500
-300
-200
-100
0

May 9-12 1998

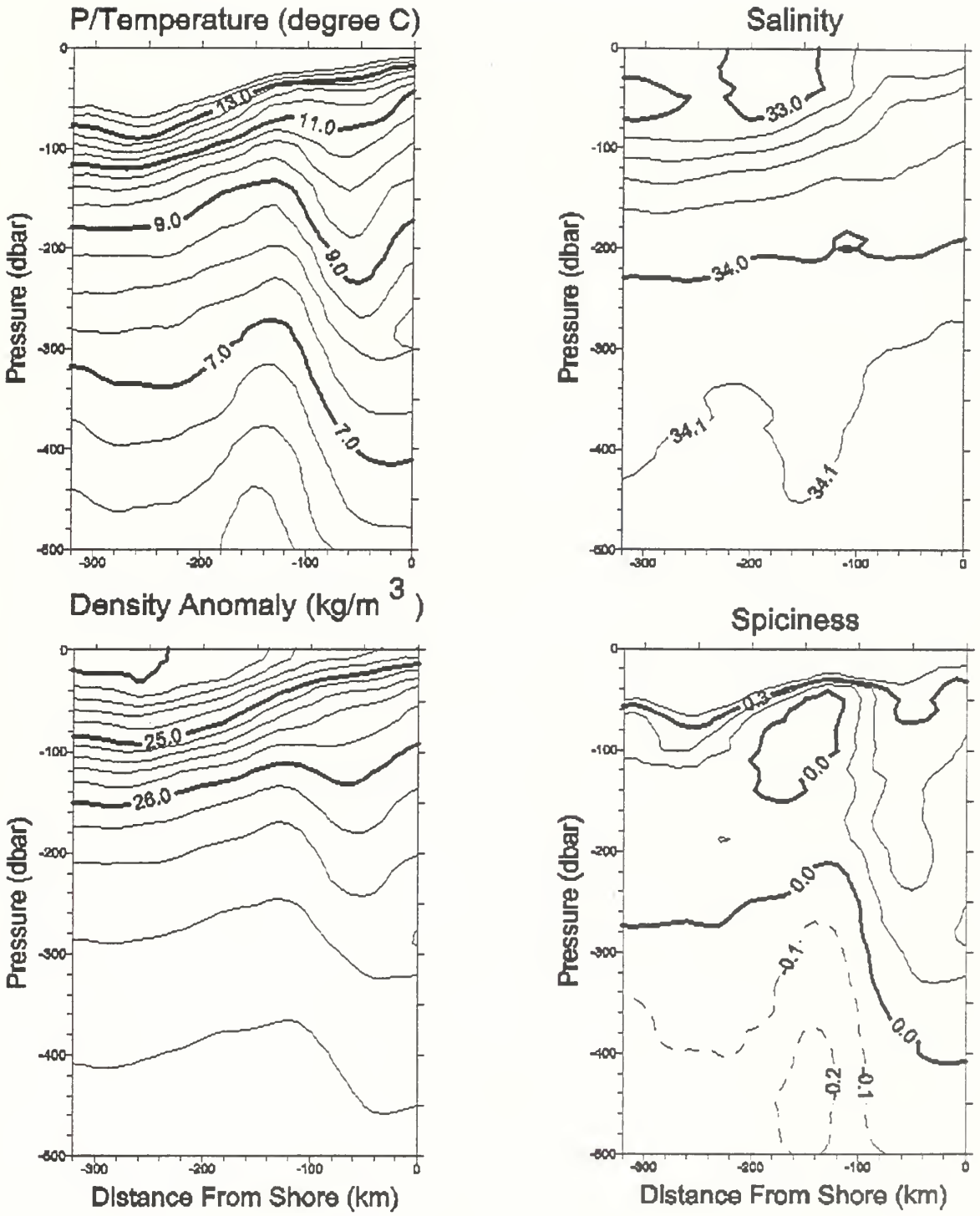
P/Temperature (degree C)
Salinity
Density Anomaly (kg/m 3)
Spiciness
Pressure (dbar)
Distance From Shore (km)
13.0
11.0
9.0
7.0
33.0
34.0
34.1
25.0
26.0
0.3
0.0
-0.1
-0.2
0
-100
-200
-300
-400
-500

July 2-4 1998

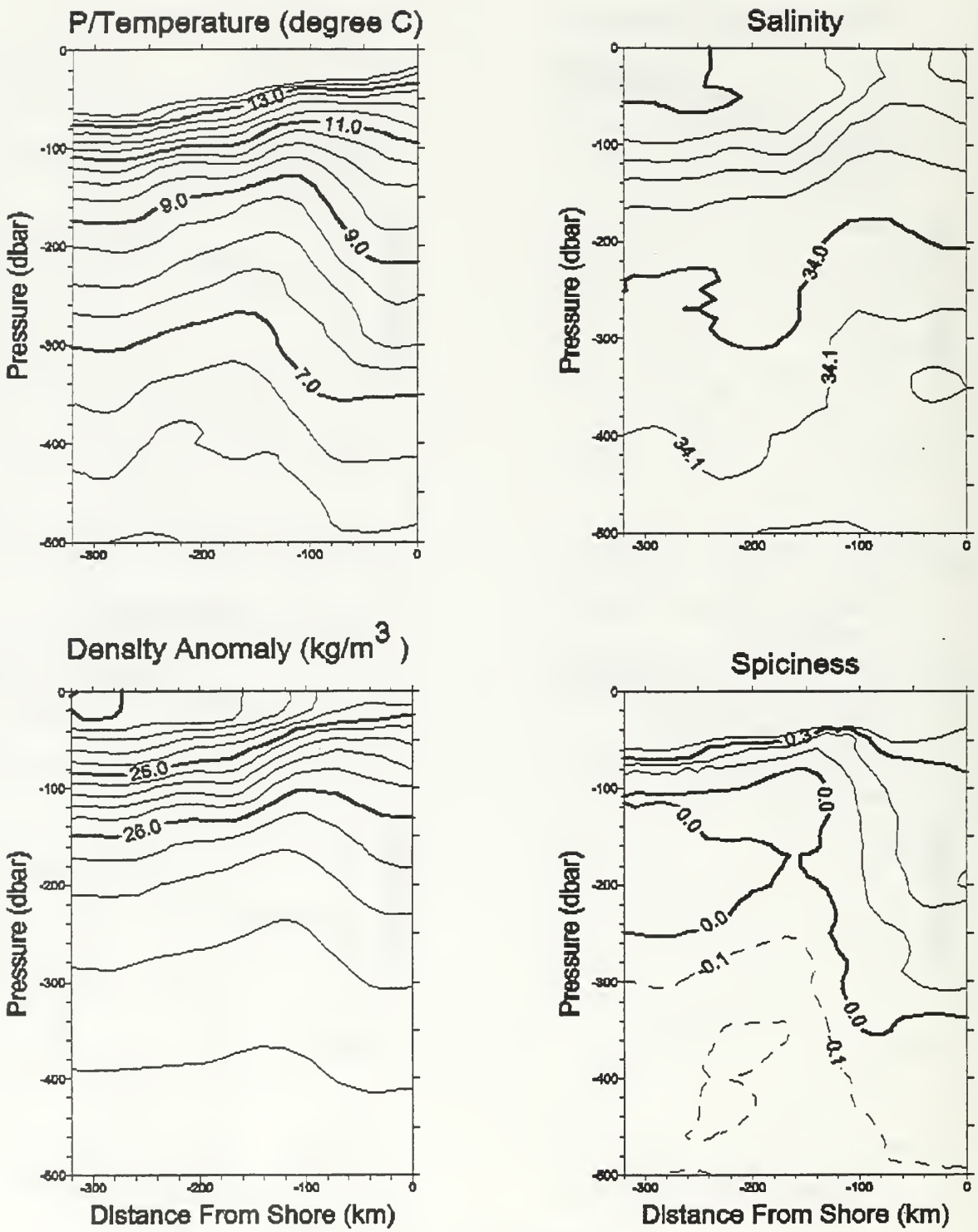

August 22-25 1998

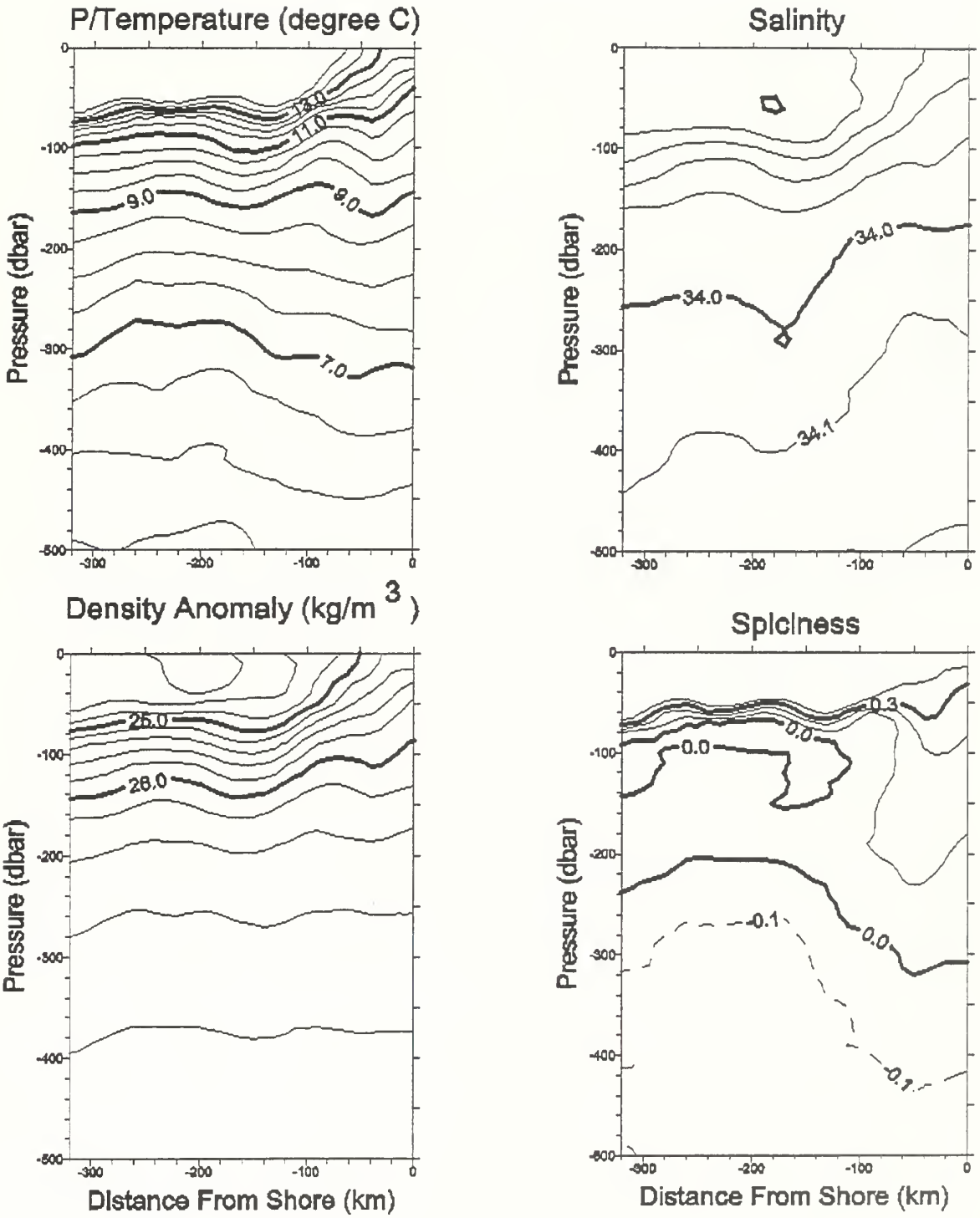

November 6-9 1998

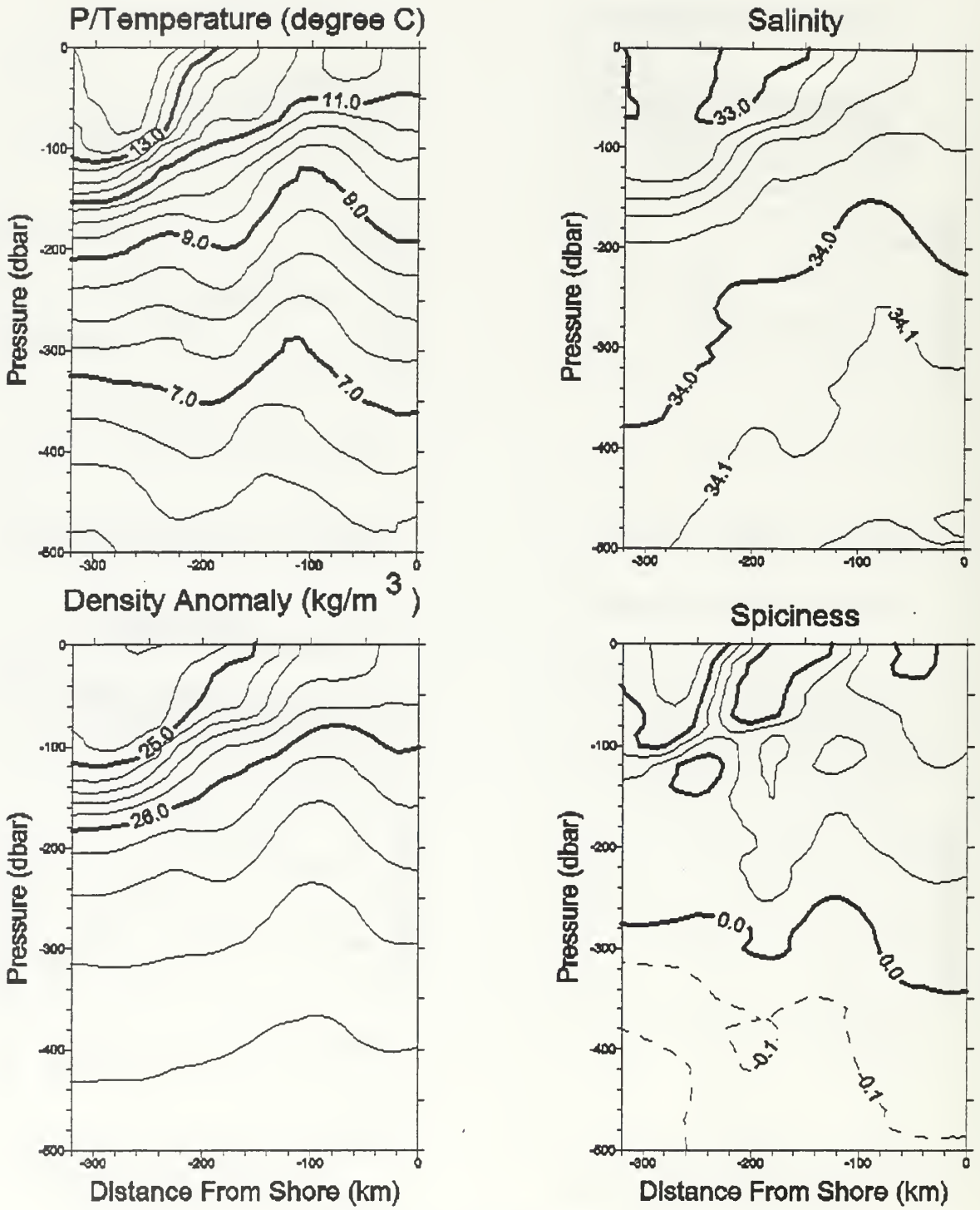

January 14-16 1999

APPENDIX B: VELOCITY CHARTS

Vector charts of observed velocity (vessel-mounted acoustic Doppler current profiler) for each cruise are included in this appendix. The vectors represent averages of all available data within a given one-hour period. Charts are included for four levels: from the first bin (11 or 12 m) to 25 m, 25 m to 75 m, 75 m to 125 m, and 125 m to 200 m. All data were processed using CODAS3 software provided by the University of Hawaii. The CODAS3 software (a program called 'vector') also produced the charts included in this appendix.

Dr. Jules Hummon and Prof. Eric Firing provided us with the CODAS3 software and taught us how to use it. We gratefully acknowledge their generosity and assistance.

February 22-23, 1997

R/V Point Sur

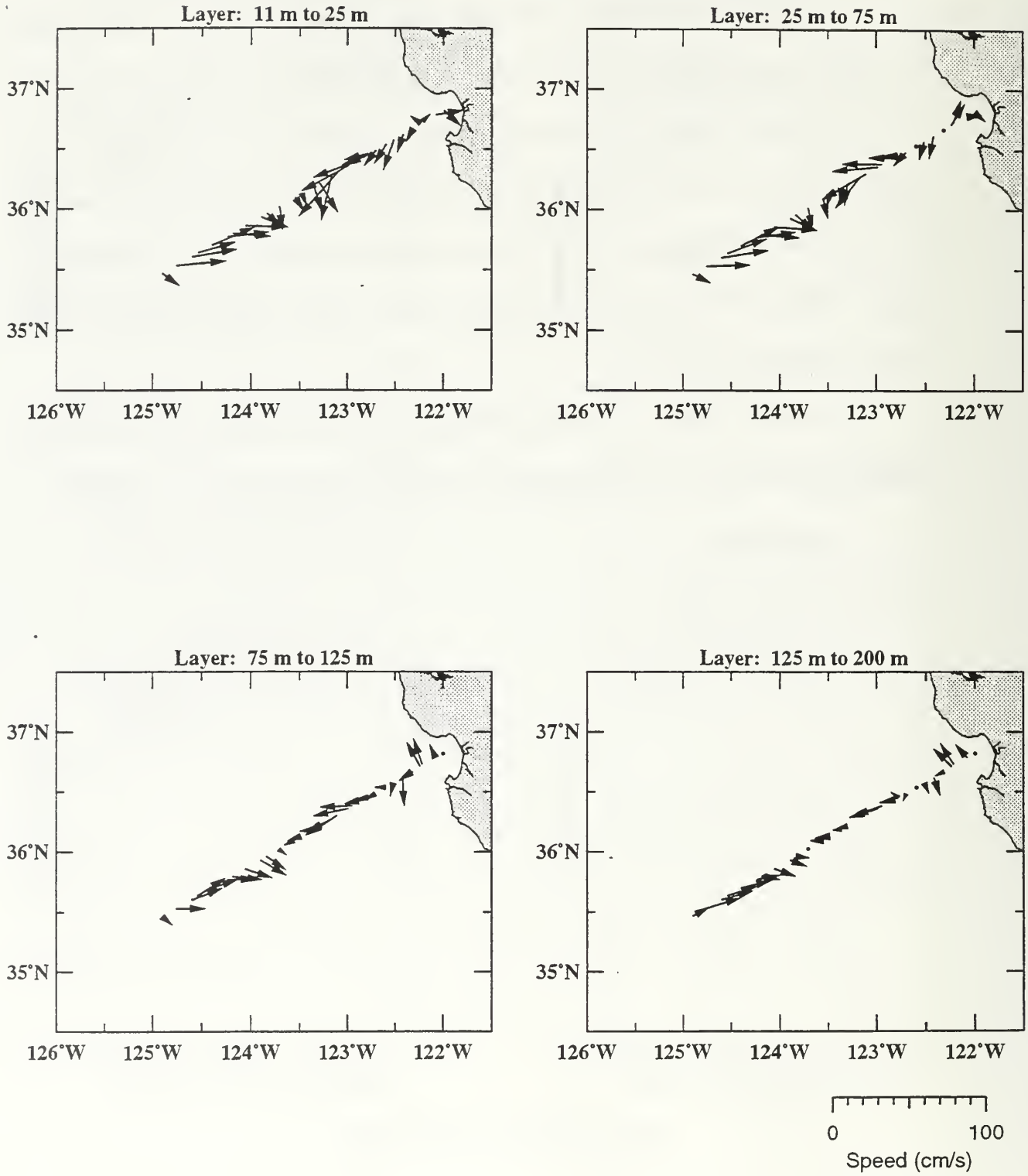

June 2-6, 1997

R/V Point Sur

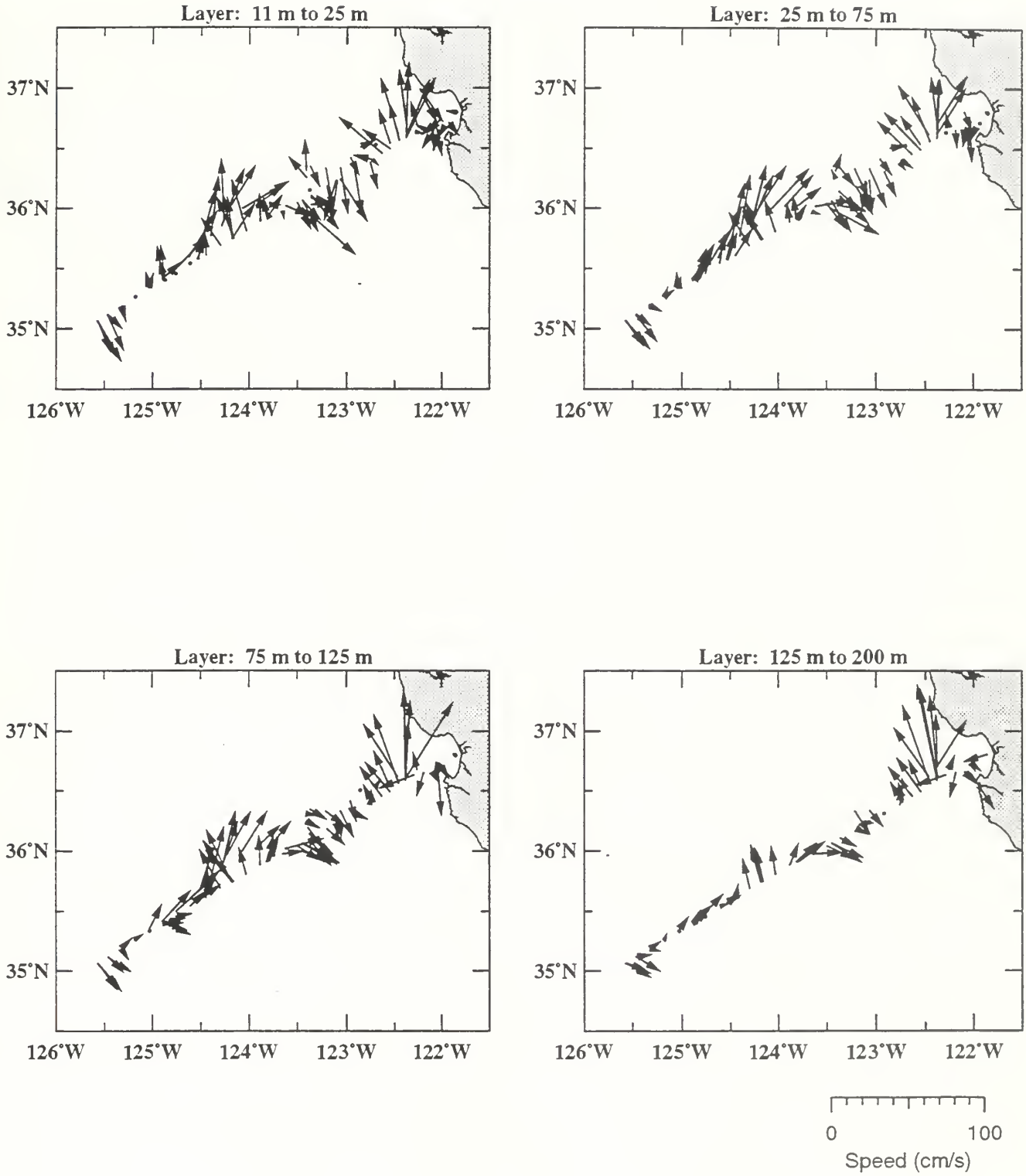

July 20-29, 1997

R/V Point Sur

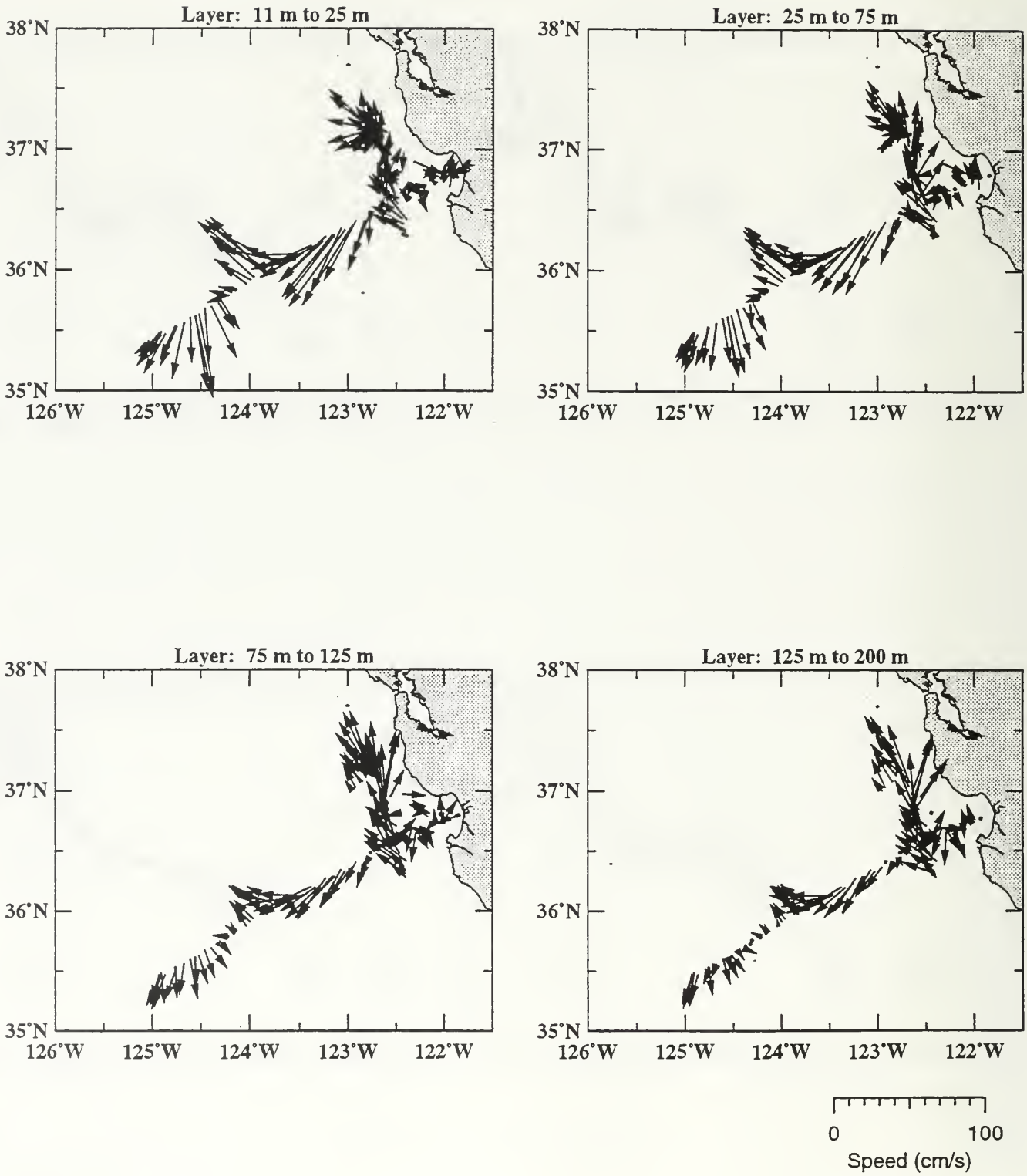

September 12-14, 1997

R/V New Horizon

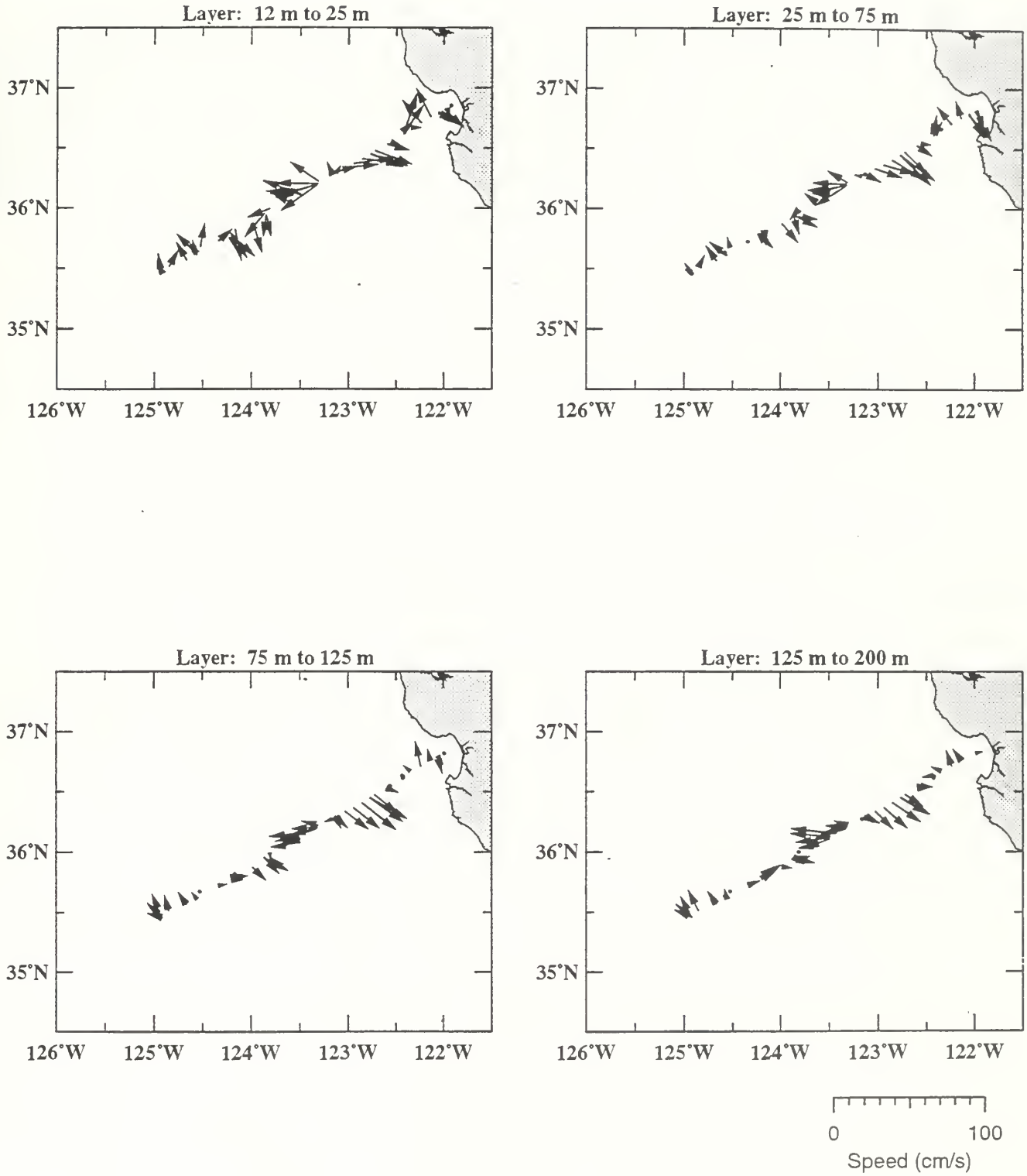

November 11-14, 1997

R/V Point Sur

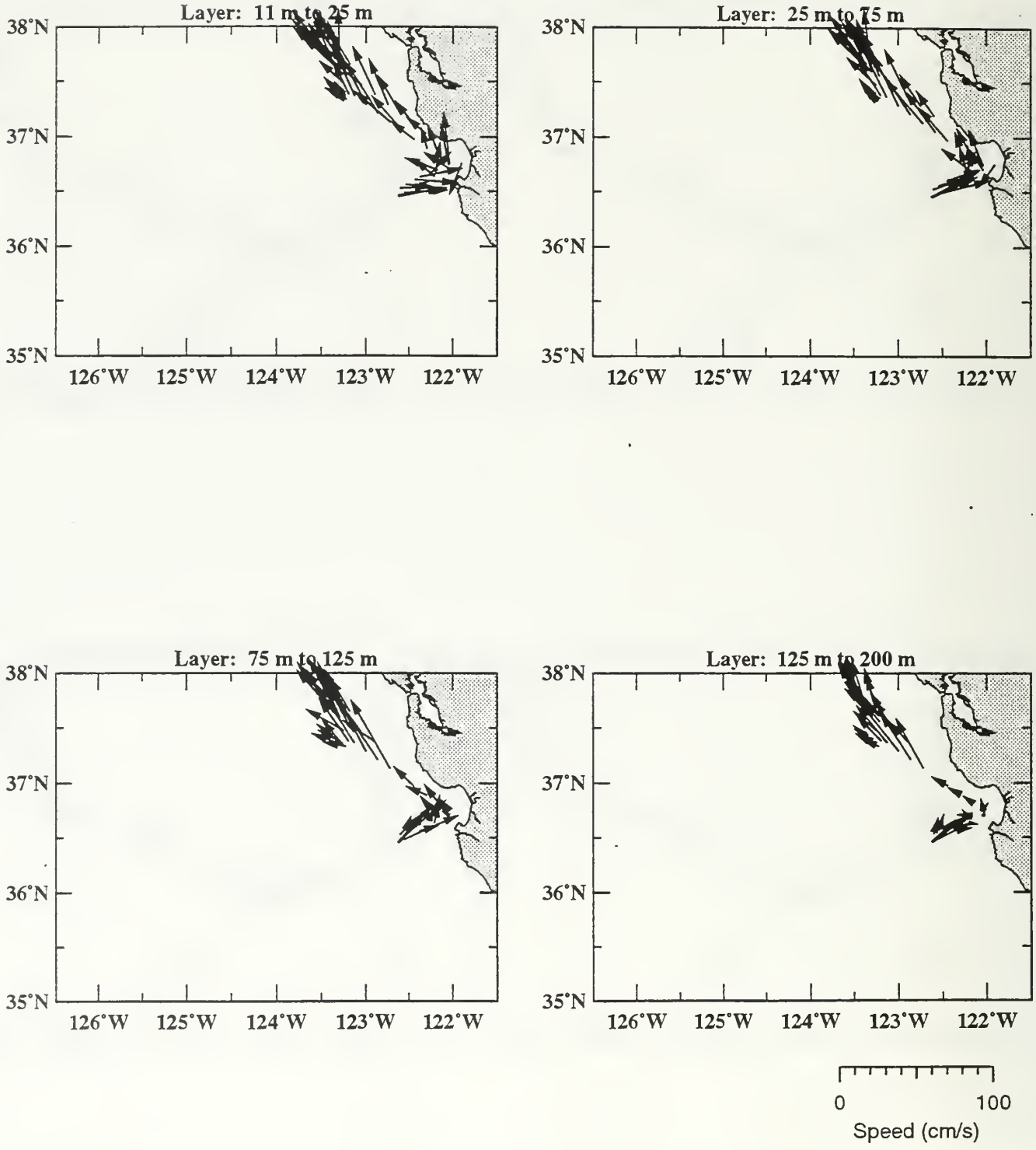

January 21-24, 1998

R/V Point Sur

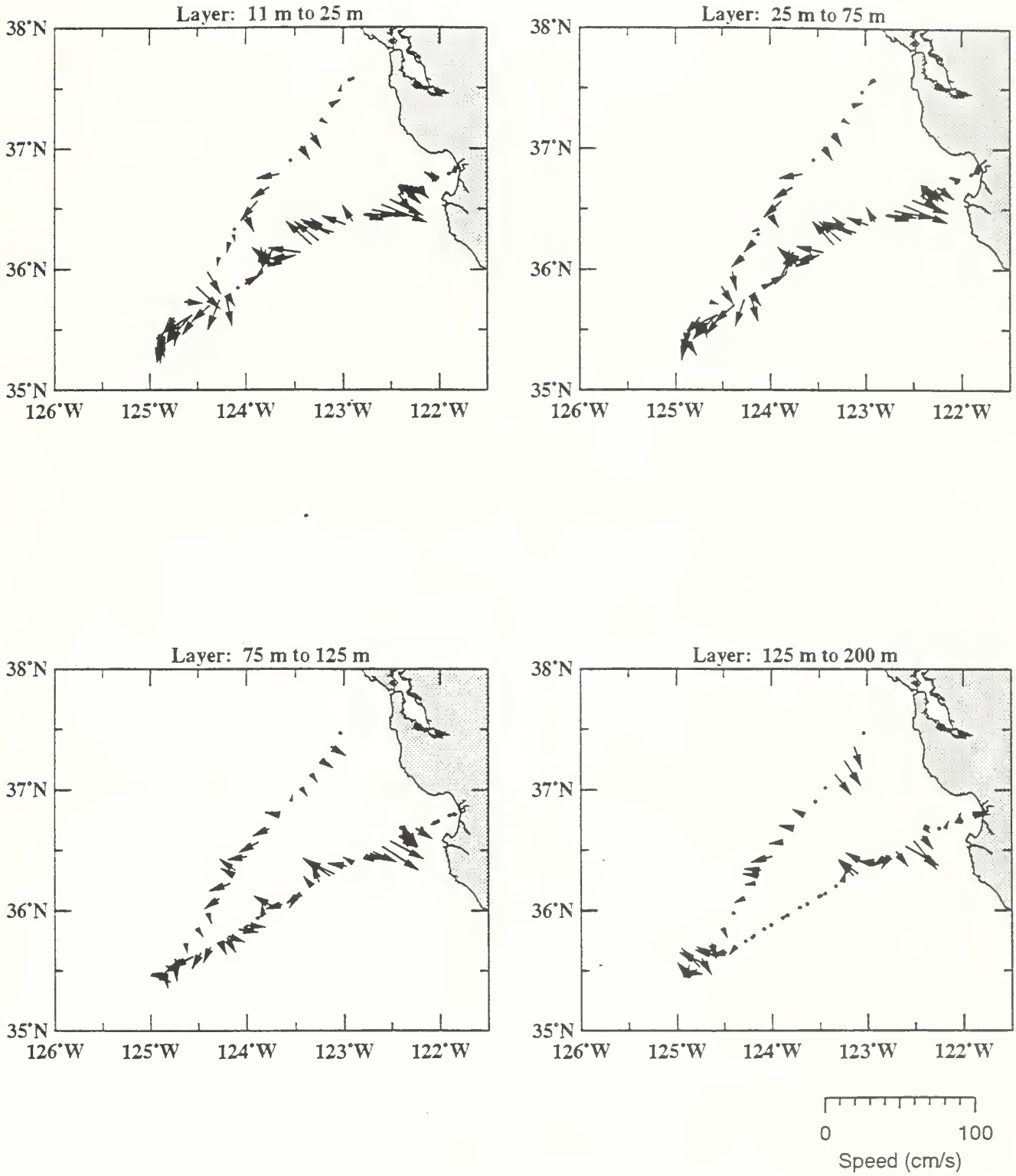

March 21-23, 1998

R/V New Horizon

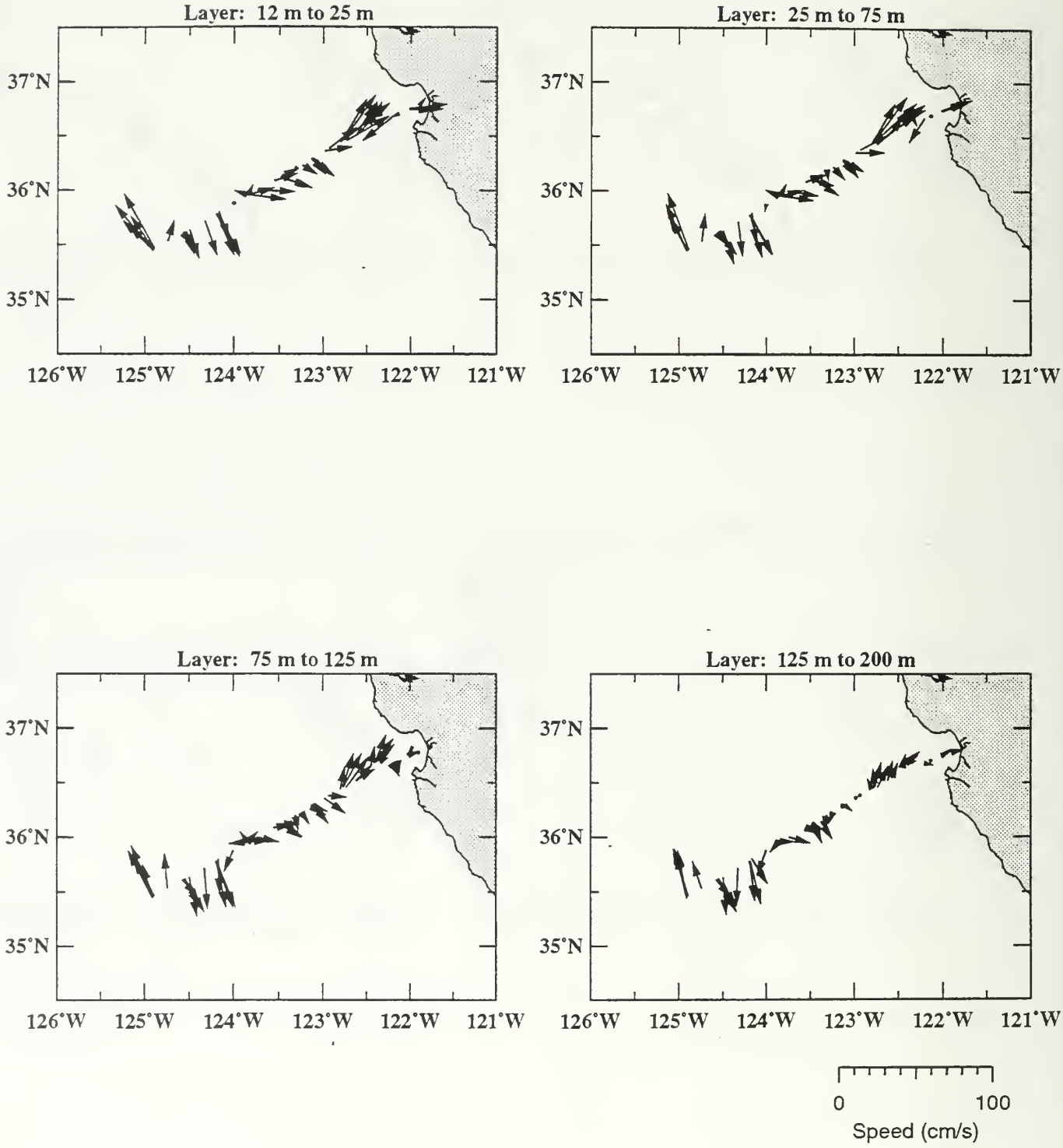

April 14-17, 1998

NOAA Ship McArthur

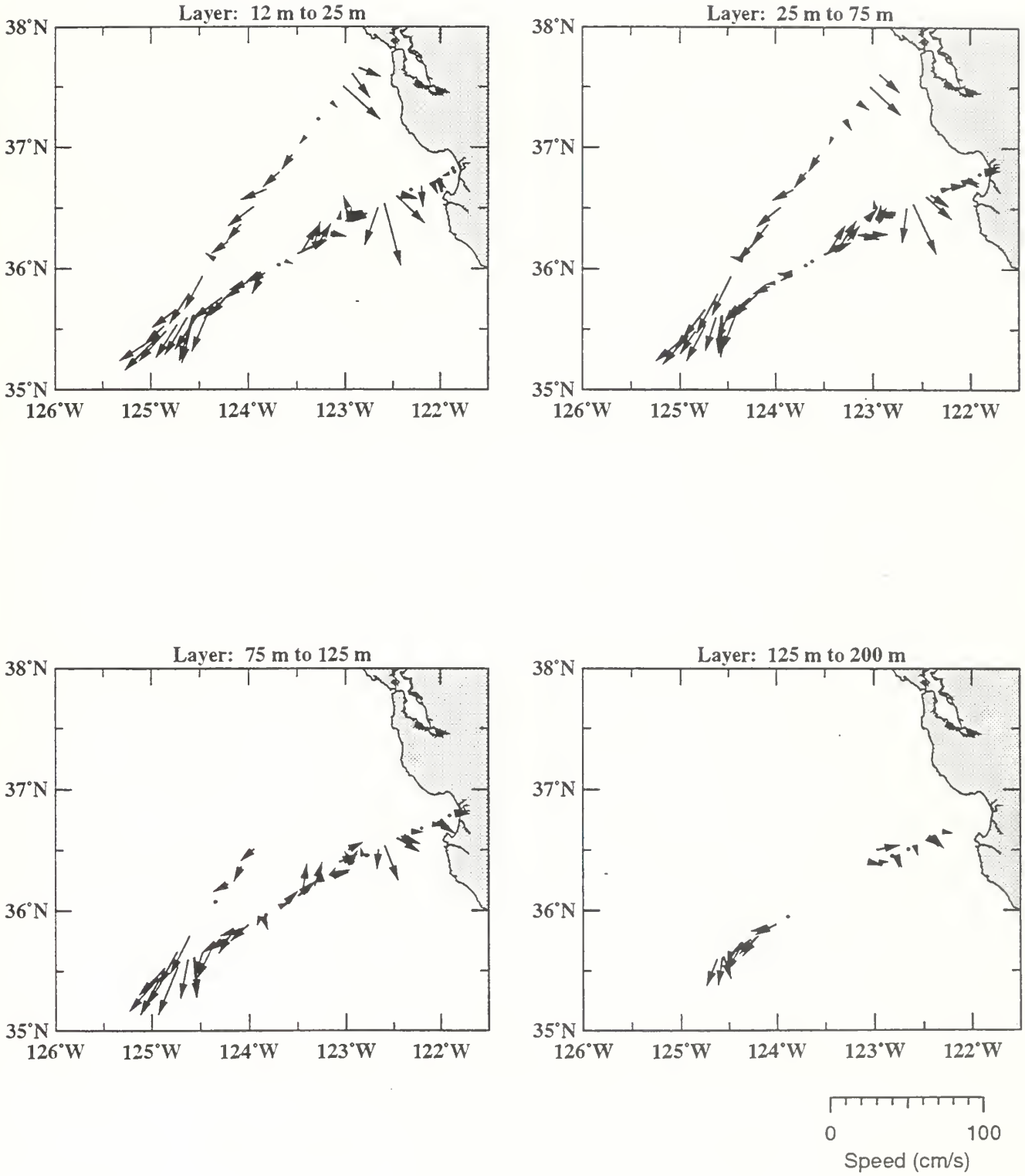

May 9-12, 1998

R/V New Horizon

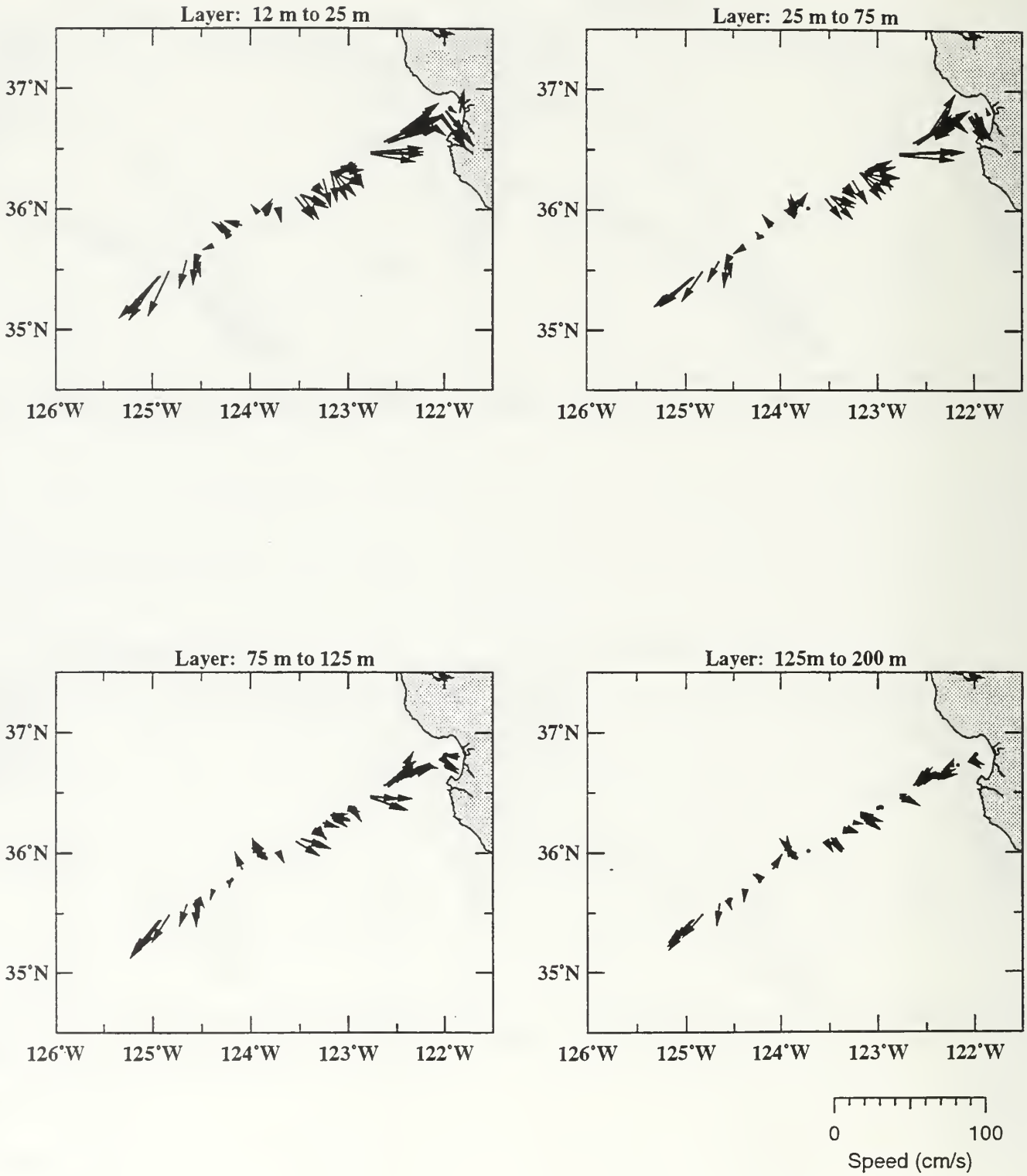

July 29-August 5, 1998

R/V Point Sur

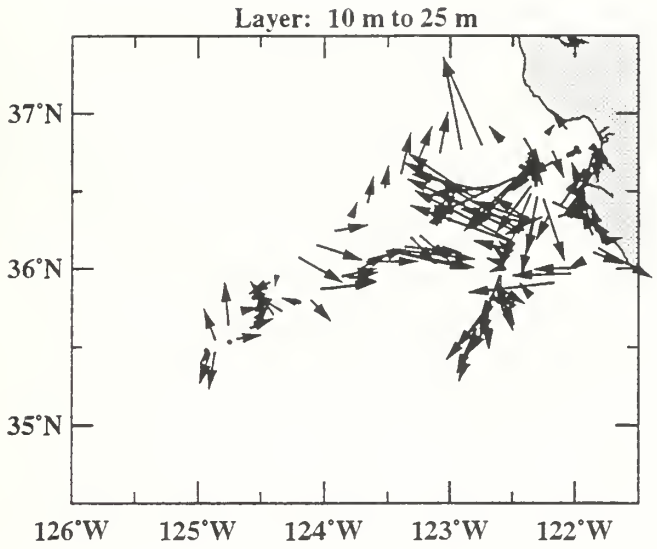

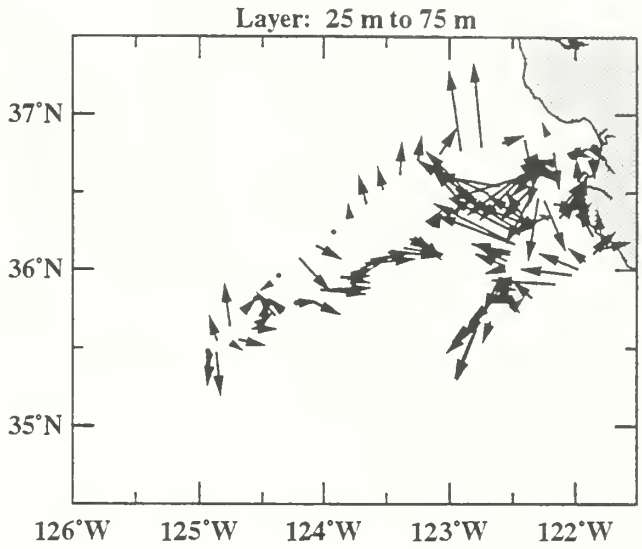

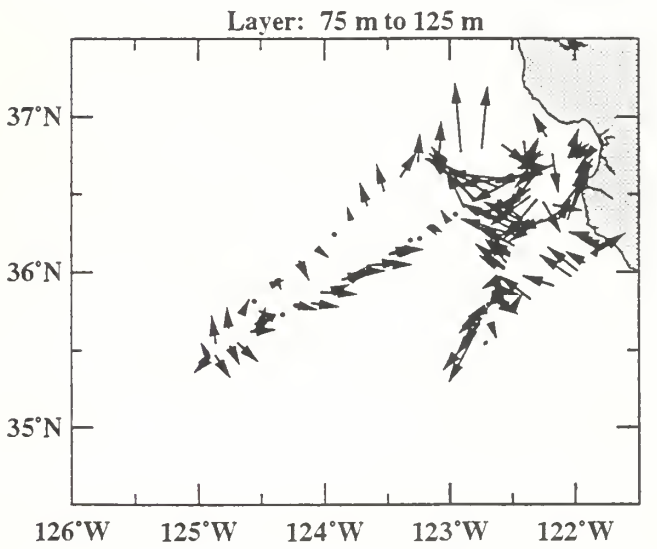

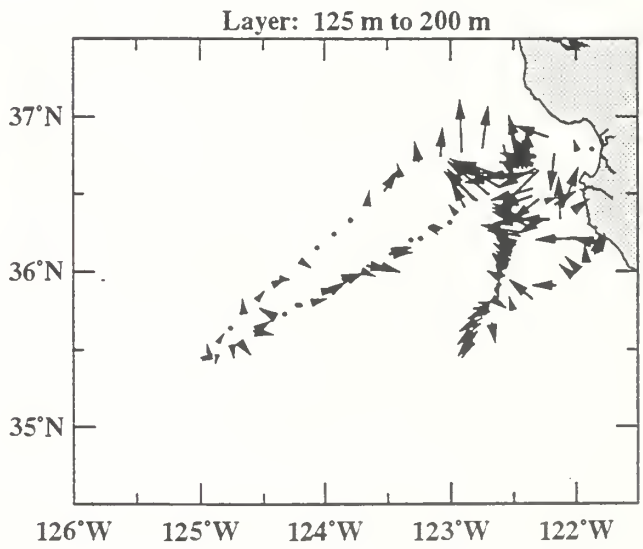

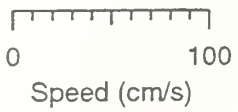

August 22-28, 1998

R/V New Horizon

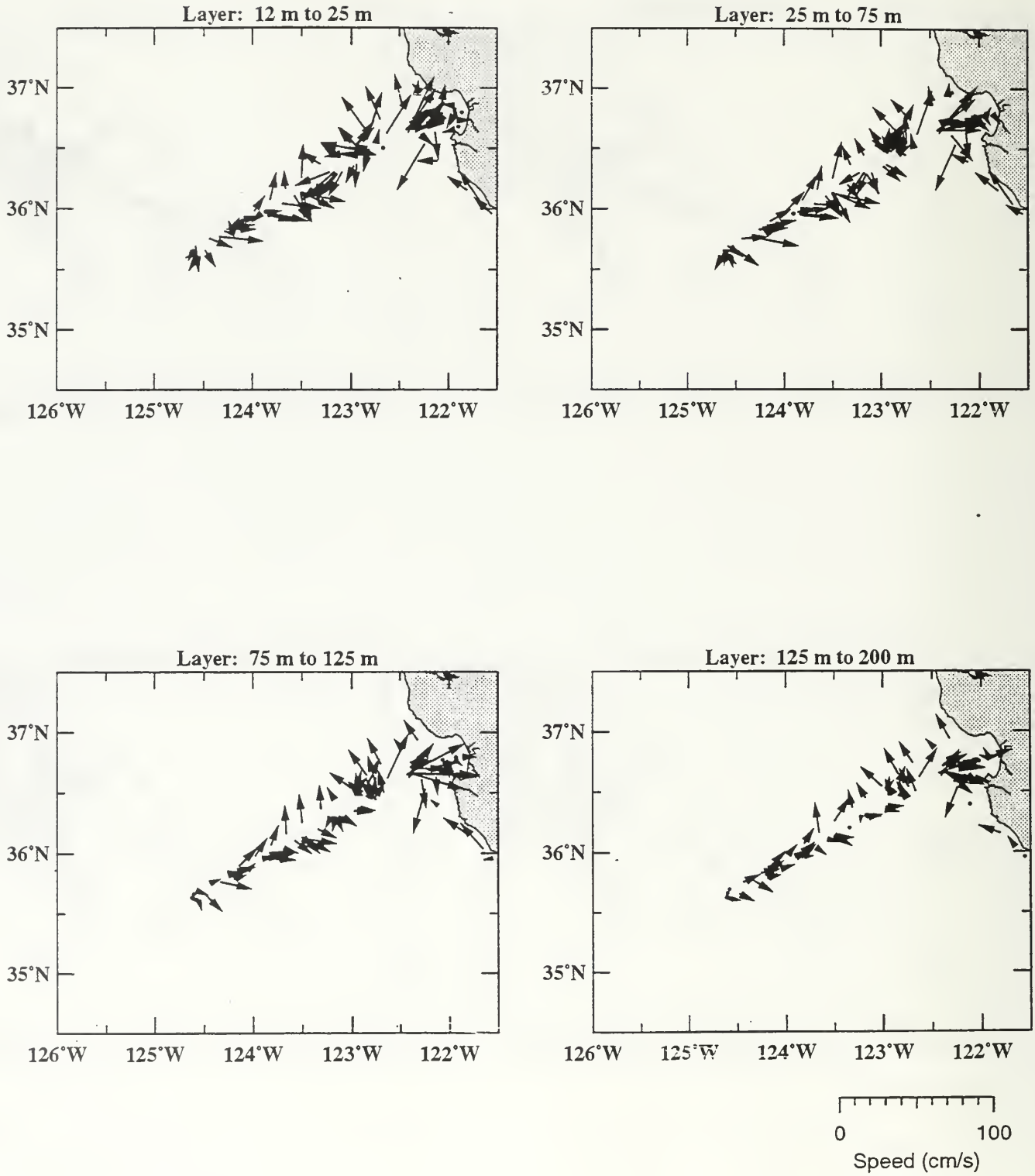

November 6-9, 1998

R/V New Horizon

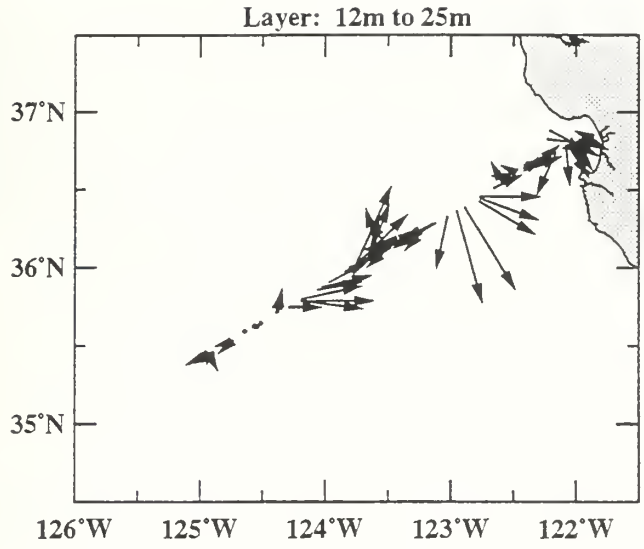

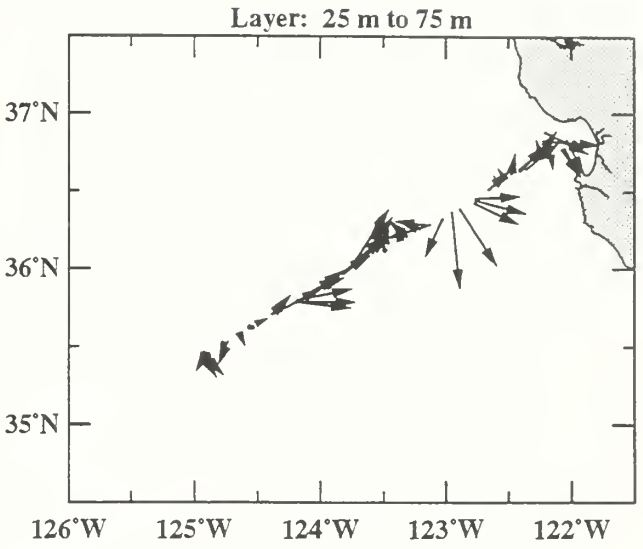

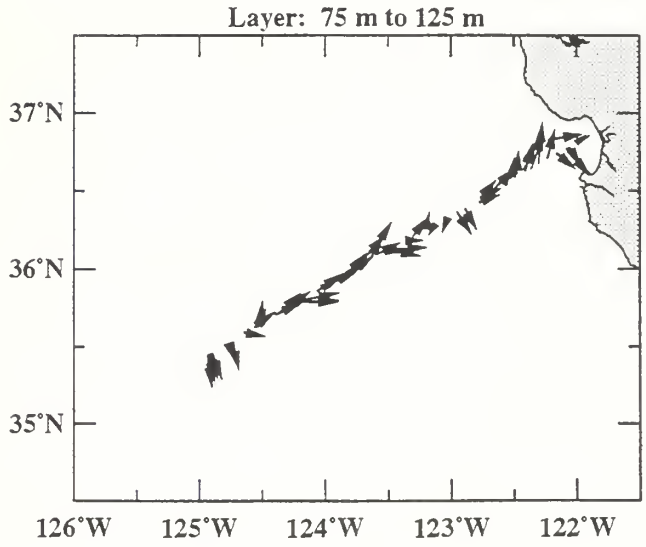

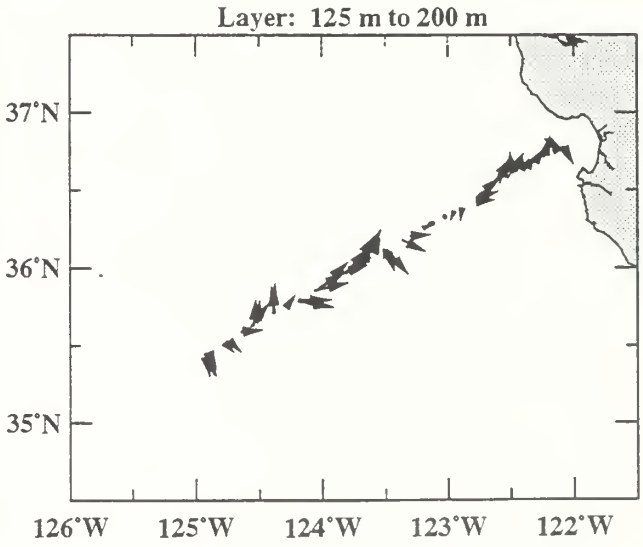

January 14-16, 1999

R/V Point Sur

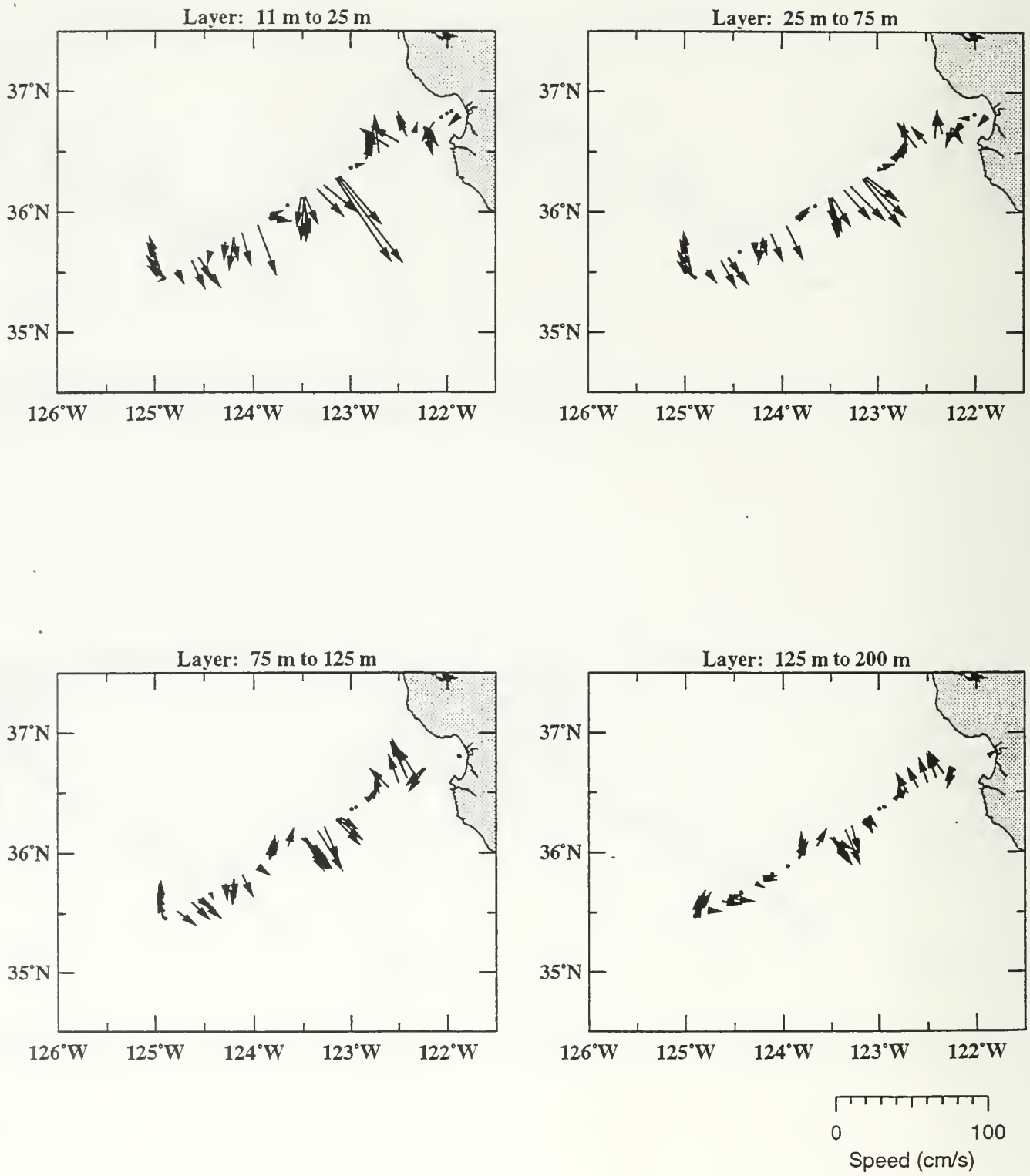

APPENDIX C: PRINCIPAL COMPONENTS

This appendix contains the first three principal components for hydrography and velocity data. Principal components were computed from objectively analyzed sections using MATLAB™ programs.

Potential Temperature (Contour Interval=0.5)

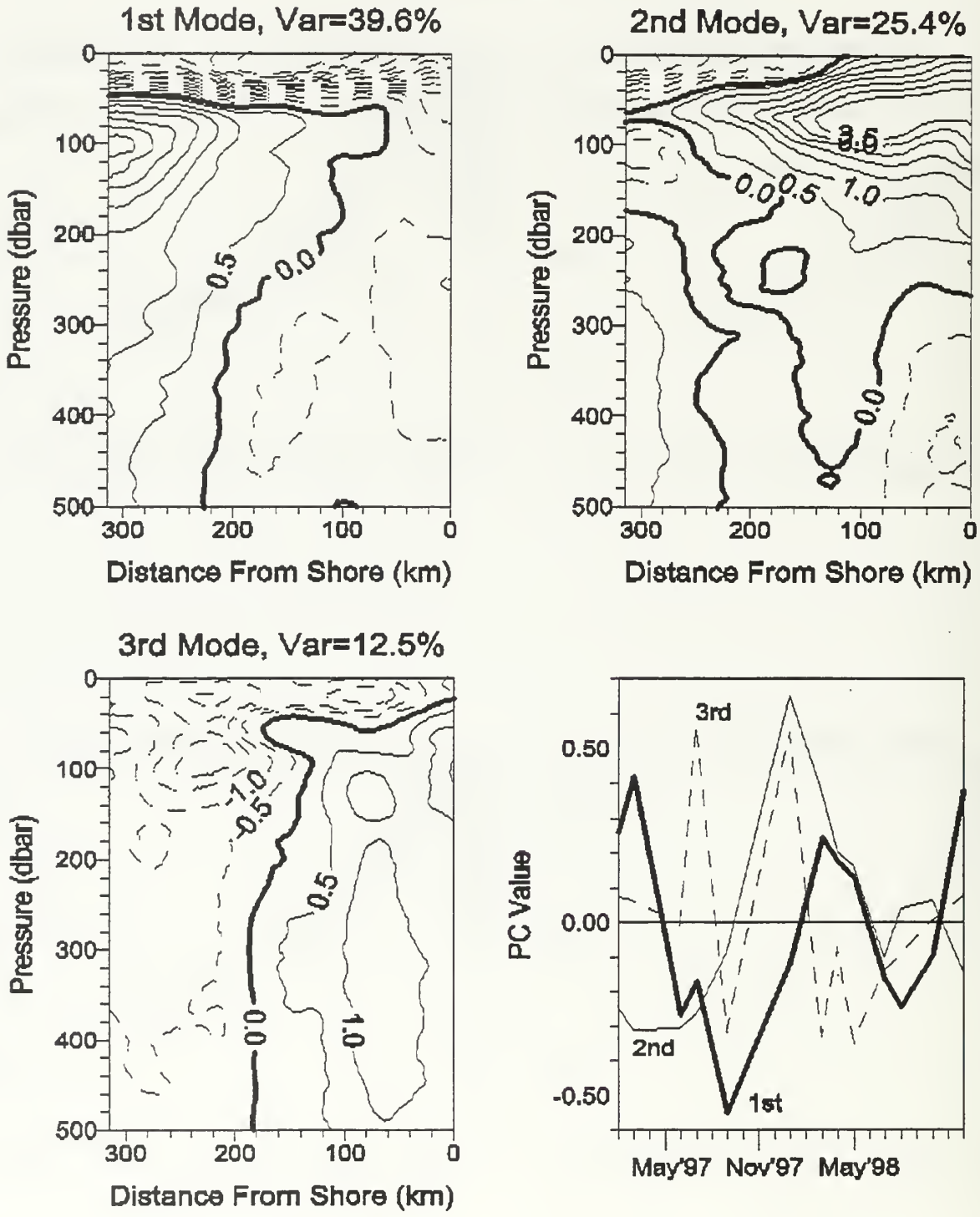

Salinity (Contour Interval=0.1)

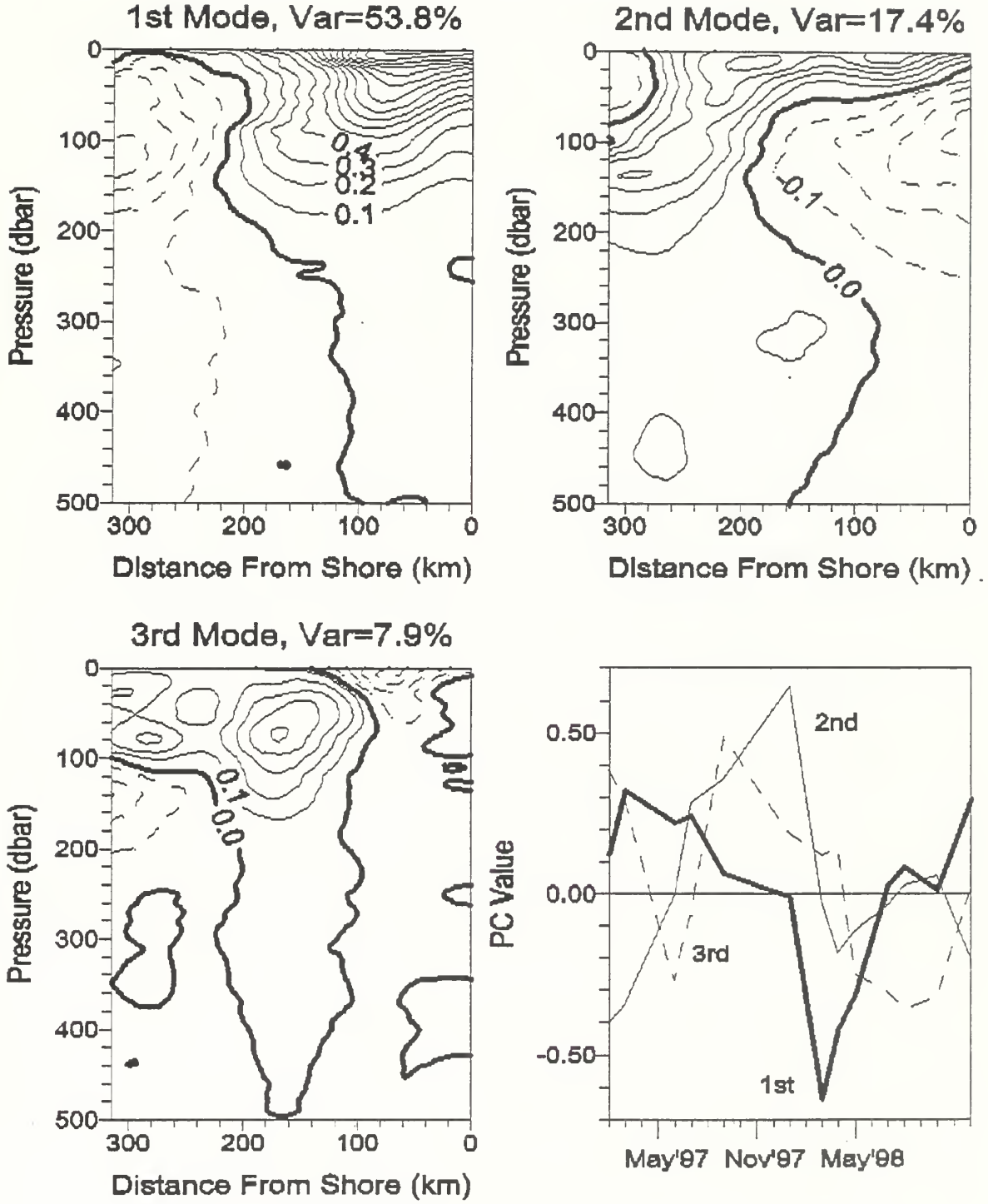

Density Anomaly (Contour Interval=0.2)

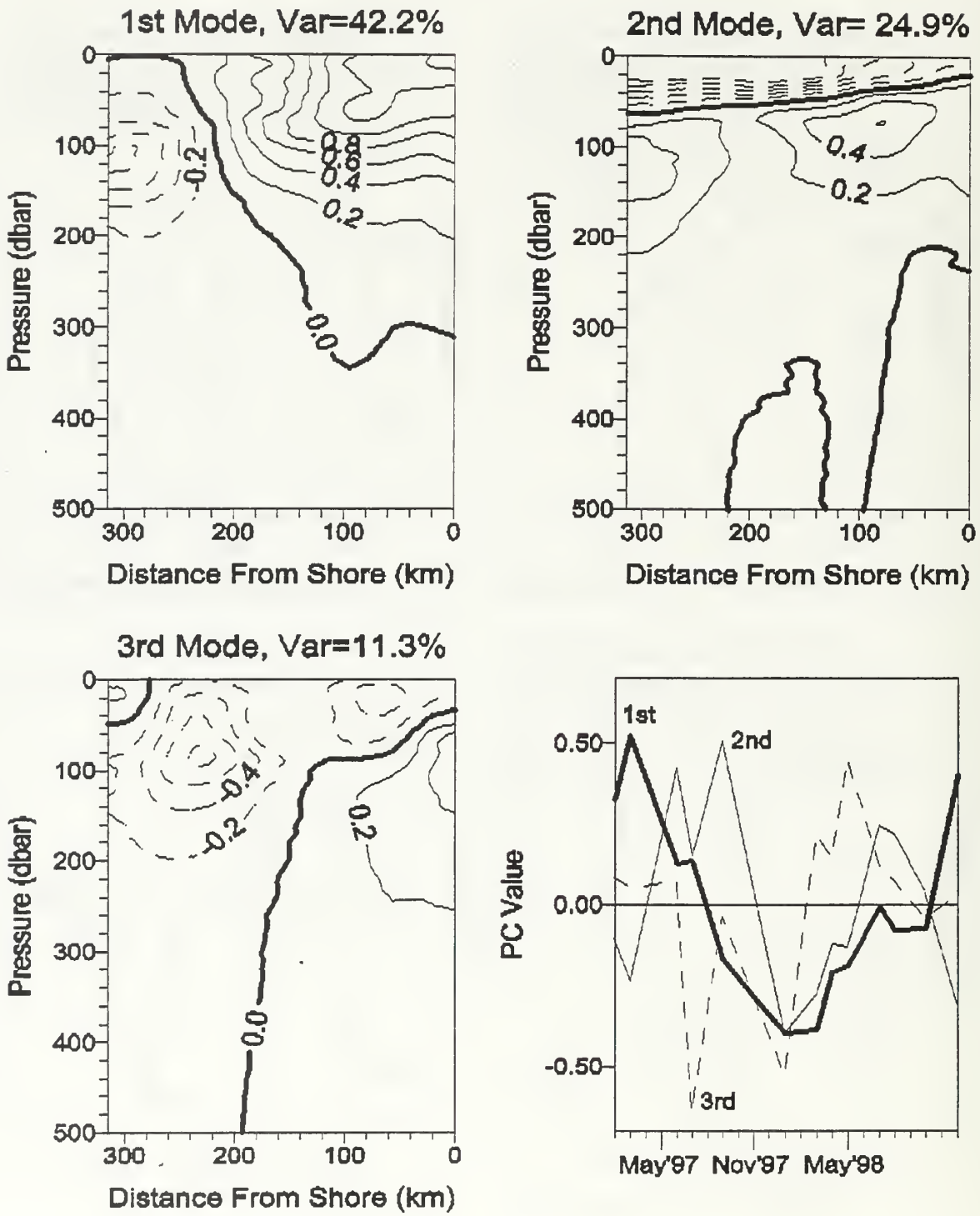

Salinity on Density Anomaly Contour Interval=0.05)

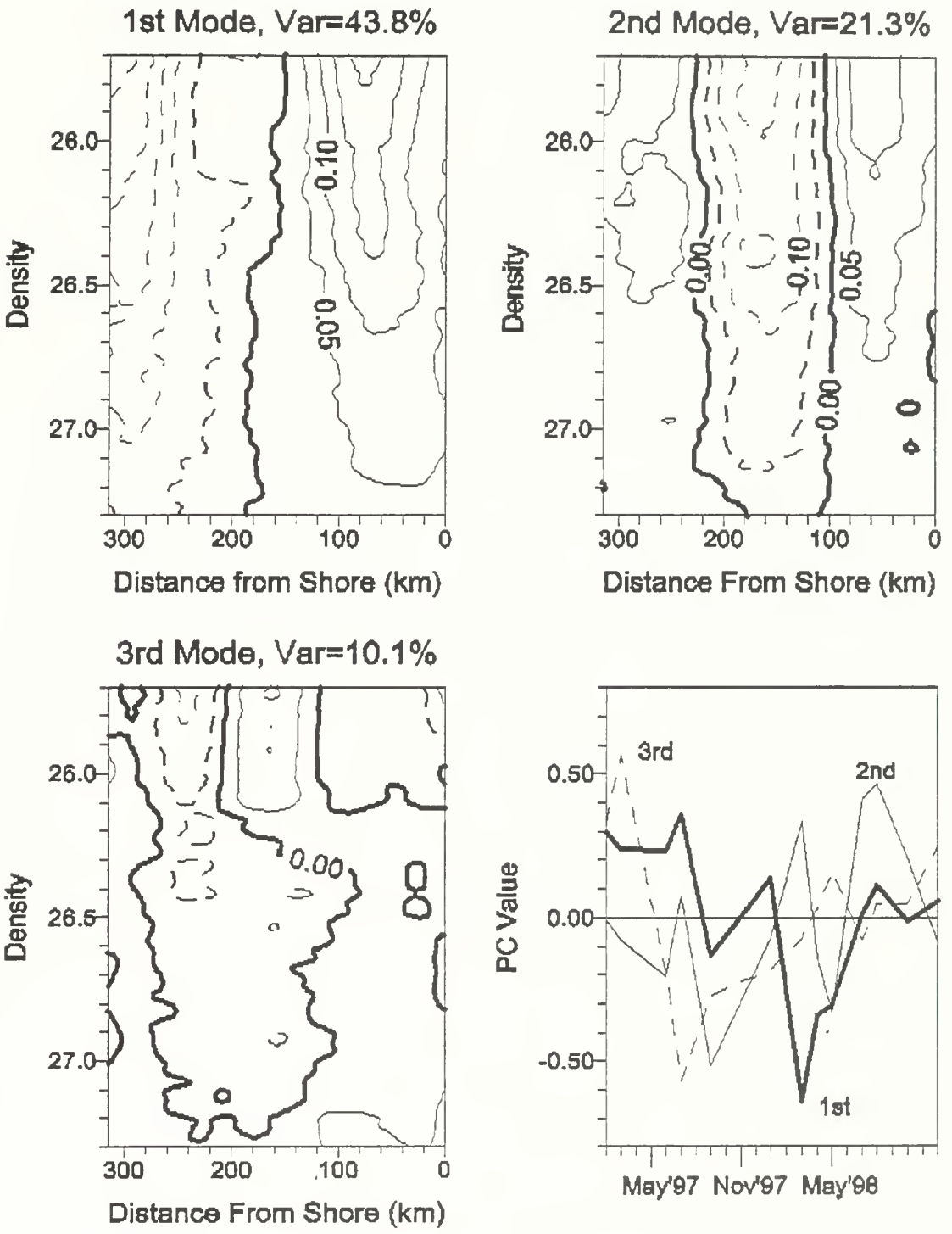

Pressure on Density Anomaly (Contour Interval=20)

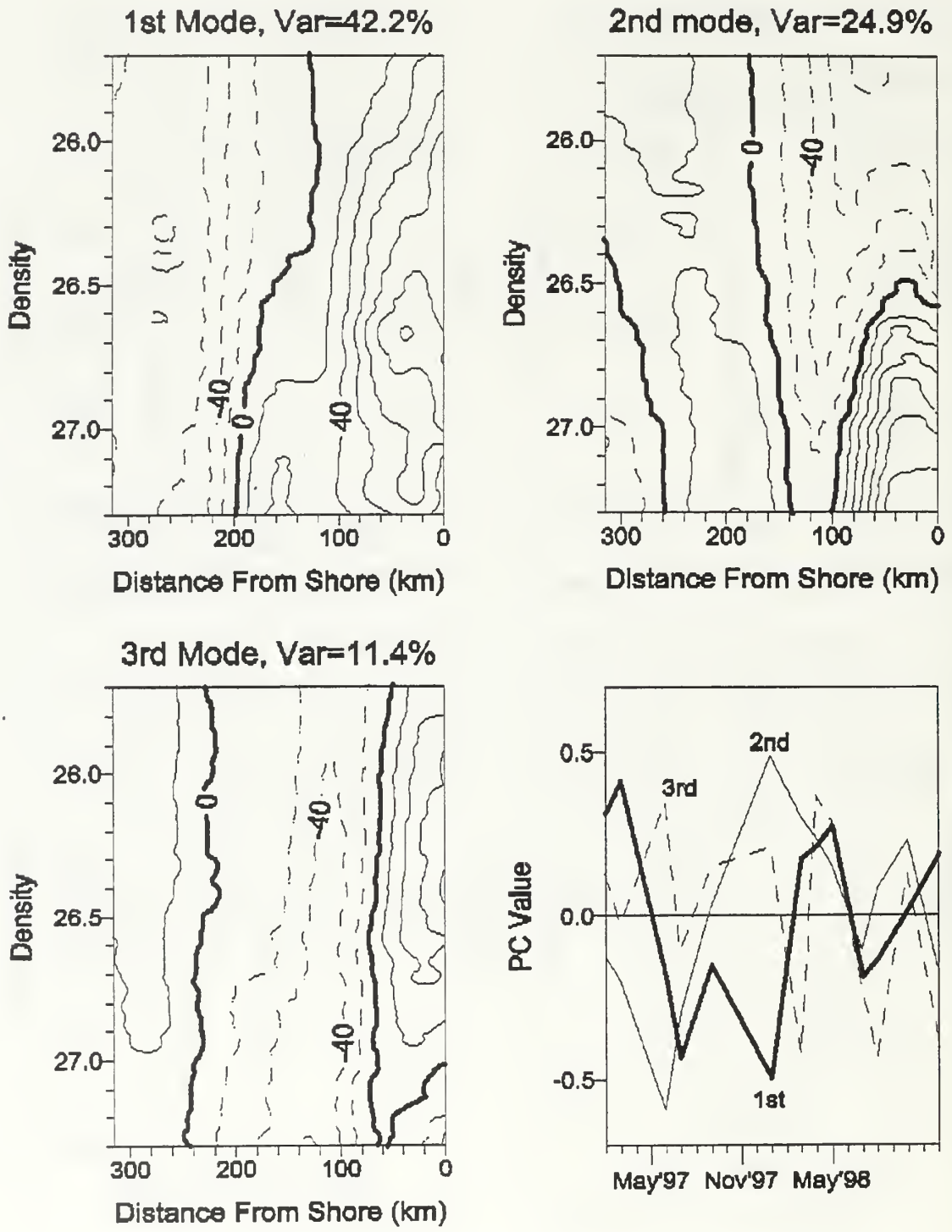

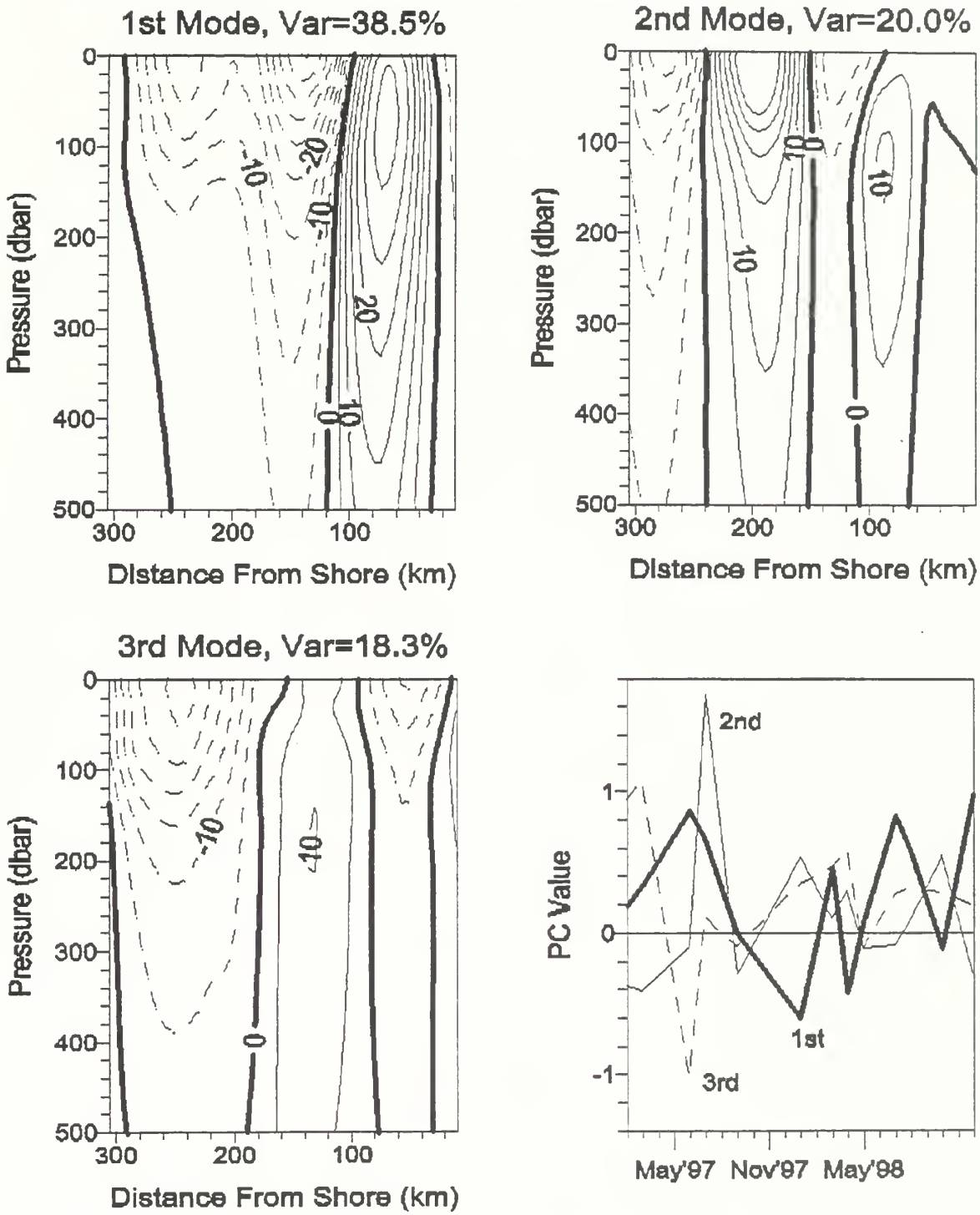
Geostrophic Velocity (Contour Interval=5)
1st Mode, Var=38.5%
2nd Mode, Var=20.0%
3rd Mode, Var=18.3%
Pressure (dbar)
Distance From Shore (km)
PC Value
2nd
1st
3rd
May'97
Nov'97
May'98

ADCP Alongshore Velocity (Contour Interval=10)

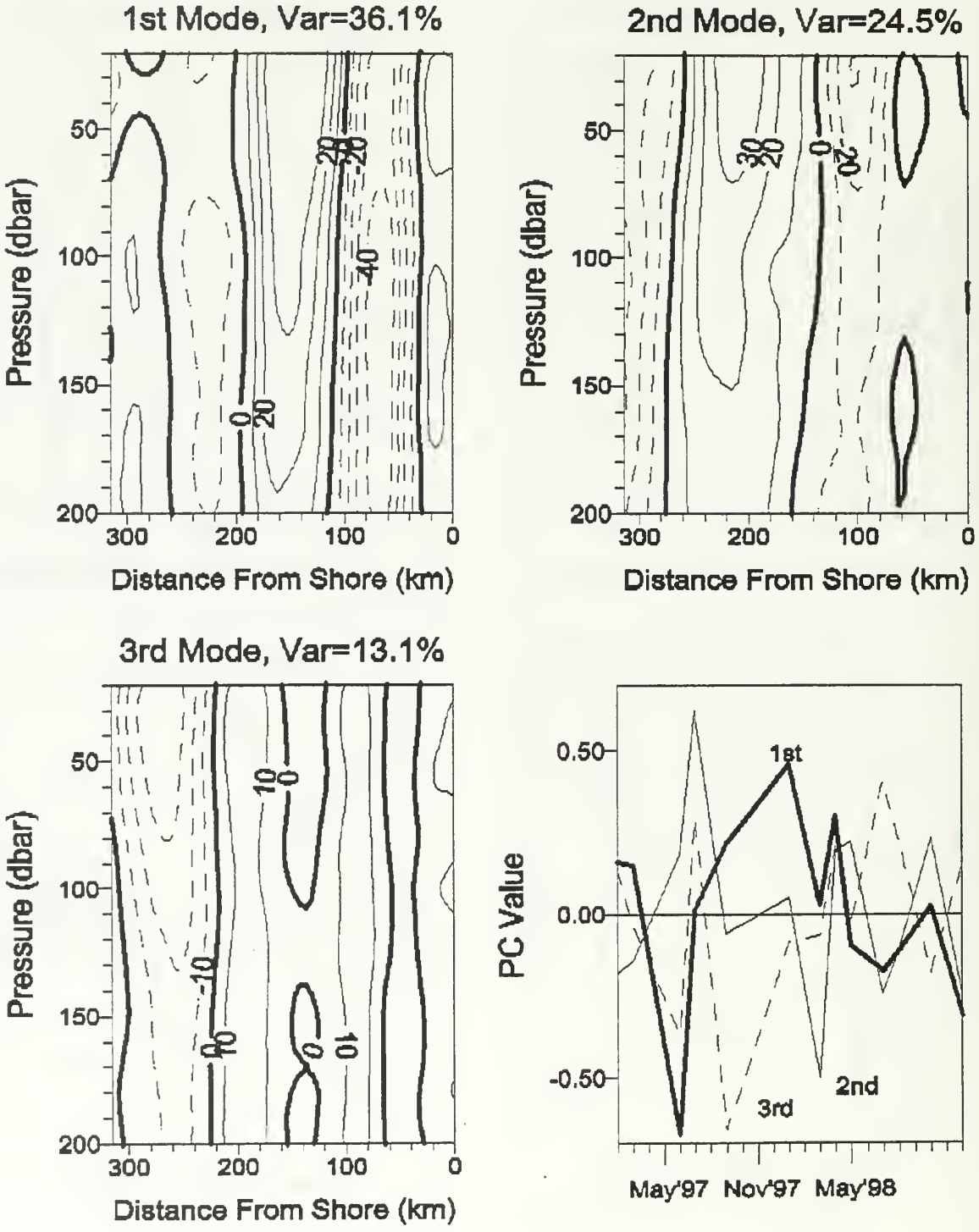

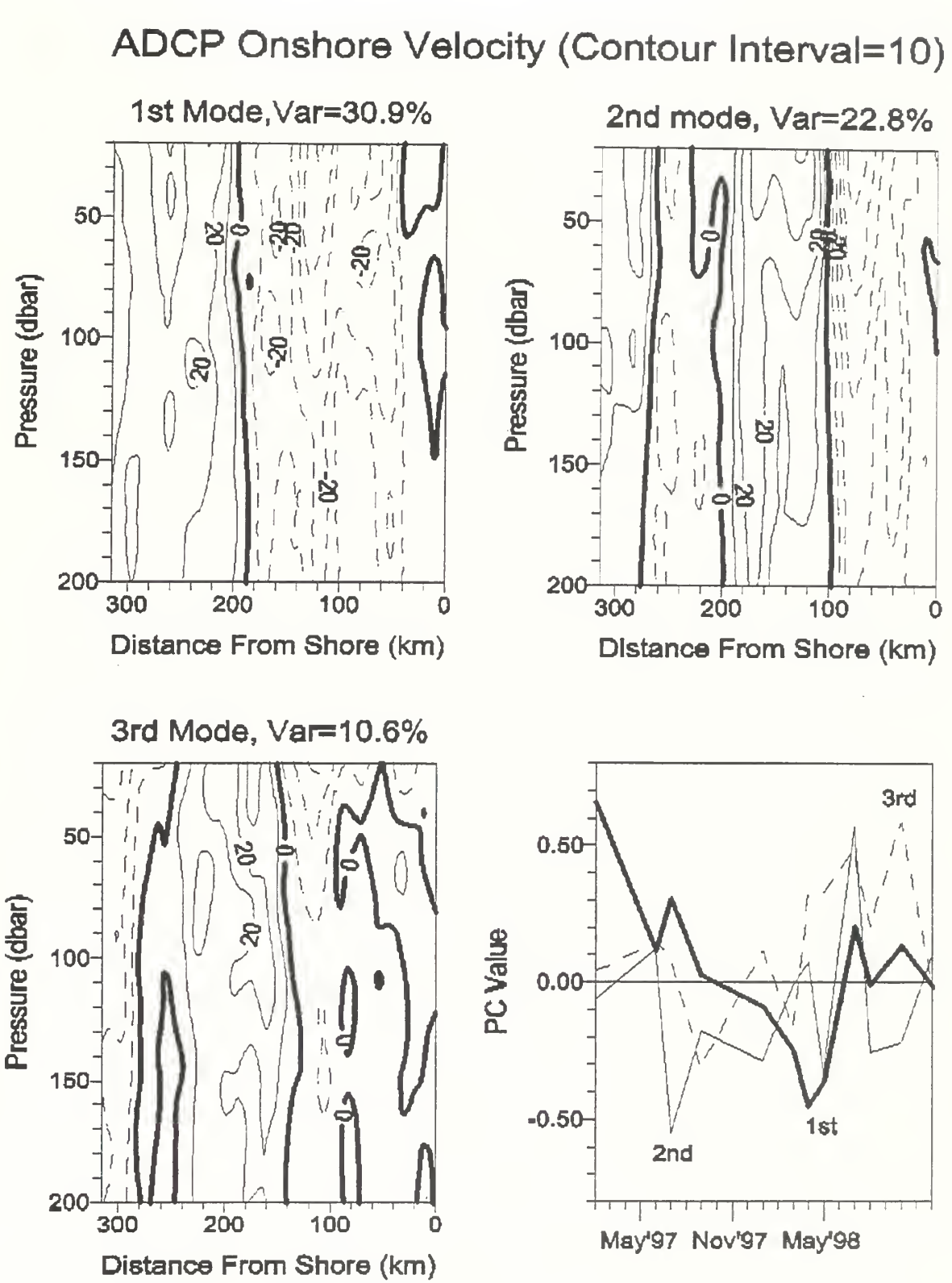
ADCP Onshore Velocity (Contour Interval=10)
1st Mode,Var=30.9%
2nd mode, Var=22.8%
3rd Mode, Var=10.6%
Pressure (dbar)
Distance From Shore (km)
50
100
150
200
300
200
100
0
20
0
-20
PC Value
0.50
0.00
-0.50
3rd
1st
2nd
May'97
Nov'97
May'98

INITIAL DISTRIBUTION LIST

No. Copies

1. Defense Technical Information Center .....(2)
   8725 John J. Kingman Rd., STE 0944
   Fort Belvoir, 22060-6218

2. Dudley Knox Library .....(2)
   Naval Postgraduate School
   411 Dyer Road
   Monterey, CA 93943-5101

3. Dr. Curtis A. Collins .....(2)
   Department of Oceanography, OC/Co
   Naval Postgraduate School
   833 Dyer Road, Rm 331
   Monterey, CA 93943-5122

4. Dr. Carmen Castro .....(1)
   Department of Oceanography, OC/Ca
   Naval Postgraduate School
   833 Dyer Road, Rm 331
   Monterey, CA 93943-5122

5. Mr. Thomas A. Rago .....(1)
   Department of Oceanography, OC/Rq
   Naval Postgraduate School
   833 Dyer Road, Rm 331
   Monterey, CA 93943-5122

6. Dr. Leslie K. Rosenfeld .....(1)
   Department of Oceanography, OC/Ro
   Naval Postgraduate School
   833 Dyer Road, Rm 331
   Monterey, CA 93943-5122

7. Dr. Steven R. Ramp .....(1)
   Department of Oceanography, OC/Ra
   Naval Postgraduate School
   833 Dyer Road, Rm 331
   Monterey, CA 93943-5122

8. Dr. Jeffrey Paduan .....(1)
Department of Oceanography, OC/Pd
Naval Postgraduate School
833 Dyer Road, Rm 331
Monterey, CA 93943-5122

9. Dr. Reginaldo Durazo .....(1)
Department of Oceanography, OC/Dj
Naval Postgraduate School
833 Dyer Road, Rm 331
Monterey, CA 93943-5122

10. Chairman .....(1)
Department of Oceanography, OC/Gd

Naval Postgraduate School
833 Dyer Road, Rm 331
Monterey, CA 93943-5122

11. Dr. Franklin B. Schwing ..... (1)
NOAA Pacific Fisheries Environmental Laboratory
1352 Lighthouse Avenue
Pacific Grove, CA 93950

12. Dr. Marlene Noble .....(1)
U.S. Geological Survey
345 Middlefield Road, MS 999
Menlo Park, CA 93025

13. Dr. Francisco Chavez .....(1)
Monterey Bay Aquarium Research Institute
700 Sandholdt Road
Moss Landing, CA 95039-1620

14. Ms. Reiko Michisaki .....(1)
Monterey Bay Aquarium Research Institute
700 Sandholdt Road
PO Box 628
Moss Landing, CA 95039-1620

15. Library .....(1)
Moss Landing Marine Laboratories
California State Colleges
P.O. Box 450
Moss Landing, CA 95039

16. LCDR Hiromi Asanuma, JMSDF .....(1)
819 Amarube Shimo Maizuru City,
Kyoto Prefecture Japan

17. Mr. Ron Lynn .....(1)
Southwest Fisheries Science Center
National Marine Fisheries Service
8604 La Jolla Shore Drive
La Jolla, CA 92038

18. Dr. James Simpson .....(1)
Scripps Institution of Oceanography
University of California, San Diego
La Jollas, CA 92093

19. Dr. Affonso Mascarenhas.....(1)
482 W. San Ysidro Blvd, Suite 731
San Ysidro, CA 92173-2410

20. Dr. Andrew DeVogelaire .....(1)
Monterey Bay National Marine Sanctuary
299 Foam Street Monterey, CA 93940